Bachelor's thesis

Jonas Jensen
Morten Fosstveit

A techno-economic analysis of hydrogen production from a 1 MW photovoltaic plant in Zambia, a feasibility study

June 2019

NTNU
Norwegian University of Science and Technology
Faculty of Engineering
Department of Energy and Process Engineering

NTNU
Norwegian University of
Science and Technology

Bachelor’s thesis

2019

NTNU

Norwegian University of
Science and Technology

Jonas Jensen
Morten Fosstveit

A techno-economic analysis of hydrogen production from a 1 MW photovoltaic plant in Zambia, a feasibility study

Bachelor's thesis
June 2019

NTNU
Norwegian University of Science and Technology
Faculty of Engineering
Department of Energy and Process Engineering

NTNU
Norwegian University of
Science and Technology

NTNU

Faculty of Engineering
Department of Energy and Process Engineering

Bachelor thesis

Project title: A techno-economic analysis of hydrogen production from a 1 MW photovoltaic plant in Zambia, a feasibility study.	**Filing date**: 03.06.2019
Oppgavens tittel: En teknisk-økonomisk analyse av hydrogen produksjon fra 1 MW solcelleanlegg i Zambia, en mulighetsstudie.	**Number of pages/appendix**: 132 /7
Study programme: Renewable energy, engineer	**Project number**: FEN1912
Group participants: Jonas Flatgård Jensen Morten Fosstveit	**Supervisor**: Bruno G. Pollet Professor, NTNU bruno.g.pollet@ntnu.no +47 735 58 984
Client: Norconsult AS	**Contact person at the client**: Harald Hesselberg / +47 454 01 439

Free for publishing ☒

Temporary banned ☐

Free for publishing after ☐

Preface

The Bachelor thesis is the final part of the Renewable Energy Bachelor's degree program at the Department of Energy and Process Engineering (EPT), Norwegian University of Science and Technology (NTNU).

This project were given by the Nordic consulting engineering company Norconsult. With the overlaying intention of examining the possibility for a future PV-hydrogen producing facility in Zambia. This thesis will present the feasibility of a small scale hydrogen production site in Zambia, as a step in this process.

We would like to express our sincere gratitude towards our internal supervisor at NTNU, Professor Bruno G. Pollet with weekly guidance and supplying abundant information. This gratitude is also directed to our external supervisors at Norconsult, Harald Hesselberg, Stian Erichsen and Eystein Helland for their time and dedication.

We will also like to thank Bjørn Gregert Halvorsen, Technology Specialist at NEL, for providing essential information.

Morten Fosstveit
Morten Fosstveit

Jonas Jensen
Jonas Flatgård Jensen

Abstract

The energy sector in Zambia is currently relying on past investment in hydropower. Over half of the electricity produced in the nation is consumed by the energy demanding copper industry, which is responsible for over three-quarters of the annual export revenues. In a nation where approximately 20% of the population has access to electricity, alternative energy solutions will have to be examined.

In this thesis, the feasibility of supplying a hydrogen electrolysis system with a 1 MW photovoltaic plant in Zambia is examined.

Information is gathered through literature review, field excursion, and interviews. Software simulations are used to assess the production from a photovoltaic plant in Zambia. Calculations and analysis have been done to evaluate the feasibility of a photovoltaic-hydrogen system.

An excursion to Zambia gave valuable information and understanding of the current situation in the region. Practical information and experience were obtained through conversation and meetings with representatives from different companies and institutions.

The results indicate that a hydrogen electrolysis module supported by a 1 MW photovoltaic plant, would be optimal with a 750 kW alkaline water electrolyzer. With an additional ideal energy storage system, a 250 kW alkaline water electrolyzer would be the more fitting choice.

The final analysis indicates that a PV-hydrogen system is technologically feasible, but not very efficient compared to the potential hydrogen production achievable from the electrolyzer module. Additional energy storage and power sources should be implemented to increase the total hydrogen production.

The PV-hydrogen system would most likely only be economically feasible in combination with the existing industry rather than for commercial electrification in Zambia.

Sammendrag

Energisektoren i Zambia støtter seg på tidligere investeringer innen vannkraft. Over halvparten av elektrisiteten produsert i nasjonen går til den energikrevende kobberindustrien, som er ansvarlig for over tre fjerdedeler av de årlige eksportinntektene. I en nasjon hvor omtrentlig 20% av befolkningen har tilgang til elektrisitet, må alternative energiløsninger undersøkes.

I denne rapporten, er muligheten for å forsyne et hydrogen-elektrolyse-system fra ett solcelleanlegg på 1 MW i Zambia blitt evaluert.

Informasjon er innhentet ved hjelp av litteratur studier, ekskursjon og intervjuer. Datasimuleringer ble gjort for å undersøke produksjonen fra et solcelleanlegg i Zambia. Beregninger og analyse har blitt gjort for å evaluere levedyktigheten til et solcelle-hydrogen-system.

Ekskursjonen til Zambia ga verdifull informasjon og forståelse av den nåværende situasjonen i regionen. Praktisk informasjon og erfaring ble innhentet gjennom samtaler og møtevirksomhet med representanter fra ulike selskaper og institusjoner.

Simuleringsresultatene indikerte at en hydrogen-elektrolyse-modul forsynt av et 1 MW solcelleanlegg, vil fungere best med en 750kW alkalisk vann elektrolysør. Hvis ett alternativt ideelt energi lagringssystem ble benyttet, ville en 250kW alkalisk vann elektrolysør være et mer passende størrelses valg

Resultatene indikerer at et solcelle-hydrogen-system er teknologisk gjennomførbart, men ikke veldig effektivt sammenlignet med den mulige hydrogen produksjonen som kan oppnås med elektrolysørmodulen. Alternative energilagringsystemer og kraftkilder bør benyttes for å øke den totale hydrogen produksjonen.

Solcelle-hydrogen-systemet kan sannsynligivs kun være økonomisk bærekraftig i kombinasjon med eksisterende industri i Zambia, snarere enn for kommersiell elektrifisering .

Contents

Preface i

Abstract ii

Sammendrag iii

Nomenclature ix

Abbreviations x

Background and Introduction 1

1 Introduction 1

1.1 Background . . . 1

1.2 Problem Definition . . . 2

1.3 Scope and Methodology . . . 3

Literature Review 5

2 The Republic of Zambia 5

2.1 Demography . . . 6

2.1.1 Climate . . . 7

2.2 Infrastructure . . . 9

2.2.1 Electric Power Industry . . . 9

2.2.2 Transportation . . . 13

2.3 Economy . . . 14

3 Photovoltaics 19

3.1 Solar Irradiation . . . 19

3.2 Operational Principle . . . 20

3.2.1 Converter . . . 22

3.2.2 Inverter . . . 23

3.3 Solar Energy Technologies . . . 24

3.3.1 Crystalline Silicon (c-Si) 24
3.3.2 Thin Film Solar Cell 26
3.4 Solar Tracking 26
3.5 PV Economics 28

4 Hydrogen Production 29
4.1 Steam Methane Reforming 32
4.2 Water Electrolysis 33
4.2.1 Thermodynamics 33
4.2.2 Kinetics and Resistance 35
4.2.3 Water Supply 37
4.3 Electrolyzer Technologies 38
4.3.1 Alkaline Water Electrolyzer 38
4.3.2 Proton Exchange Membrane Water Electrolyzer 40
4.3.3 Solid Oxide Water Electrolyzer 42
4.3.4 Molten Carbonate Water Electrolyzer 43

5 Hydrogen Storage 45
5.1 Hydrogen Transformation 45
5.2 Compressed Hydrogen 46
5.2.1 Piston Compressor 46
5.2.2 Diaphragm Compressor 47
5.3 Liquid Hydrogen 48
5.4 Metal Hydride Storage 49
5.5 Chemical Storage 50

6 Alternative Energy Storage Systems 51
6.1 Battery Energy Storage System 51
6.2 Mechanical Energy Storage 52
6.2.1 Pumped Hydroelectric Storage 53
6.2.2 Compressed Air Energy Storage 54
6.2.3 Flywheel Energy Storage 56

7 Economics 57

7.1 Capital Expenditure 57
7.2 Operating Expenditure 58
7.3 Levelized Cost of Energy 58
7.4 Hydrogen Prices 59

Methods and Approach 61

8 Photovoltaic 62
8.1 PVsyst 62
8.2 Land Coverage and PV-Orientation 63
8.3 PV Price Estimate 64

9 Electrolyzer System 65
9.1 Power Consumption 66
9.2 Hydrogen Production 67

10 PV-Hydrogen System 69
10.1 Hydrogen Price Estimate 71
10.2 Additional Energy Storage System 72

Results 73

11 Photovoltaics 73
11.1 PVsyst Simulation 73
    11.1.1 Solar Irradiation 73
    11.1.2 Fixed Tilt vs Tracking System 75
    11.1.3 Power Production 77
11.2 Economics 81

12 Alkaline Water Electrolyzer 83
12.1 Power Consumption 83
12.2 Hydrogen Production 87
12.3 Hydrogen Compression and Storage 92
12.4 Economics 93

13 Proton Exchange Membrane Water Electrolysis 95
13.1 Power Consumption 95
13.2 Hydrogen Production 99
13.3 Hydrogen Compression and Storage 104
13.4 Economics 105

14 Surplus Energy 107
14.1 Ideal Energy Storage 109
14.2 Economics 111

Discussion 113

15 Zambia 113

16 Photovoltaics 114
16.1 Inverter 116
16.2 Fixed Tilt and Tracked Configuration 116
16.3 PV Economics 117

17 Electrolyzer Module 118
17.1 Electrolyzer Technology 118
17.2 Electrolyzer Stack Size 119
17.3 Electrolyzer Degradation 121
17.4 Hydrogen Transformation and storage 122

18 Surplus Energy Storage System 123
18.1 Battery Energy Storage System 124
18.2 Pumped Hydroelectric Storage 125
18.3 Compressed Air Energy Storage 125
18.4 Flywheel Energy Storage 126

19 System Economics 126

20 Assumptions and Limitations 128

Conclusion **131**

21 Future Work **132**

A Appendix: NEL M-series datasheet **I**

B Appendix: NEL A-series datasheet **IV**

C Appendix: SAPP Members **V**

D Appendix: Canadian Solar datasheet **VI**

E Appendix: PV land coverage **IX**

F Appendix: DOE hydrogen production targets **X**

G Appendix: Hydrogen price equivalent **XI**

Nomenclature

AM	Air Mass coefficient
Cell stack	Multiple electrolyzer cells
Covalent bond	Atoms that share electrons to fulfill the octet rule
Diaphragm	Semi-penetrable seperator
Electrolyte	Electrical conduction solution
Electrolyzer Cell	The component that includes the separator and the electrodes
Fuel Cell	Component that converts hydrogen into electricity
Membrane	Semi-penetrable separator
Nm^3	Normal cubic meter (volume at STP)
STC	Standard Test Condition (25°C & 1 000 W/m^2 & AM 1.5)
STP	Standard Temperature and Pressure (0°C & 1 atmosphere)

Abbreviations

AC	Alternating Current
AHP	African Hydrogen Partnership Association
a-Si	Amorphous Silicon
AWE	Alkaline Water Electrolyzer
BESS	Battery Energy Storage System
CAES	Compressed Air Energy Storage
CAPEX	Capital Expenditure
CBU	Copperbelt University
CdTe	Cadmium Telluride
CEC	Copperbelt Energy Corporation
CGV	Coventional Gasoline Vehicle
CIS/CIGS	Copper Indium Gallium Selenide
c-Si	Crystalline Silicon
DC	Direct Current
DHI	Direct Horizontal Irradiance
DNI	Direct Normal Irradiance
DoD	Depth of Discharge
DOE	Department of Energy
DRC	Democratic Republic of Congo
EIB	European Investment Bank
ESS	Energy Storage System
EPT	Energy and Process Engineering
FCE	Fuel Cell Engine
FCEV	Fuel Cell Electrical Vehicle
FES	Flywheel Energy Storage
GDP	Gross Domestic Product
GHI	Global Horizontal Irradiation
HES	Hydrogen Energy Storage
HER	Hydrogen Evolution Reaction
HHV	Higher Heating Value
ICE	Internal Combustion Engine
IDC	Industrial Development Corporation

IFC	Industrial Financing Corporation
IRENA	International Renewable Energy Agency
OER	Oxygen Evolution Reaction
LCoE	Levelized Cost of Energy
LHPC	Lunsemfwa Hydro Power Company
LHV	Lower Heating Value
MCWE	Molten Carbonate Water Electrolyzer
MH	Metal Hydride
MPPT	Maximum Power Point Tracker
NREL	National Renewable Energy Laboratory
NTNU	Norwegian University of Science and Technology
NWEC	North Western Energy Corporation
O&M	Operation & Maintenance
OPC	Organic Photovoltaic Cell
OPEX	Operating Expenditure
PEM	Proton Exchange Membrane
PEMWE	Proton Exchange Membrane Water Electrolyzer
PHS	Pumped Hydroelectric Storage
PV	Photovoltaic
RES	Renewable Energy System
RSZ	Railway Systems of Zambia
SAPP	Southern Africa Power Pool
SOWE	Solid Oxide Water Electrolyzer
STC	Standard Test Conditions
STP	Standard Temperature and Pressure
TAZARA	Tanzania and Zambia Railway Authority
TFSC	Thin-film Solar Cells
USD	United States Dollar
ZDA	Zambian Development Agency
ZESCO	Zambia Electricity Supply Corporation Limited
ZPC	Zengamina Power Company Limited

List of Figures

1.1 Photo taken at the excursion to Zambia. 4
2.1 Zambia's geographical location highlighted on the African continent. 5
2.2 The population distribution in Zambia. 6
2.3 The elevation distribution in Zambia. 8
2.4 The long-term average temperature in Zambia. 8
2.5 The long-term average GHI in Zambia. 9
2.6 Illustration of the transmission and installed capacity in Zambia 10
2.7 Installed electricity capacity in Norway and Zambia 11
2.8 Illustration of the road infrastructure in Zambia 13
2.9 The export distribution in Zambia (2014) 15
3.1 World long-term average GHI 19
3.2 Solar irradiation on a horizontal module. 20
3.3 Solar irradiation on a tilted module. 20
3.4 A principle sketch of a PV-cell. 21
3.5 Difference between: cell, module and array. 22
3.6 Efficiency vs load characteristics for DC/DC Converters 23
3.7 Efficiency versus load characteristics for inverters 24
3.8 Space utilization and appearance differences in PV-modules. 25
3.9 Illustration of the terminology regarding the suns position 27
3.10 Total cost of PV-system with fixed tilt and one-axis tracker 29
4.1 A flowchart of the hydrogen cycle 31
4.2 Water decomposition, energy consumption versus temperature 35
4.3 Equivalent circuit of an electrolyzer cell 36
4.4 Illustration of an Alkaline Water Electrolysis 39
4.5 Illustration of a Proton Exchange Membrane Water Electrolyzer 40
4.6 Illustration of a Proton Exchange Membrane 41
4.7 Illustration of a Solide Oxide Water Electrolyzer 43
4.8 Illustration of a Molten Carbonate Water Electrolyzer 44
5.1 Simple schematic of piston compression 47
5.2 Simple schematic of diaphragm compression 48
5.3 The interaction between Metal Hydride and hydrogen atoms 49

6.1 Layout of a hydroelectric facility 53
6.2 The layout of a large scale CAES system 55
6.3 Layout of a carbon fibre flywheel 56
7.1 CAPEX versus electrolyzer plant capacity 60
7.2 Visual representation of the system simulated in the thesis 61
11.1 Global horizontal irradiation in Chililabombwe, Zambia 74
11.2 Power output versus land coverage with fixed tilt 75
11.3 Power output versus land coverage with north-south tracking 76
11.4 Fixed versus tracking, mean monthly power production 78
11.5 Fixed versus tracking, daily power output 79
11.6 Effect of PV degradation on annual power production 80
11.7 Extrapolated prices for PV-modules 82
12.1 Daily consumption versus energy available, 250 kW and 500 kW AWE . . . 84
12.2 Daily consumption versus energy available, 750 kW and 1000 kW AWE . . . 84
12.3 Hourly consumption versus energy available, 250 kW and 500 kW, AWE . . 85
12.4 Hourly consumption versus power available, 750 kW and 1000 kW, AWE . . 86
12.5 Daily hydrogen production, 250kW & 500kW, AWE 88
12.6 Daily hydrogen production, 750kW and 1000kW, AWE 88
12.7 Monthly hydrogen production, AWE 89
12.8 Hydrogen production over 25 years, AWE 91
12.9 Hydrogen production the first year, AWE 92
12.10 Accumulated cost and income, AWE 94
13.1 Daily consumption versus energy available, 250 kW and 500 kW, PEMWE . 96
13.2 Daily consumption versus energy available, 750 kW and 1000 kW, PEMWE 96
13.3 Hourly consumption versus energy available, 250kW and 500kW, PEMWE . 97
13.4 Hourly consumption versus energy available, 750kW and 1000kW PEMWE . 98
13.5 Daily hydrogen production, 250kW and 500kW, PEMWE 100
13.6 Daily hydrogen production, 750kW and 1000kW, PEMWE 100
13.7 Monthly hydrogen production, PEMWE 101
13.8 Hydrogen production over 25 years, PEMWE 103
13.9 Hydrogen production the first year, PEMWE 104
13.10 Accumulated cost and income, PEMWE 106
14.1 Daily surplus energy, 250 kW and 500 kW, AWE 107

14.2 Daily surplus energy, 750 kW and 1000 kW, AWE 108
14.3 Energy consumption with an ESS, 250 kW & 500 kW, AWE 109
14.4 Hourly power consumption with an ESS, AWE 110
A.1 Datasheet of the M-Series electrolyzers produced by NEL III
B.1 Datasheet of the A-Series electrolyzers produced by NEL IV
C.1 The companies involved in the Southern African Power Pool V
D.1 Datasheet for the PV-module used in PVsyst .VIII
E.1 Land coverage due to shading from PV IX
F.1 DOE Technical Targets for Hydrogen Production from Electrolysis X

List of Tables

2.1 Zambia compared with the world average and Norway 7
2.2 Electric power industry status in Zambia 12
3.1 PV benchmark assumptions from NREL 28
4.1 Different water purification processes 37
4.2 Specific Heat Capacity, water and air 37
4.3 Comparison between different electrolysis technology 38
5.1 Properties of hydrogen and diesel at STP 45
5.2 Phase transition, hydrogen and water at 1 atm 48
6.1 Comparison between lead acid and lithium ion batteries 52
6.2 Comparison between PHS, CAES and FES 53
8.1 Specific design inputs for the PVsyst simulations 63
9.1 Simulation parameters used for the electrolyzer in Matlab modelling 66
9.2 Electrolyzer system range used in Matlab modelling 66
10.1 Storage tank and compressor values used in the simulations 69
10.2 CAPEX for electrolyzer and compressor combined 70
10.3 0&M for electrolyzer and tanks combined 70
10.4 Vehicle range CGV and FCEV 71
10.5 Gasoline prices USA and Zambia 71
11.1 Average GHI in Chililabombwe, Zambia 74
11.2 Summarized results after module orientation simulations 77
11.3 Annual power production from the PV-system 81
12.1 System and stack ranges for AWE at different installed capacities 83
12.2 First year electrolyzer consumption and surplus energy, AWE 87
12.3 First year performance, AWE 87
12.4 First year hydrogen production, AWE 90
12.5 Hydrogen production and stack degradation over 25 years, AWE 92
12.6 Compressor and tank size for each evaluated stack size, AWE 93
12.7 Total CAPEX and OPEX, and the LCOE, AWE 93
13.1 System and stack ranges at different installed capacities, PEMWE 95
13.2 First year electrolyzer consumption and surplus energy, PEMWE 99
13.3 First year performance, PEMWE 99

13.4 First year hydrogen production, PEMWE 102
13.5 Hydrogen production and stack degradation over 25 years, PEMWE 104
13.6 Compressor and tank size for each evaluated stack size, PEMWE 105
13.7 Total CAPEX and OPEX, and the LCOE, PEMWE 105
14.1 Surplus energy of the system, relative to the stack size, AWE 108
14.2 Hydrogen production with an Ideal ESS, AWE 111
14.3 Cost of an additional energy storage system 111

Background and Introduction

1 Introduction

1.1 Background

The Republic of Zambia is facing major energy challenges in the future. An energy-dependent mining industry, lack of public electrical access and under-investment in infrastructure are some of the problems that the landlocked nation will have to deal with in the coming years. To have a sustainable and renewable future for in the energy sector, hydrogen might be part of a comprehensive solution, with keywords such as solar- and hydro-power playing important roles in the energy supply of the future.[1]

The total installed electrical generation capacity in the nation is 2 347 MW (2017), where hydropower is responsible for approximately 96%. The demand for electricity in Zambia has been increasing with about 3% annually, and the connected Southern Africa Power Pool (SAPP) electrical power consumption has been increasing with an average of 5% per year. The increase in power consumption is expected to accelerate in the coming years, with a high demand for reliable, sustainable and renewable power sources. [2]

Hydrogen is the simplest and most abundant element in the known universe, despite this, hydrogen does not exist naturally on earth. Since hydrogen reacts easily with other elements, hydrogen must be separated from other elements. Hydrogen is therefore classified as an energy carrier and not an energy source. [3, 4]

Attention towards hydrogen as a reliable, sustainable, energy storage medium has rapidly been increasing. Pairing hydrogen electrolysis with renewable energy sources such as solar or hydropower could yield clean, reliable energy in large quantities. This is also applicable for off-grid production and storage, which could be relevant in rural regions of the nation. If the Sub-Saharan region growth is going to happen in a climate-sustainable way, the commitment to clean, renewable technology should be made. [1, 2]

1.2 Problem Definition

Due to poor rural infrastructure and a power demanding mining industry the ability to store energy reliably, either for large scale mining/refining facilities or rural villages is needed in Zambia. Due to the high solar irradiance in the region, a PV-facility and coupled with hydrogen electrolysis could meet the current and future energy demand in a sustainable and renewable way.

The following questions can be asked:

- Is hydrogen electrolysis from a 1 MW Photovoltaic system feasible?
- Could a PV-hydrogen system be economical feasible in Zambia?

This thesis will analyze the possibilities for a hydrogen production and storage unit, powered by a 1 MW PV-plant, in Chililabombwe, Zambia.

The PV-plant will be on the scale of 1 MW nominal power production. The daily and yearly solar irradiation will be taken into account, when looking at the available power supplied for hydrogen production.

The choice of electrolyzer cell will be based on efficiency, cost, durability and commercially available technology. Hydrogen production volume is going to be calculated for on-site storage. Storage alternatives will be taken into consideration when designing the overall system.

A calculation for the accumulated cost and income will be conducted for the perceived optimal system, with different hydrogen prices, to estimate the economical feasibility.

1.3 Scope and Methodology

Scope

- Get a comprehensive overview of the power production from the PV-system through simulations.
- Research existing electrolysis technology.
- Evaluate the efficiency, cost and methods of different hydrogen storage technologies.
- Obtain information about cost and performance parameters of the different components through calculations.
- Research the existing electricity and transport infrastructure.
- Estimate the economical sustainability of the system.

Methodology

This thesis is based on the theory and information gained by the participants through literature review, online sources, excursion, mail correspondence, other research groups and meetings with industry. With the knowledge obtained through these means coupled with simulations and calculations, a complete PV-Hydrogen system will be proposed. Weekly information exchange and transparency with guidance counsellors were used to receive vital feedback and expertise during the process.

Excursion

An excursion to Zambia were realized during the project period, from 8th of April to the 14th of April. It included a conversation with Boyd Simposya (NB solar Africa), meeting with Moses Mubanga, Chief Engineer in ZESCO, presentation of a PV facility by Hilton M. Fulele (Engineer, Copperbelt Energy Corporation (CEC)) and a tour of the Copperbelt University (CBU) given by Robert Ngoma and Francis Mulolani. Valuable information and understanding of the situation in Zambia were obtained through the various conversations and discussions during the trip. First-hand experience and information about infrastructure and existing PV-facilities in Zambia were attained.

Figure 1.1: *Photo taken at the excursion to Zambia. In the background is the PV-plant the Copperbelt Energy Corporation (CEC) have constructed, which is situated right outside the CBU campus. From left to right: Robert Ngoma (CBU), Jonas Jensen (NTNU), Hilton M. Fulele (CEC) and Francis Mulolani (CBU).*

Literature Review

2 The Republic of Zambia

The nation is located on a high plateau in south-central Africa [5]. Zambia has a total area of 752 612 km^2 and a population of 17.9 million (per February of 2019). The capital is Lusaka, and the landlocked nation borders with Zimbabwe, Botswana, Namibia, the Democratic Republic of the Congo, Angola, Tanzania, Malawi, and Mozambique, as seen in figure 2.1. [6]

Figure 2.1: *Zambia's geographical location highlighted on the African continent.[5]*

2.1 Demography

Lusaka is both the capital and the largest city, with approximately 2.5 million inhabitants. Much of Zambia's population is centered around Lusaka and the Copperbelt province (Kitwe and Ndola). As shown in figure 2.2. The nation is one of the most urbanized countries in sub-Saharan Africa. Zambia is the 30th largest country in the world, and with a population density of $24/\text{km}^2$ combined with an urbanization percentage of 44 % resulting in scarcely populated rural areas. [6]

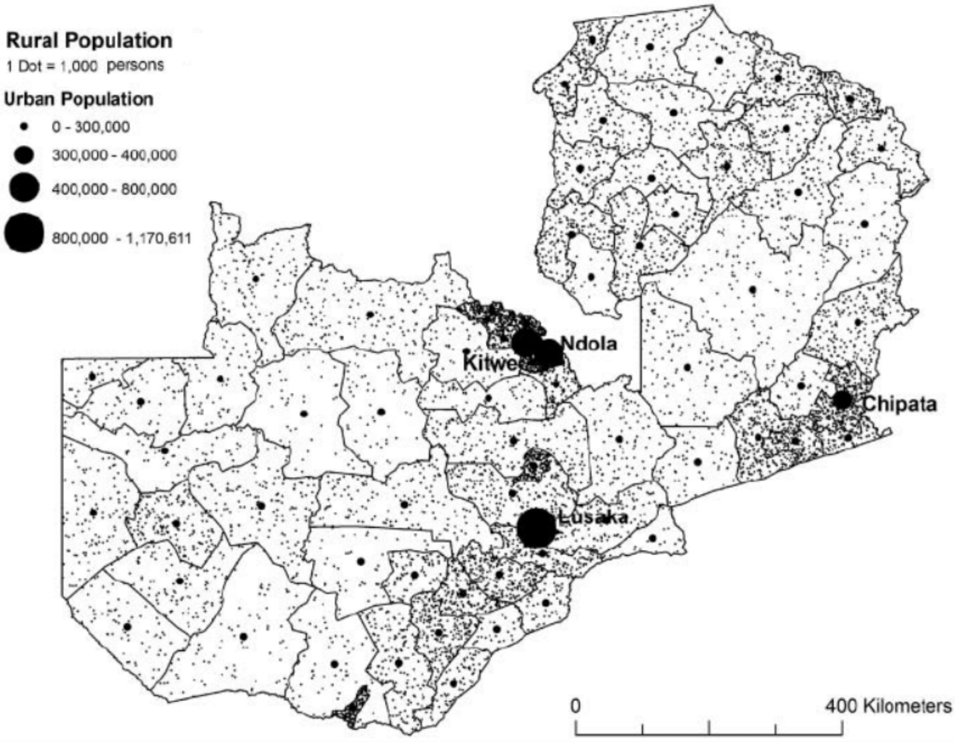

Figure 2.2: *The population distribution in Zambia. [7]*

Zambia consists of 72 indigenous groups, where most speak a native language in the Bantu-family. English serves as the common language and is declared the national language.
The two largest immigrant groups from outside the African continent are Indians (13 000) and Chinese (80 000). There are also approximately 89 000 asylum seekers and refugees from the following nations: the Democratic Republic of Congo (47 000), Angola (27 000), Zimbabwe (5 000) and Rwanda (5 000). [6]

In table 2.1, Zambia is compared to the World average and Norway in terms of median age, life expectancy, fertility rate and GDP per capita.

Table 2.1: *Zambia compared with the world average and Norway. [5, 8, 9, 10]*

	Zambia	**World average**	**Norway**
Median age	16.8	30.6	39.3
Life expectancy	52.7	69.8	82
Fertility rate	5.63	2.42	1.85
GDP per capita [USD]	1 513.3	10 721.6	75 504.6

It is predicted that the population in Zambia could reach 43 million by 2050, and 104 million by 2100. [11]

Roughly 65 % have access to clean drinking water, and scarcely 43.9 % have access to improved sanitation[6]. The risk of infectious diseases is high, and the number of antibiotic-resistant virus strains is increasing in the sub-Saharan region.[5]

2.1.1 Climate

Since Zambia is located on a plateau in South-central Africa, the mean elevation in the nation is 1138 meters above sea level, ranging from 329 meters above sea level, at the Zambezi river in the south-west. To above 2 300 meters above sea level in the north-east. Figure 2.3 shows the elevation distribution. Zambia has a rainy season from October to April and is classified as tropic/sub-tropic, depending on the region. Figure 2.4 shows the long-term average temperature. [5]

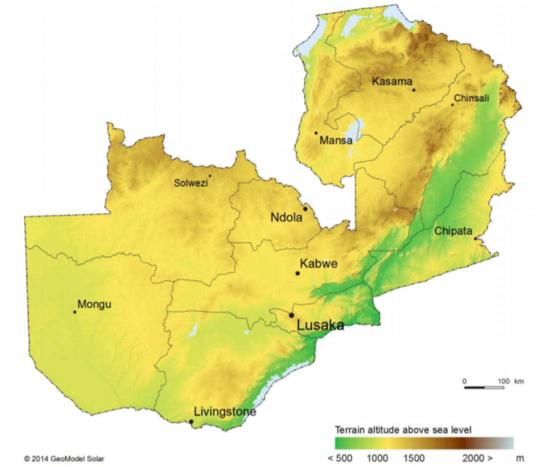

Figure 2.3: *The elevation distribution in Zambia.[12]*

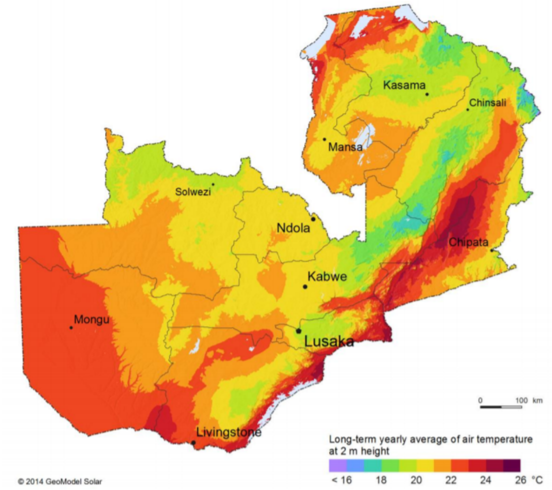

Figure 2.4: *The long-term average temperature in Zambia. [12]*

The solar irradiance in Zambia is quite high. Figure 2.5 illustrates the long-term variation in Global Horizontal Irradiation (GHI). The regional variance can be explained by the geography of Zambia. Comparing figure 2.3 and 2.4 gives some explanation about the GHI, since cloud-formation would likely be happening correspondingly to the elevation and the average temperature on the plateau where Zambia is located. [12]

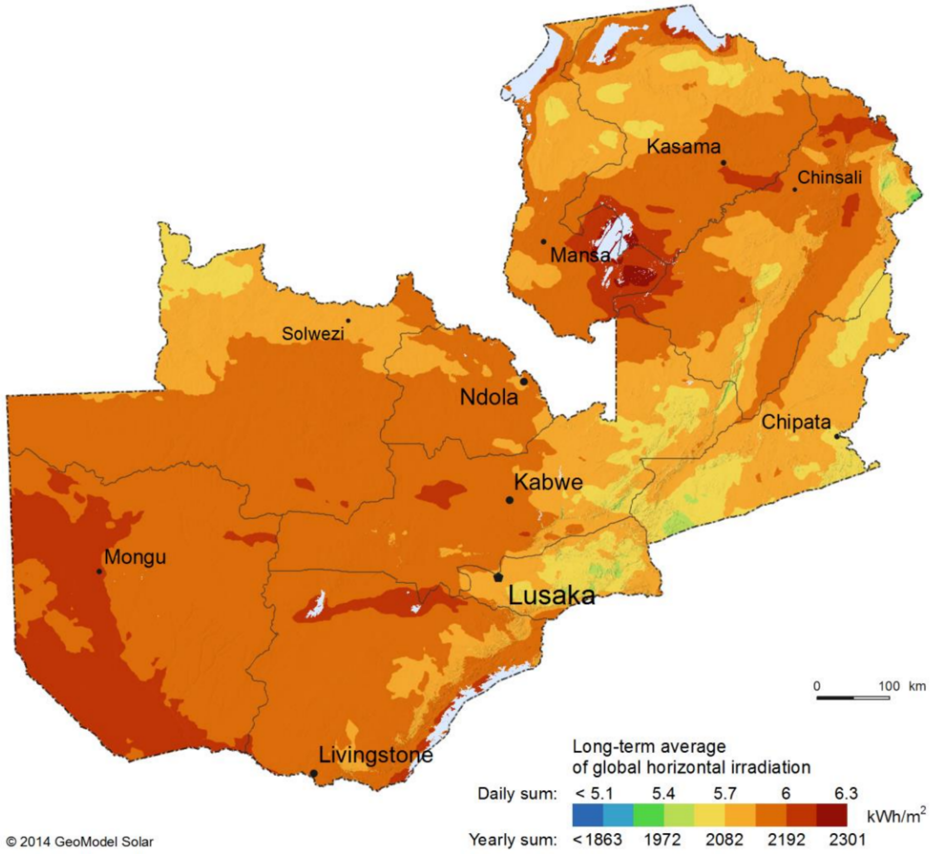

Figure 2.5: *The long-term average GHI in Zambia. [12]*

2.2 Infrastructure

2.2.1 Electric Power Industry

Zambia's total installed electrical production capacity is 2 347 MW (2017) [2]. Of the electricity produced, little is available for the population, and in 2010 only 20% had access to electricity. This is because of the power demanding mining sector, which consumes more than 50% of the electricity produced in the nation [13]. The grid is mainly tailored around the mining sectors, as seen from figure 2.6. [1]

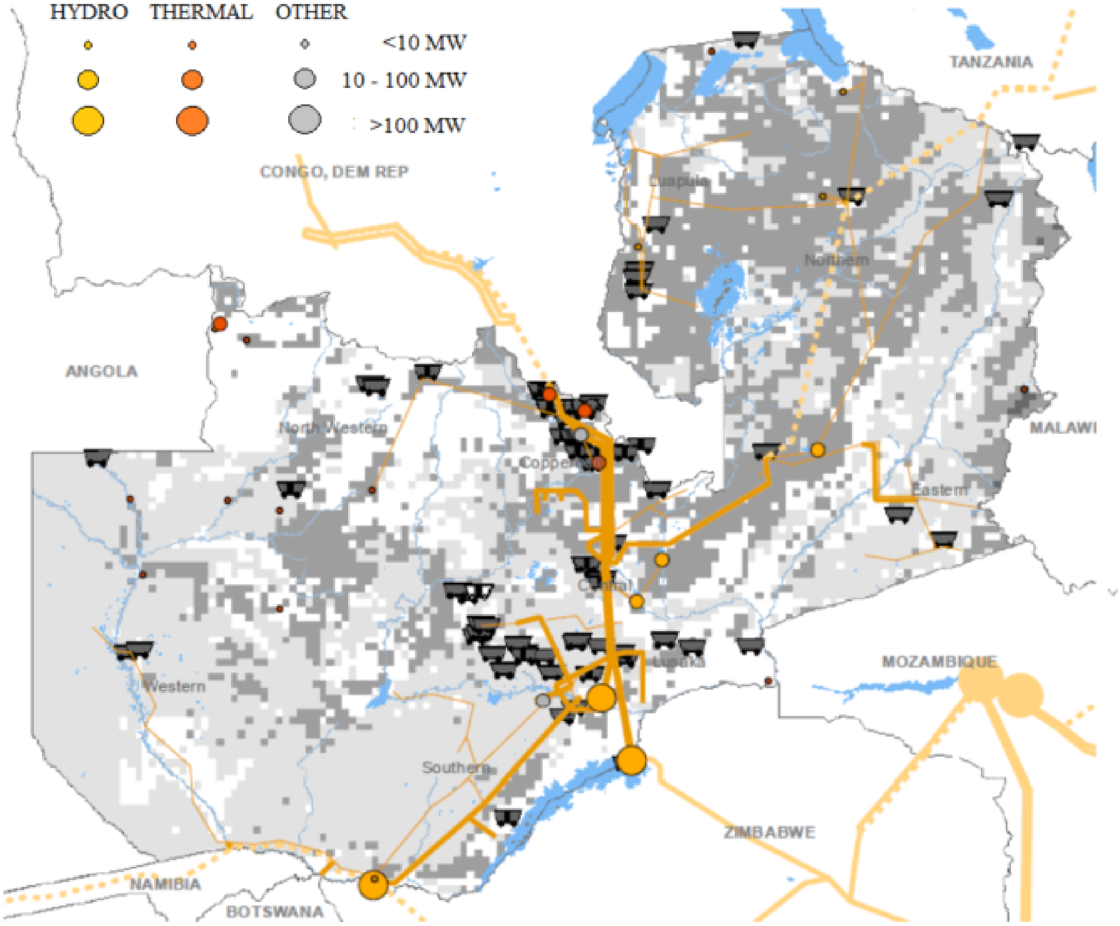

Figure 2.6: *Illustration of the transmission and installed capacity in Zambia. [1]*

Zambia has a relatively large percentage share of hydropower installed, even compared with Norway, see figure 2.7. It is estimated that there is about 6 000 MW of unexploited hydropower potential in the nation. Due to the large energy demand from the mining sector, Zambia has a large generation capacity and power consumption per capita compared to other Sub-Saharan nations. The hydro resources allows the nation to produce electricity for approximately 0.08 USD/kWh. [1]

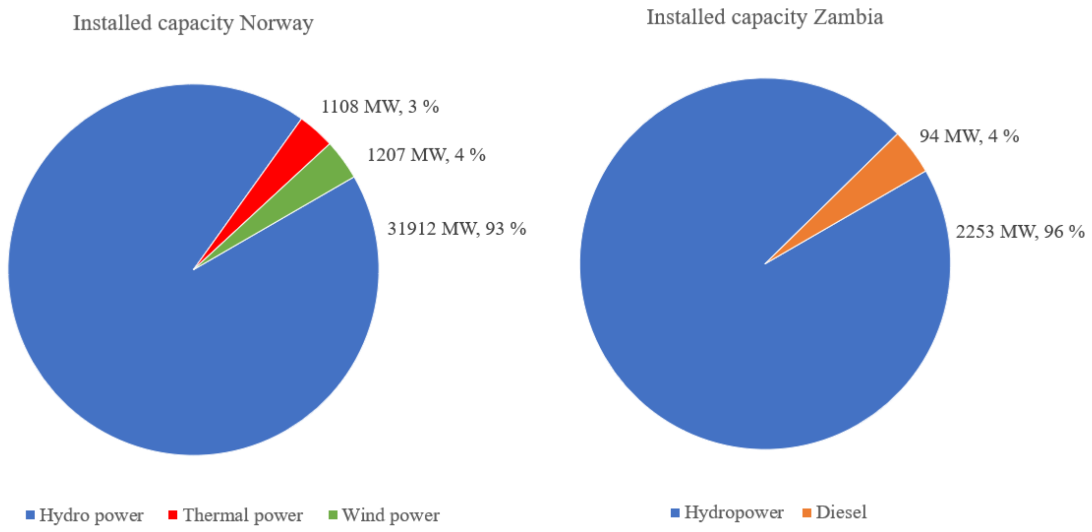

Figure 2.7: *Installed electricity capacity in Norway and Zambia. [14, 2]*

Although Zambia has mainly cost-effective hydropower, the power sector is being undermined by even lower power tariffs, at 0.03–0.04 USD/kWh. The power sector in Zambia is mainly living on past investments, and the groundwork is not being facilitated for the future. [1]

The long-term power supply will be influenced by the regional power trading organization, Southern African Power Pool (SAPP), see attachment C for the companies involved. Especially the import of low-cost hydropower from the Democratic Republic of the Congo, which is around 0.014 USD/kWh. In the medium term, Zambia is facing a strategic choice of the investment distribution in the domestic expansion of renewable energy, the construction of new thermal power stations or expanding the cross-border interconnectors and transmission. [1]

There are multiple challenges to face, especially regarding electricity access and power stability. Only 3.5% of the rural population have access to electricity, but make up the majority of the population. Those who have access to electricity often experience load shedding and numerous blackouts throughout the year. [1, 13]. Table 2.2 shows the power status in 2010.

Table 2.2: *Electric power industry status in Zambia. [1, 2]*

Status in Zambia (2010)		
Installed power-generation capacity	[MW/mill. people]	154.9
Installed electrical production	[MW]	2 347
Yearly power consumption	[kWh/capita]	771.0
Power outages	[Day/year]	49.8
Access to electricity	[%]	20.1
Urban access to electricity	[%]	50.0
Rural access to electricity	[%]	3.5
Growth access to electricity	[%/year]	0.3
Transmission losses	[%]	12.0

The time period from September to December, 2015, the nation experienced a major power deficit due to shortage of rainfall in the 2014/2015 rainy season. The deficit varied between 560 and 1 000 MW. This resulted in frequent load shedding, often eight hours per day. [13]

In Zambia, the main electricity supplier is the state-owned Zambia Electricity Supply Corporation (ZESCO) who is responsible for over 80% of the electricity consumed in the nation. Private companies in the electricity sectors includes the Copperbelt Energy Corporation (CEC), Lunsemfwa Hydro Power Company (LHPC), Zengamina Power Company Ltd (ZPC) and North Western Energy Corporation (NWEC). [15, 16, 17])

2.2.2 Transportation

Road

Three-quarters of the primary and secondary road network, which connects the most important cities, mining facilities and border crossing points, are paved and in good condition. Heavy-duty trucks are vital for Zambia's mineral-based economy and are the most competitive for large bulk copper transportation in the nation. The allocation of resources is enough to maintain and improve the primary and secondary road networks. Only 21 % of the rural network is in good or fair condition. [1]. See figure 2.8 for an illustration of the road network.

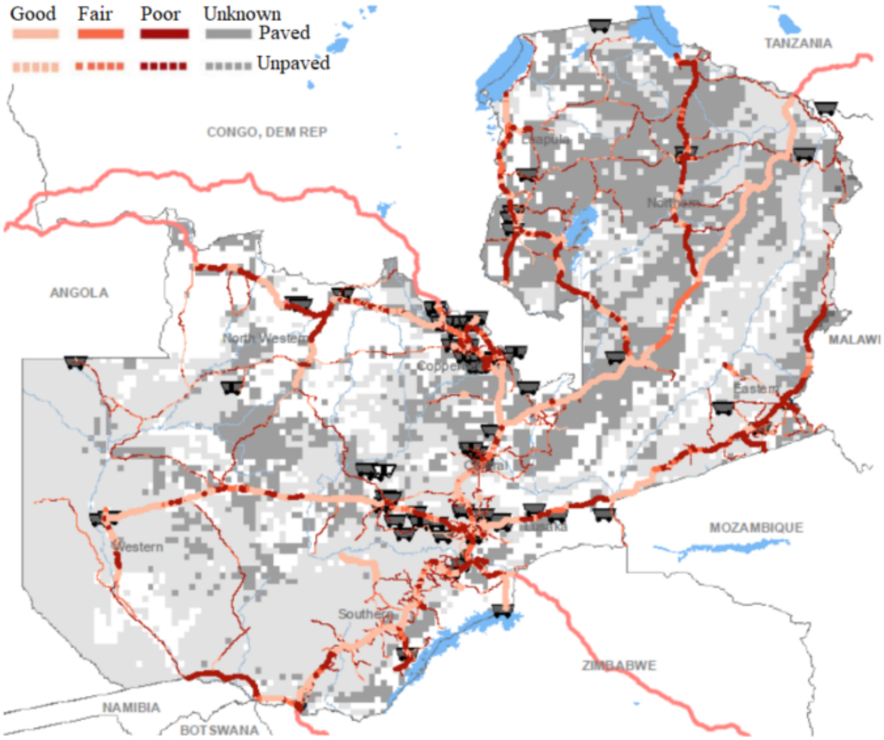

Figure 2.8: *Illustration of the road infrastructure in Zambia. [1]*

Rail Road

The railroad infrastructure is not the most cost-competitive for large bulk copper transportation. The reason for this is neglect in the maintenance of the railroad. The average speed from Lusaka to Ndola is 15 km/h. There are currently two operators: The Railway Systems of Zambia (RSZ) and The Tanzania and Zambia Railway Authority (TAZARA). The RSZ serves the north-south and TAZARA operates an eastward route. Due to delays associated with clearance, rail quality, loading, access rights and technical difficulties the transport of goods from the DRC border, to the port of Durban, South Africa, a journey of 3 000 km, takes 38 days to complete, 9 days of travel and 29 days of delay.[1]

Aviation

The domestic air transport is modest and is a fraction compared to neighboring countries such as Angola, Mozambique, and Tanzania. Although the domestic air transport is modest, Lusaka has good inter- African connectivity, and the Zambian air traffic is increasing, due to investment from foreign aviation companies.[1]

2.3 Economy

After the millennium change, and the following decade and a half, Zambia experienced substantial economic growth. With an average of 6.7 % increase in GDP per year, this was mainly due to an increase in international copper prices. The copper industry is the backbone of the Zambian economy. Figure 2.9 shows the distribution of export products in 2014. Where 77 % of all the exports were copper. In 2014 the total exports was 12.6 billion USD, and imports was 9.6 billion USD. Which results in a positive trade balance of 3 billion USD. [18]

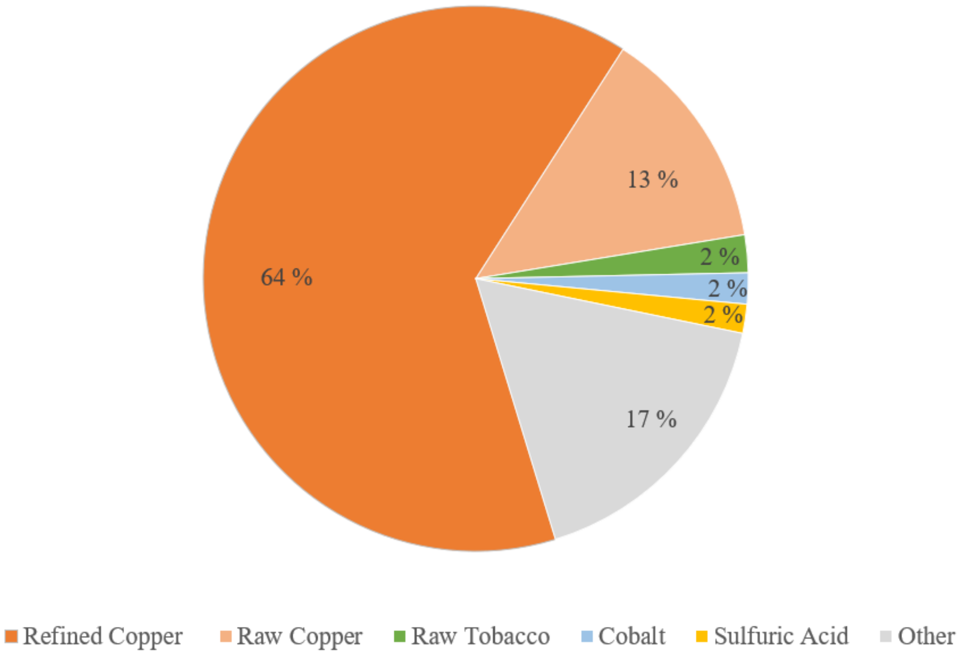

Figure 2.9: *The export distribution in Zambia (2014). [18]*

Zambia experienced major economic setbacks in 2015. In 2014 the Zambian GDP was 27.1 billion USD, while in 2015 it declined to 21.2 billion USD. The decline was due to multiple reasons. After the election in 2015, the rise in expenditure, fiscal deficit, decrease in copper prices and nationwide electricity shortage was the main reasons for the major economic setback. It seems that the economy has stabilized, with an increase in GDP of 4.1 % in 2017 and 4.0 % in 2018. The medium outlook remains positive, but this could change quickly. The nation is highly vulnerable to fluctuations in both: international copper prices and weather conditions. Because of the reliance on hydropower and climate, the seasonal rainfall directly dictates electricity and agricultural production in the nation. [18, 19]

Incentives

Over the last two decades, there have been some regulatory reforms and the development of private sector incentives programs. This was done to make Zambia more attractive and streamlined for businesses. The Zambia Development Agency (ZDA) was established in 2006 by the parliament. The agency took over for five different mandated functions and made the processes of applying for permissions, exemptions, authorization, licensing, the establishment of companies more streamlined and efficient. [17]

In 2014, the Industrial Development Corporation (IDC) was instituted by the Minister of Finance. The corporation was established, so that the government could make more precise and long-term investments in conjunction with private investors, to create new industries. [20]

The following excerpt was posted by Enel, on the 20.06.2018:

"The Enel Group and Zambia's Industrial Development Corporation (IDC) signed today in Lusaka a financing agreement of around 34 million US dollars for the construction of the 34 MW Ngonye solar plant in the country. The financing involves senior loans of up to 10 million US dollars from the International Financing Corporation (IFC), a member of the World Bank Group, up to 12 million from the IFC-Canada Climate Change Program and up to 11.75 million from the European Investment Bank (EIB)"[21]

The following excerpts were posted on zambiareports.com, the 11.03.2019:

"President Edgar Lungu has commissioned the 54 megawatts solar power plant, Zambia's largest renewable energy project constructed at a cost of $60 million."[22]

"The project represents a total investment of $60 million, $39 million of which were contributed by the International Finance Corporation and the Overseas Private Investment Corporation."[22]

There are currently no specific hydrogen storage infrastructure in Zambia, but there are emerging organizations in the Sub-Saharan region that are looking promising for the hydrogen expansion. Especially The African Hydrogen Partnership Association (AHP).

Excerpt found on their website, (accessed the 19.05.2019)[23]:

"AHP will:

1. *Initiate and support economically and commercially feasible programs that combine large scale Power-to-Gas/Hydrogen (P2G) and Hydrogen (H_2) Fuel Cell (FC) applications.*
2. *Form strategic alliances, consortium's and syndicates with the strongest partners from business, industry, finance, governments, research and science.*
3. *Connect with supranational organizations to implement hydrogen strategies."*

3 Photovoltaics

A photovoltaic (PV) cell consists of semiconductors that react with the sun's incoming energy, called photon. When the photon is absorbed by the PV-cell, an electric current forms through whats called the photovoltaic effect.[24]

3.1 Solar Irradiation

Our sun releases a large amount of energy every second, a portion of this is reaching the earths atmosphere, on average 1367 W/m^2. Some of this energy is reflected and absorbed by the atmosphere, while the rest of the energy is distributed unevenly across the earth's surface, as seen in figure 3.1.[25].

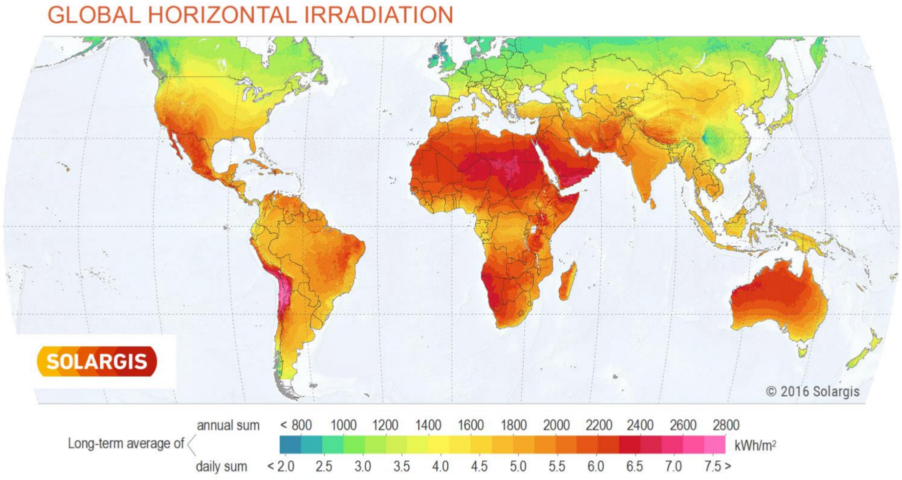

Figure 3.1: *World long-term average GHI.[26]*

The variation in sunlight hitting a regions surface depends on the time of day and the earths rotational axis, as this affects the hours of sunlight. The climate, mainly cloud formation and regional air pollution affects the amount of solar irradiation available to produce photovoltaic energy.[25]

The total solar irradiation reaching the earths surface, horizontal to the ground is called Global Horizontal Irradiation (GHI). The GHI consists of Direct Normal Irradiance (DNI) which is the radiation that comes in a straight line from the suns direction, and the Diffuse Horizontal Irradiance (DHI) which is the radiation scattered by particles in the atmosphere. A tilted PV module receives additional irradiation reflected by the ground. This reflection effect is referred to as the Albedo. [27] An illustration of the this can be seen i figure 3.2 and figure 3.3.

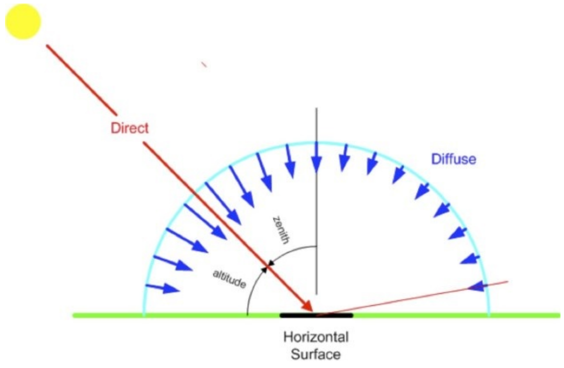

Figure 3.2: *Solar irradiation on a horizontal module.[28]*

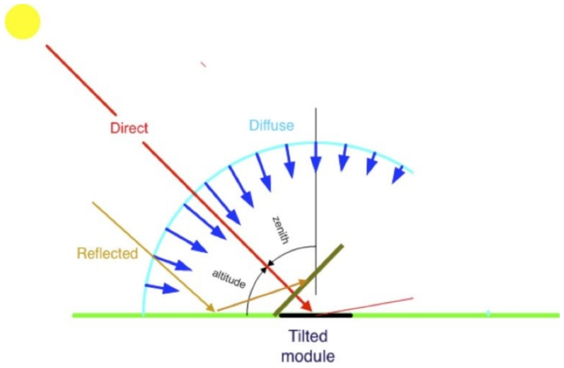

Figure 3.3: *Solar irradiation on a tilted module.[28]*

3.2 Operational Principle

A PV-cell consists of two layers of silicon. A layer that is negatively doped (N-type) and a layer lying below, which is positively doped (P-type). When the two layers are combined a PN-junction (Depletion zone) forms between the layers. The energy of the solar irradiation (photon) penetrates the negative layer and hits the PN-junction. This results in a potential difference between the layers, and an electron is freed. When connected to an external circuit the electrons will generate electrical current. The voltage that occurs can then be utilized as a DC power source. This is illustrated in figure 3.4.[29]

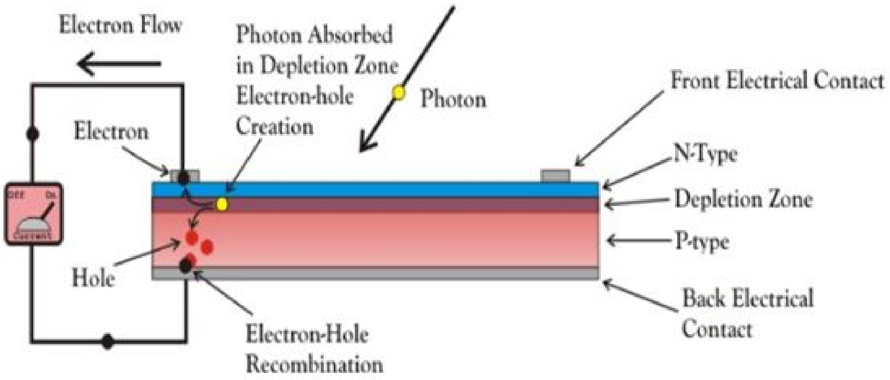

Figure 3.4: *A principle sketch of a PV-cell.[30]*

Nominal power rating of a solar module is determined at STC. Which equals a temperature of 25°C, irradiation of 1 000 W/m^2 and air mass (AM) of 1.5. The nominal power is denoted as watt peak (Wp) [31, 32]. The theoretical efficiency of a PV cell is about 33%. Silicon has a band gap of 1.12 electrol volts, if a photon has higher or lower energy than the band gap, it is absorbed as heat by the PV-cell. [24] The effect of temperature on a PV-cell can be seen in the I-V characteristic figure in appendix D.

A single cell can provide an open circuit voltage of 0.5-0.6 V at 25° C. Cells are connected in series-parallel configuration to form modules (panel). This is commonly done to achieve outputs of 12 V, 24 V or higher. Modules can be combined in multiple ways, the most common is in series (string) to form an array, as seen in figure 3.5. A PV system usually consist of multiple strings. [33, 34]

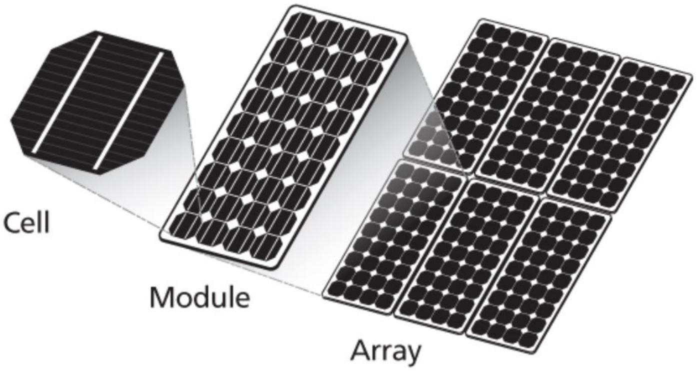

Figure 3.5: *Difference between: cell, module and array.[35]*

3.2.1 Converter

By implementing a DC-DC converter with a PV-system the voltage level can be transformed to a desirable value matching the DC load requirement. Converters can also include a Maximum Power Point Tracker (MPPT). This is to reduce the mismatched output from individual modules in a PV-system, due to the variation of environmental conditions such as solar irradiation, shading, temperature, etc.[32]. DC-DC converters can reach approximately 90% efficiency, dependent on temperature and rated output power[36], shown in figure 3.6.

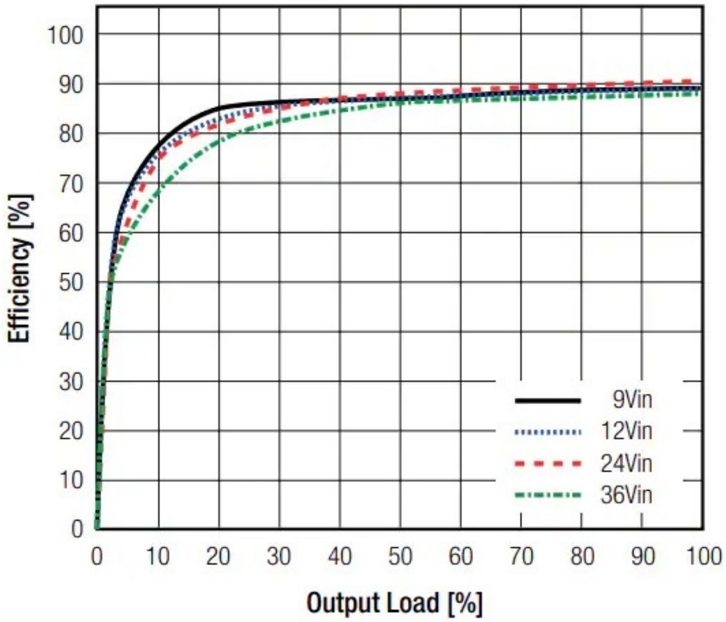

Figure 3.6: *Efficiency vs load characteristics for RECOM Power REC15E-Z Series DC/DC Converters.[36]*

3.2.2 Inverter

If a PV-system is connected to the grid or is to supply a household that uses AC-current, a DC-AC inverter is utilized, in order to convert DC-current from the PV-system into AC-current supplying the electrical load. A DC-AC inverter can typically reach 95% efficiency dependent on the DC-voltage, the rated AC output power and temperature. This is shown in figure 3.7. [37]

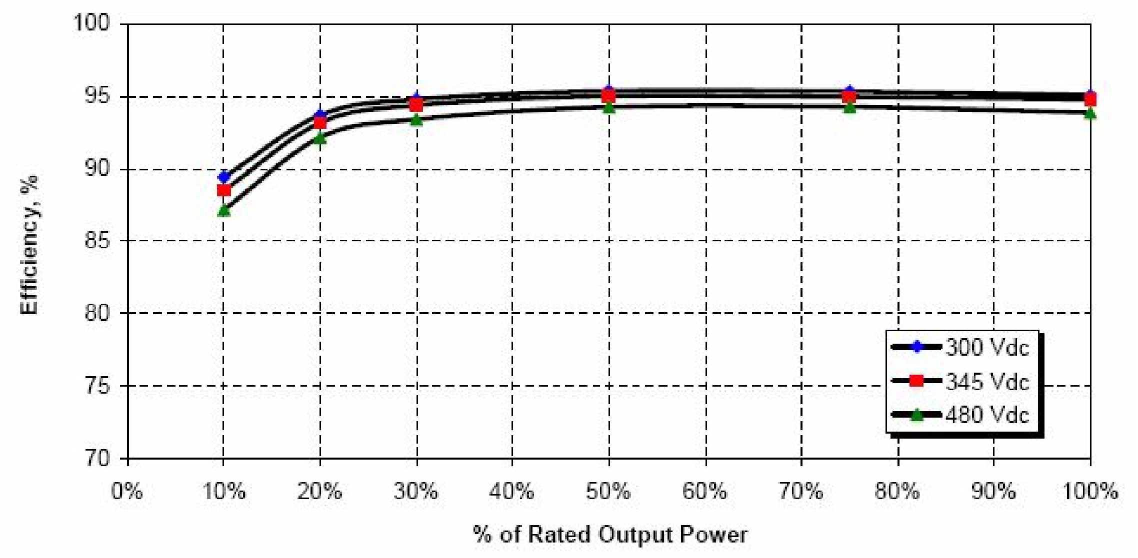

Figure 3.7: *Efficiency versus load characteristics for inverters.[37]*

3.3 Solar Energy Technologies

The most commonly used PV technology is crystalline silicon (c-Si) and thin-film solar cells (TFSC).[38]

3.3.1 Crystalline Silicon (c-Si)

Silicon is the main element present in a solar panel, about 90% of all solar panels are made up of silicon. There are several different types where the main difference is the degree of purity achieved by the production method. High precision is required when achieving high purity and is considered an expensive process. The efficiency is directly related to the degree of silicon purity. The c-Si is mainly divided into mono- and poly-crystalline solar cells (wafers).[38]

Monocrystalline solar cells are made of silicon ingots which are cylindrically shaped due to the Czochralski process when cutting into wafers, there is a relatively high amount of waste which increases the production cost. While the polycrystalline silicon is melted from raw silicon and cast into quadratic shapes. Cutting the quaderatic silicon into wafers will result in less production waste compared to the cylindrical monocrystalline, and a cheaper product. The visual difference of mono- and polycrystalline can be seen in figure 3.8.[38]

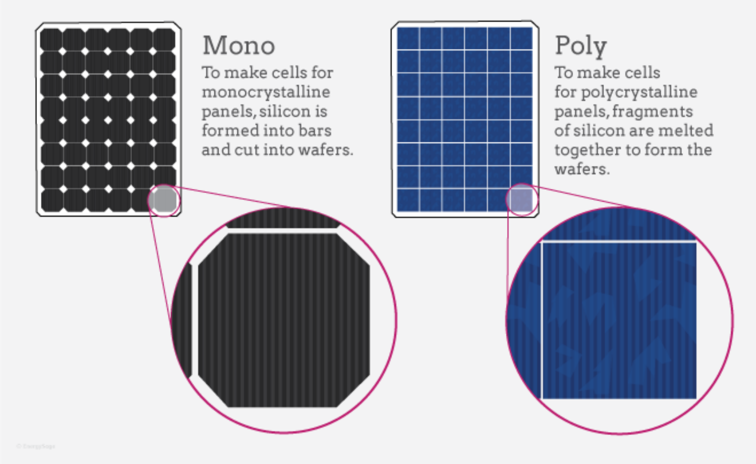

Figure 3.8: *Space utilization and appearance differences in PV-modules.[39]*

The standard warranty of c-Si is 25-years, however life expectancy can reach 40-50 years, with an approximated degradation rate of 0.5%/year.[40, 41]

Monocrystalline Silicon Solar Cell

Has the highest purity of the PV technologies and are made of single-crystal silicon. The efficiency is typically about 15-20%. The high degree of purity contributes to the long lifetime relative to other PV cells. They also work better in low light conditioning, when a cell is partially covered eg due to shade, snow or sand. The efficiency of the PV-cell is reduced at high temperatures, but monocrystalline is less affected then a polycrystalline.[38]

Polycrystalline Silicon Solar Cell

Has a lower heat tolerance and therefore has a lower life expectancy and performance at high temperatures than monocrystalline. Because of a lower degree of silicon purity, efficiency is often around 13-16%. [38]

3.3.2 Thin Film Solar Cell

TFSC is made up of several sub-technologies, amorphous silicon (a-Si), cadmium telluride (CdTe), copper indium gallium selenide (CIS/CIGS) and organic photovoltaic cells (OPC). The efficiency of TFSC is around 7-13% dependent on the technology. As a result of the simple mass production methods, thin-film modules are cheaper than crystalline-based modules. Because of the lower efficiency, TFSC requires more space to achieve similar nominal power as the crystalline-based modules. As a result of this, the cost of support structures, cables, etc, increases. TFSC also has an increased degradation rate (≈1%/year)[41], which leads to shorter lifetime and manufacturer warranty.[38]

3.4 Solar Tracking

The Earth rotates once on a daily basis and has one rotation around the sun per year. These rotations will cause variations in the angle of DNI relative to a solar cell. To harvest the maximum amount of solar irradiation, the PV-module can be positioned normal relative to the DNI by tilting the module or utilizing a solar tracking system. Figure 3.9 shows the different terminology regarding the suns position.[42]

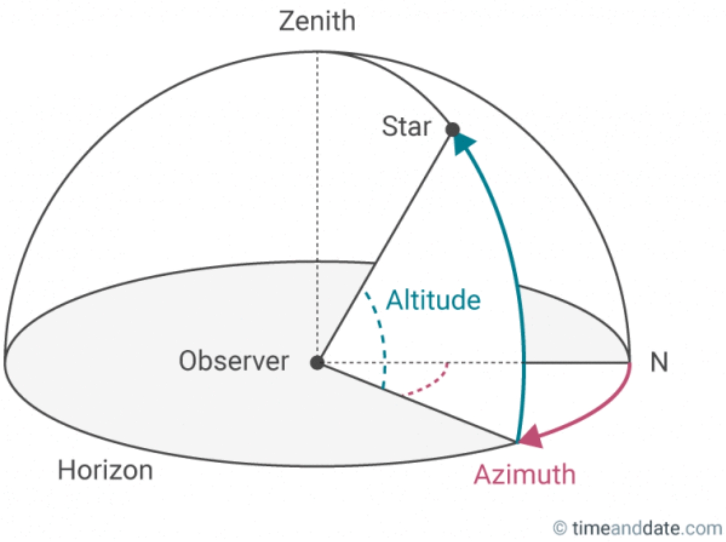

Figure 3.9: *Illustration of the terminology regarding the suns position.[43]*

As the earth rotates around the sun, environmental conditions vary throughout the year due to the solar altitude. Which is caused by the tilt of the Earth's rotation axis (23.4°) [42]. Since the solar altitude only varies a small amount on a day-to-day basis, it may be sufficient to have a fixed tilt on the east-west axis, or to manually adjust this angle 2-4 times a year, since an automatic control system is costly.[44]

To get the optimal configuration, it may be cost-effective to adjust the azimuth angle by installing a single-axis tracking system for the north-south axis. By keeping the DNI normal on the solar cell throughout the day solar energy production can be increased by 25-35%. While a dual-axis tracker adjusts both east-west and north-south, will yield an additional 5-10% increase in energy production compared to single-axis tracking. Trackers are often used in commercial or industrial applications (>1 MW), due to the high investment and an increase in maintenance cost. It can also be suitable for high altitude installations because of the sun's altitude relative to the horizon. [44]

3.5 PV Economics

The total cost of a PV-system is highly dependent on the region, and the size of the project due to the economics of scale. From NREL's "U.S Solar Photovoltaic System Cost Benchmark: Q1 2017" the benchmark assumption is divided into three categories, residential, commercial and utility-scale. Description and the range for each one are presented in table 3.1. [45]

Table 3.1: *PV benchmark assumptions from NREL. [45]*

PV Sector	Description	Size [MW]
Residential	Residential system	0.003 - 0.01
Commercial	Commercial rooftop system, ballasted racking	0.01 - 2
Utility scale	Ground-mounted system, fixed-tilt and one-axis tracker	>2

The benchmark is based on the installed cost which represents the value paid to the developer and installer. It does not take into account any supply agreements or other contracts. The costs of an utility-scale system is presented in figure 3.10. [45]

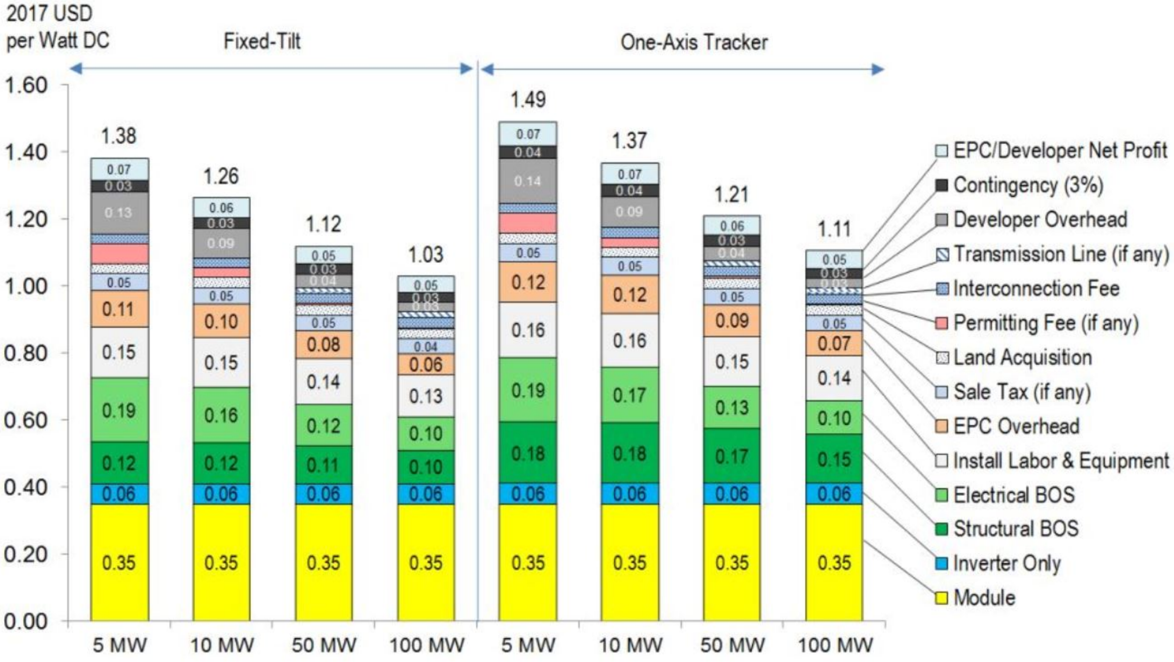

Figure 3.10: *Total cost of PV-system with fixed tilt and one-axis tracker, on an utility-scale. [45]*

According to a report published by the International Renewable Energy Agency (IRENA) in 2016, the global weighted average cost of electricity could decrease with 59% for photovoltaics between 2015 and 2025. [46]

4 Hydrogen Production

The world's total energy consumption in 2016 was approximately $400 \cdot 10^{18}$ joules. About 3% of this energy was used to produce hydrogen. Pure hydrogen does not exist naturally in any meaningful quantities since it reacts easily with other substances. It has to be separated from other chemical components. This is the reason why hydrogen is called an energy carrier, and not an energy source. [3]

Approximately 90% of all hydrogen produced (2017), is used as a chemical component in industrial applications such as ammonia production, methanol production and in oil refineries. Most of this hydrogen is produced for use in industry. About 96% is produced on-site for on-site consumption, and only 4% are available for marked trading. A small percentage of the world's hydrogen consumption ($\approx$ 1000 tonnes or 0.002%) is currently used in hydrogen vehicles. However, this is an increasing sector. The hydrogen vehicle capacity, delivered per year, for transport applications increased from 37 MW in 2014 to 456 MW in 2017. This is more than a tenfold increase in the annual delivered capacity.[3]

Although the world's consumption of hydrogen as a chemical component in industrial applications is expected to continue to grow, hydrogen has started to receive attention as an energy carrier for reducing greenhouse gas emissions[3]. The most common production methods are water electrolysis, steam reforming of natural gases or gasification of hydrocarbons in coal. [47] Figure 4.1 shows different hydrogen cycles.

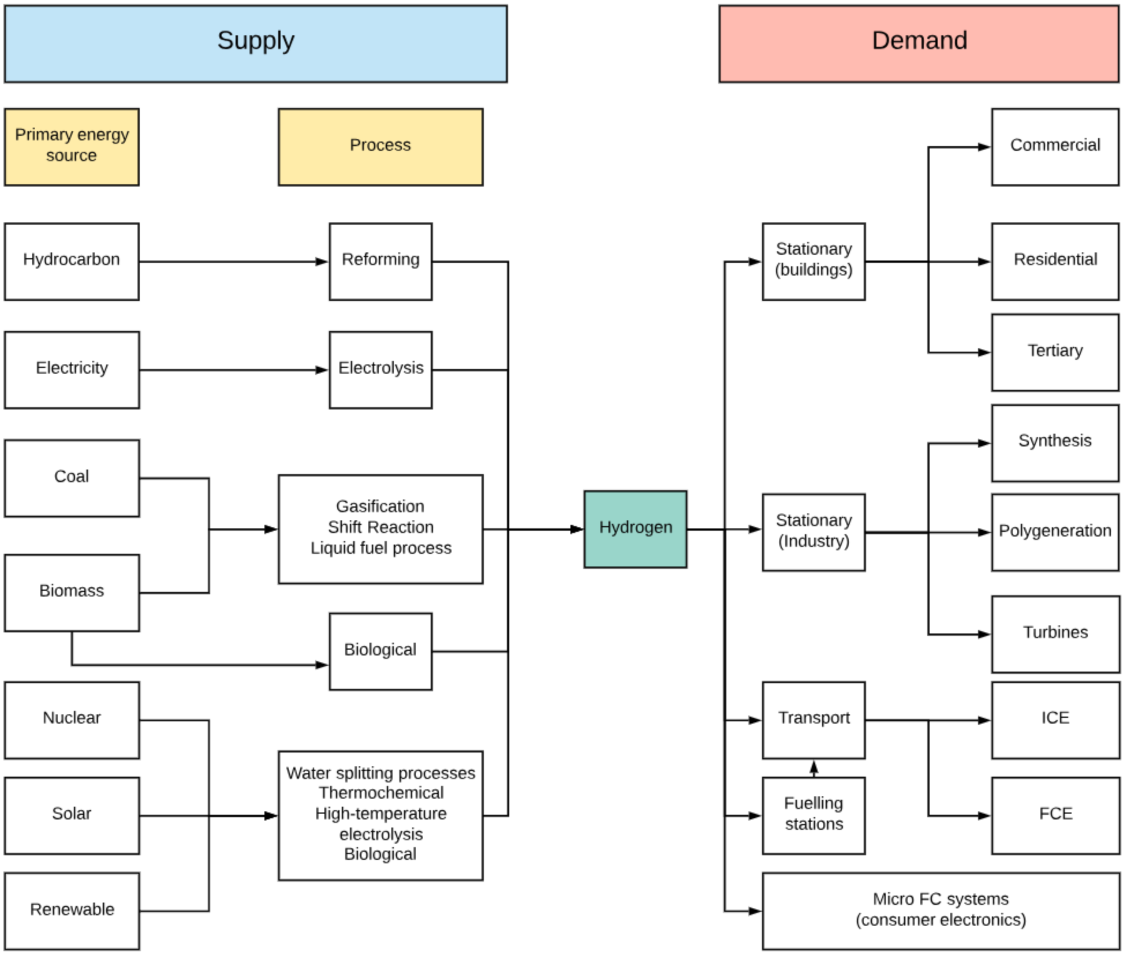

Figure 4.1: *A flowchart of the hydrogen cycle.* [4]

One of the major challenges with solar power is the variations in production, that does not necessarily vary with the demand. The implementation of hydrogen storage could help solve this issue. Through hydrogen water electrolysis coupled with clean solar power, large quantities of hydrogen could be produced and stored. With the use of a fuel cell, the chemical energy in the hydrogen could be released, and the only by-products being water and electricity. The process is quick, and consequently, it can help solve the problems with abrupt energy demand and intermittent renewable energy sources. [47]

4.1 Steam Methane Reforming

The most common way to produce hydrogen is through steam-methane reforming. About 95% of the hydrogen produced in the United States is through natural gas reforming. It's a mature technology that can utilize pre-existing natural gas pipeline infrastructure. [48]

The process uses high-temperature steam (700 – 1 000° C) which reacts with methane under pressure (3-25 bar). With the presence of a catalyst, this reaction produces hydrogen, carbon monoxide and small amounts of carbon dioxide. The process is endothermic, so a continuous supply of heat is required. The steam-methane reforming equation is described in equation 4.1 below. [48, 49]

$$CH_4 + H_2O + Heat \rightarrow CO + 3H \tag{4.1}$$

An additional process called "water-gas shift reaction" can be deployed to further increase efficiency. The carbon monoxide from the previous reaction can be used to produce more hydrogen and carbon dioxide. This is described in equation 4.2. [48, 49]

$$CO + H_2O \rightarrow CO + H + Heat \tag{4.2}$$

If the end carbon is captured, this technology can be deployed to reduce the carbon footprint of current facilities that utilize natural gas. Steam reforming can be deployed to produce hydrogen from other fuels, such as ethanol, propane, ammonia or gasoline. [48, 49]

4.2 Water Electrolysis

Water electrolysis is the definition of decomposing water molecules H_2O into hydrogen H_2 and oxygen O_2. This is done by separating two electrodes with an ionic-conducting electrolyte and apply an electrical potential across the electrodes. The potential will create a hydrogen evolution reaction (HER) at the negative cathode and an oxygen evolution reaction (OER) at the positive anode. The total reaction is represented in equation 4.3. [50]

$$H_2O_{(l)/(g)} + Energy \rightarrow H_{2(g)} + \frac{1}{2}O_{2(g)} \tag{4.3}$$

.

4.2.1 Thermodynamics

The thermodynamic energy can be classified into reversible and irreversible energy. Reversible energy in a chemical reaction is referred to as the change in Gibbs free energy (ΔG). ΔG is the theoretical minimum energy required to decompose a water molecule into hydrogen and oxygen, and is often referred to as the lower heating value (LHV) at standard temperature and pressure (STP). [51, 52]

Irreversible energy changes linearly with temperature (T), as the temperature increases to the transition phase from liquid to gaseous state a change in entropy (ΔS) occurs. Change in enthalpy (ΔH) includes both reversible and irreversible energy and is the minimum energy required for water electrolysis also called the higher heating value (HHV). The thermodynamic connection is seen in equation 4.4. [51, 52]

$$\Delta H = \Delta G + T\Delta S \tag{4.4}$$

The minimum theoretic potential is expressed from Nernst's equation and is dependent on Faraday's constant ($F = 96485\frac{C}{mol}$) and the number of electrons ($z = 2$). Calculation for the reversible potential for water decomposition (V_{rev}) and the thermo-neutral potential (V_{enth}) which is the ideal potential for electrolysis is presented in equation 4.5 and 4.6 respectively. [52]

$$V^{\circ}_{rev} = -\frac{\Delta G^{\circ}}{zF} \tag{4.5}$$

$$V^{\circ}_{enth} = -\frac{\Delta H^{\circ}}{zF} \tag{4.6}$$

At STP the reversible potential is $1.23V$, the process is endothermic and therefore requires energy. If deviations from the STP is present reversible potential changes as described in Nernst's equation 4.7. [51]

$$V^{rev} = V^{\circ}_{rev} - \frac{RT}{zF} ln\left(\frac{p_{H_2}\sqrt{p_{O_2}}}{p_0^{3/2} a_{H_2O}}\right) \tag{4.7}$$

V^{rev} = Reversible potential [V]
V°_{rev} = Reversible potential (STP) [V]
R = Universal gas constant (8.314) $\left[\frac{J}{K\cdot mol}\right]$
T = Temperature [K]
F = Faraday's constant 96 485 $\left[\frac{C}{mol}\right]$
z = Number of electrons
p = Partial pressure, subscript denotes element [Pa]

At STP (1.23V) the theoretical energy consumption rate (ΔG) is 2.94 kWh/Nm^3 H_2 or 32.7kWh/kg H_2. It decreases with increasing temperature as illustrated in figure 4.2. In reality, the potential used by industry lies approximately between 1.8-2.6V due to the kinetics and resistance in the electrolyzer cell.[52]

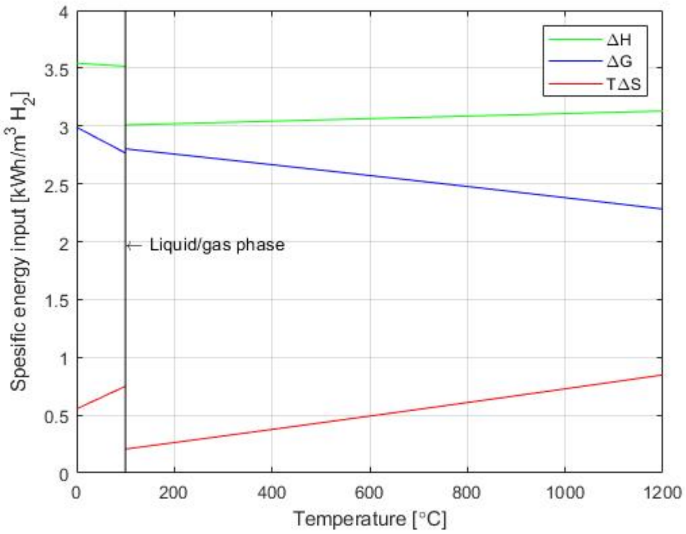

Figure 4.2: *Water decomposition, energy consumption versus temperature. [52]*

4.2.2 Kinetics and Resistance

As the applied cell voltage of an electrolysis cell is greater than the reversible potential. The overpotential (η) at the anode and cathode, and the total ohmic potential ($r_{tot}j$) has to be taken into consideration, shown in equation 4.8. The energy required to overcome the overpotential is highly dependent on the electrocatalytic properties of the electrode material.[53, 52]

$$V^{cell} = V^{rev} + |\eta_A| + |\eta_C| + r_{tot}\, j \tag{4.8}$$

V^{cell} = Cell potential [V]
V^{rev} = Reversible potential [V]
η_A = Anodic/Oxygen overpotential [V]
η_C = Cathodic/Hydrogen overpotential [V]
r_{tot} = Total ohmic resistance $[\Omega \cdot cm^2]$
j = Current density $\left[\frac{A}{cm^2}\right]$

Overpotential/kinetics can be described as the activation loss occurring at the electrode surfaces due to the chemical reactions. The magnitude of the activation loss is affected by the absorption of reactant molecules, electron transferred through the membrane and the electrode itself. The overpotential is described by the Tafel equation 4.9.[54, 50]

$$\eta = a + b \cdot log[j] \tag{4.9}$$

The total losses due to ohmic resistance from the membrane r_{mem}, the electrolyte r_{ele}, the bubble formation at the electrode r_{bub} and the circuit r_{cir} contributes to increase in the actual potential, as seen in equation 4.10.[52] Figure 4.3 shows an electric equivalent circuit for an electrolyzer cell.

$$r_{tot}j = j \cdot (r_{mem} + r_{ele} + r_{bub} + r_{cir}) \tag{4.10}$$

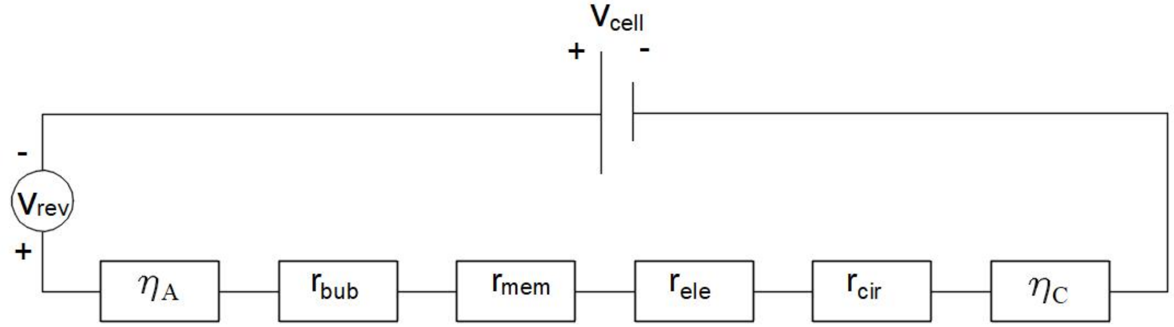

Figure 4.3: *Equivalent circuit of an electrolyzer cell.*

4.2.3 Water Supply

Steady water supply for water electrolysis is important for mainly two reasons: feedwater for hydrogen production and cooling water for the overall system. [55]

Feedwater
The feedwater in an electrolyzer has to be free of undesired particles, contaminants and objects that could harm or contaminate the cell. The presence of undesirable conducting material in an electrolysis cell could lead to less efficiency or short-circuiting of the cell. The water has to undergo a purification process before it is introduced to the cell. Some of these processes are mentioned in table 4.1. [55]

Table 4.1: *Different water purification processes.[55]*

Process	Technique
Physical	Filtration, sedimentation and distillation
Biological	Sand filters and biologically active carbon
Chemical	Flocculation and chlorination
Electromagnetic radiation	Ultraviolet light

Cooling water
Multiple components require specific temperature ranges to operate optimally. Water as a cooling medium is an effective means to do so, especially compared to air, due to the high specific heat capacity of water, see table 4.2. If a facility is located close to an area where natural cooling water is accessible, this will help reduce the overall cost of the facility. [56]

Table 4.2: *Specific Heat Capacity, water and air, at 25°C. [57]*

Specific Heat Capacity		
Water	[kJ/kg°C]	4.184
Air	[kJ/kg°C]	1.020

4.3 Electrolyzer Technologies

For commercial use, there are two main types of electrolyzers: alkaline water electrolyzer (AWE) and proton exchange membrane water electrolyzers (PEMWE) [50]. There are also different emerging technologies that look promising in the field, such as solid oxide water electrolyzer (SOWE) and molten carbonate water Electrolyzer (MCWE) [58]. The next section presents a more detailed explanation of the different technologies mentioned. In table 4.3 some key values are presented for the different technologies.

Table 4.3: *Comparison between electrolysis technology. [58, 59]*

		AWE	**PEMWE**	**SOWE**	**MCWE**
Maturity		Mature	Commercial	Demonstration	-
Stack lifetime	[hours]	60 000-90 000	20 000-60 000	<10 000	-
System response		Seconds	Milliseconds	Seconds	-
Cell voltage	[V]	1.8 - 2.4	1.8 -2.2	0.7-1.5	-
Current density	[A/cm^2]	0.2-0.4	0.6 -2.0	0.3 -2.0	-
Temperature	[°C]	60 - 80	50 - 80	600 - 900	600 - 700
Consumption	[kWh/kg H$_2$]	53.4 - 70.1	54.2 - 90.4	26.9	-
Efficiency	[%]	56 - 73	48 - 65	90	90

4.3.1 Alkaline Water Electrolyzer

When an electrical potential is applied across the electrodes in the AWE, water decomposes into hydrogen (H_2) and hydroxide ion (OH^-). The positively charged anode attracts OH^- through the semi-conducting diaphragm, which is permeable to hydroxide ions and water molecules. As the covalent bond forms, gases escape the electrode surface. The anodic and cathodic half-cell reactions is presented in equation 4.11 and 4.12, respectively. The AWE uses an alkaline electrolyte (lye), most common a potassium hydroxide (KOH) solution which increases the ionic conductivity of OH^-.[60] The solution is also corrosive, which makes maintenance of the cell more demanding [61]. A schematic of AWE is presented in figure 4.4.

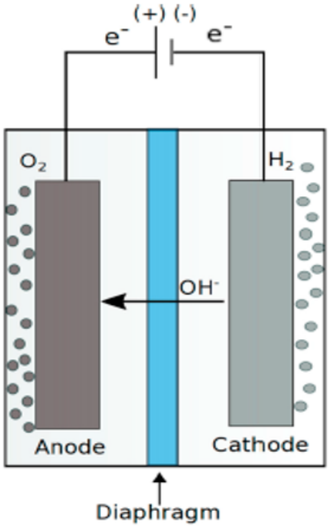

Figure 4.4: *Illustration of an Alkaline Water Electrolysis. [58]*

$$2OH^-_{(aq)} \rightarrow \frac{1}{2}O_{2(g)} + H_2O_{(l)} + 2e^- \tag{4.11}$$

$$2H_2O_{(l)} + 2e^- \rightarrow H_{2(g)} + 2OH^-_{(aq)} \tag{4.12}$$

AWE is a mature and well-tested technology. Although there are still some challenges to solve: low current density, low operating pressure and the limited ability to operate at low cell voltages. This would make the cell vulnerable to rapid fluctuations in input power. The limitations are due to the risk of gas molecules that could transfer through the diaphragm. The transfer of gas molecules will increase when the pressure at the cathode increases and the cell voltage decreases on the anode side. This could cause the presence of hydrogen in the oxygen stream. If the H_2 concentration is above 4% it could cause an explosion in the cell. [60]

4.3.2 Proton Exchange Membrane Water Electrolyzer

PEMWE uses a gas-tight polymeric membrane as the electrolyte, most commonly Nafion or Fumapem. The membrane has the properties to conduct positively charged hydrogen ions (H^+) from the anode to the cathode and to minimize the gas crossover. A covalent bond of hydrogen is formed when re-combined with electrons.[62] When the hydrogen bonding occurs, the hydrogen becomes neutrally charged. At the anode, oxygen is formed as a result. The layout for a PEMWE can be seen in figure 4.5. The anodic and cathodic half cell reactions can be seen in equation 4.13 and 4.14 respectively.

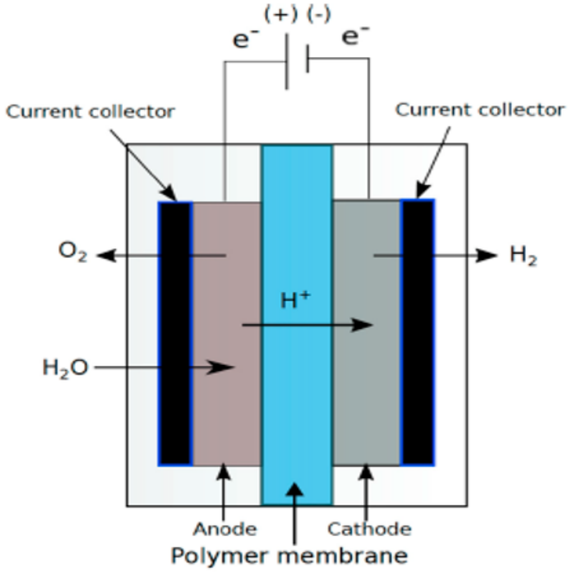

Figure 4.5: *Illustration of a Proton Exchange Membrane Water Electrolyzer. [58]*

$$H_2O_{(l)} \rightarrow \frac{1}{2}O_{2(g)} + 2H^+_{(aq)} + 2e^- \tag{4.13}$$

$$2H^+_{(aq)} + 2e^- \rightarrow H_{2(g)} \tag{4.14}$$

A PEMWE has a higher current density compared to AWE, which reduces the overall operational costs. The ohmic loss is dependent on the thickness of the membrane, which is often $\approx 20 - 300\mu m$ thick. It is desirable to have a thin membrane to reduce resistance, but thick enough to handle the desired operational pressure. Some commercial cells can achieve output pressures of 350 bar due to electrochemical compression. Electrochemical compression reduce or eliminate the energy demand for further compression. Low gas crossover through the membrane allows the PEMWE to operate in a wide area of power inputs. The membrane also allows protons to be transported quickly across, resulting in the cell to be able to respond to power input fluctuations. There is no delay by inertia as it would be in liquid electrolytes. [62]

The PEMWE have an high investment costs due to corrosion-resistant materials required to withstand corrosive environment (pH≈ 2), but also to withstand relatively high overpotentials ($\approx 2V$). Precious metals such as platinum, iridium, and ruthenium are mostly used as catalysts, current collectors and separator plates often use titanium-based metals. [62] The layout of the PEM is shown in figure 4.6.

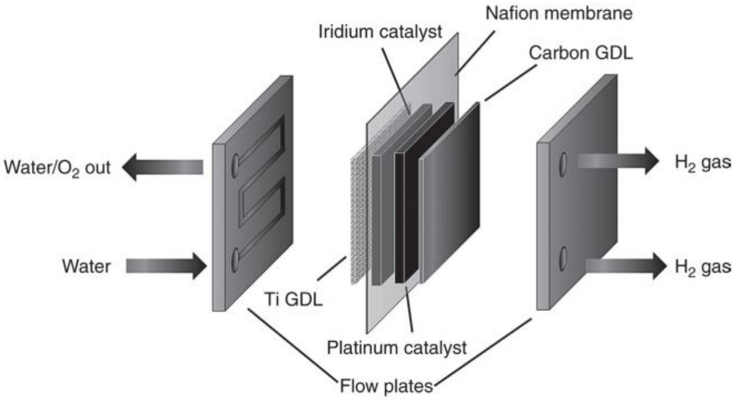

Figure 4.6: *Illustration of a Proton Exchange Membrane. [60]*

4.3.3 Solid Oxide Water Electrolyzer

SOWE differs from both PEMWE and AWE because of the high operating temperature required. Thermal energy must be supplied to achieve the necessary operating temperature. This energy is mainly compensated for, because the need for electrical energy decreases as the temperature increases. The total energy consumption is almost unchanged as the temperature rises. If the heat is supplied by thermal intensive industries, a high overall efficiency could be achieved, see table 4.3. [60, 63]

SOWE and PEMWE are similar in the way that both use a solid electrolyte to achieve ionic conductivity in the cell. The state of the art electrolyte for SOWE is the yttria-stabilized zirconia (YSZ). For the conductivity to be sufficient, this material requires high operational temperatures (≈1000°C). There are several problems associated with the high operating temperature in the cell, and these include integrity, long-lasting stability, interlayer diffusion, production, and material difficulties. Many studies have been conducted to find a suitable electrolyte, that has sufficient ionic conductivity at intermediate temperatures, to help solve some of the issues. [60, 63]

Figure 4.7 depicts the principle behind an SOWE cell. The half-cell reaction for the anode and the cathode is presented in equation 4.15 and 4.16 respectively. [52]

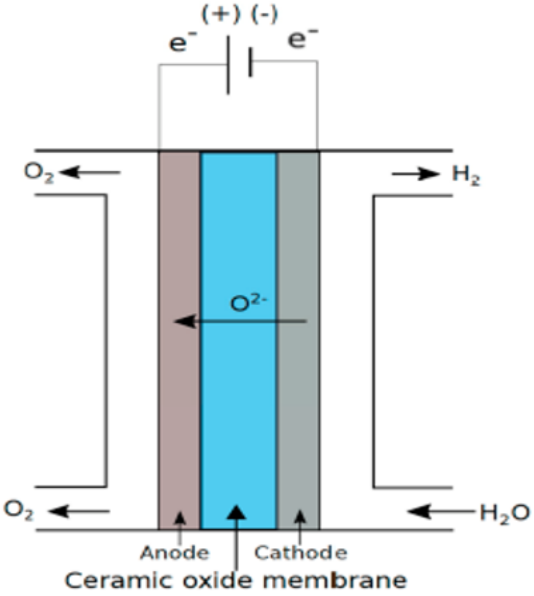

Figure 4.7: *Illustration of a Solide Oxide Water Electrolyzer. [58]*

$$O^{2-}_{(aq)} \rightarrow \frac{1}{2}O_{2(g)} + 2e^- \tag{4.15}$$

$$H_2O_{(g)} + 2e^- \rightarrow H_{2(g)} + O^{2-}_{(aq)} \tag{4.16}$$

4.3.4 Molten Carbonate Water Electrolyzer

MCWE uses nickel-based porous electrodes and a molten carbonate electrolyte, because of this, the cell has to have a high operating temperature to achieve sufficient ionic conductivity of oxygen. Figure 4.8 shows the principle behind an MCWE. It differs from other electrolysis cells in the way that carbon dioxide and water, must be present in the inlet portion of the cell. This is because CO_2 is a reactant when producing carbonate ions. The half-cell reaction for the anode and the cathode is presented in equation 4.17 and 4.18 respectively. [64]

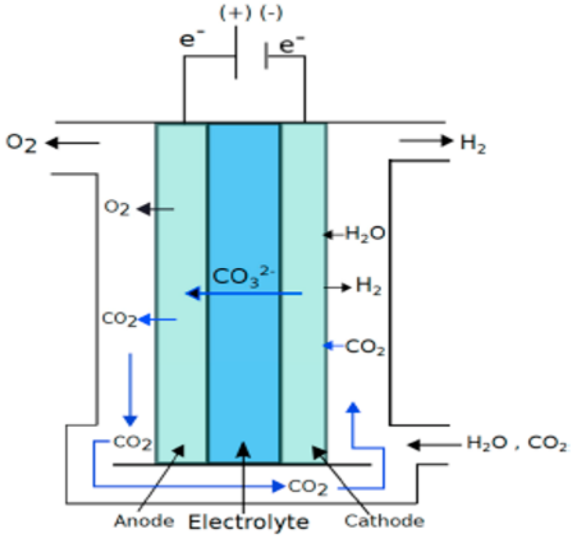

Figure 4.8: *Illustration of a Molten Carbonate Water Electrolyzer. [58]*

$$H_2O_{(g)} + CO_{2(g)} + 2e^- \rightarrow H_{2(g)} + {CO_3}^{2-} \tag{4.17}$$

$${CO_3}^{2-} \rightarrow \frac{1}{2}O_{2(g)} + CO_{2(g)} + 2e^- \tag{4.18}$$

MCWEs are generally used in large scale facilities, and have high a efficiency, as shown in table 4.3. With integrated combined heat and power (CHP), or combined cooling and power (CCP), overall efficiency's of 90 % can be achieved. [64] There are two main disadvantages to the MCWE:(i) loss of electrolyte and (ii) dissolution of the cathode. During operation, the electrolyte is consumed due to vaporization and corrosion. This results in a shorter lifespan for atmospheric systems. The cathode usually consists of nickel oxide, which is soluble with the electrolyte. This leads to nickel ions, which transfers to the anode. This could causes metallic nickel to precipitate in the electrolyte, leading to internal short-circuiting, and limit the lifespan of the pressurized systems in the electrolyzer. Many investigations are being carried out to fix the challenges associated with the particle carbonate composition. Mainly in cathode materials, modifying the present electrode and examining different carbonate compositions. [64]

5 Hydrogen Storage

Hydrogen has a low volumetric energy density at standard temperature and pressure (STP), see table 5.1. Hydrogen storage at moderate temperature and atmospheric pressure is therefore impractical for any industrial applications. [60]

Table 5.1: *Properties of hydrogen and diesel at STP (0°C and 1 atm). [4, 60, 65]*

		Hydrogen	**Diesel**
LHV	[MJ/kg]	119.96	42.6
HHV	[MJ/kg]	141.80	45.6
Density	[kg/Nm^3]	0.0899	0.846
Gravimetric energy density	[MJ/kg]	141.80	45.6
Volumetric energy density	[MJ/Nm^3]	10.7	360.4

5.1 Hydrogen Transformation

Hydrogen can be stored in gas-, solid- or liquid state. Hydrogen electrolysis delivers hydrogen in a gas state [4]. The industrial methods to increase the volumetric energy density of hydrogen are: [3]

- Compression to higher pressures.
- Cryogenic liquid storage (below -252.8° C at 1atmosphere).
- Metal Hydride Absorption
- Chemical conversion or mixture with a substance that is liquid or solid in moderate pressures and temperatures.

5.2 Compressed Hydrogen

Compression is a way to increase the volumetric energy density of the fuel. By pressurizing the hydrogen, the density will increase. In a gaseous state, hydrogen is usually stored in high-pressure tanks in the range of 300-700 bar. At 300 bar, the density of hydrogen is approximately 20 kg/m^3 at 700 bar the density is 40 kg/m^3. 700 bar is the pressure-specifications in hydrogen tanks used in most fuel cell cars. By combining pressurizing (1 000 bar) and low temperature (-60°C), densities above 60 kg/m^3 can be achieved. [3, 66]

These densities will make hydrogen competitive with fossil fuels, but the compression does demand energy. The compression from 1 to 30 bar will demand energy equivalent to 4-5 % of the original energy content for hydrogen. Compression to 350 or 700 bar will require an additional 4-8 % of energy. Therefore the trade-off between investment costs for adequate storage volume and costs associated with compression has to be considered. [3]

5.2.1 Piston Compressor

There is different wayw of supplying the force to a piston. The basic principle involving piston compression is to have suction through an one-way valve, then compress the substance and force it through another one-way valve, with the help of external force. This principle is shown in figure 5.1. [4]

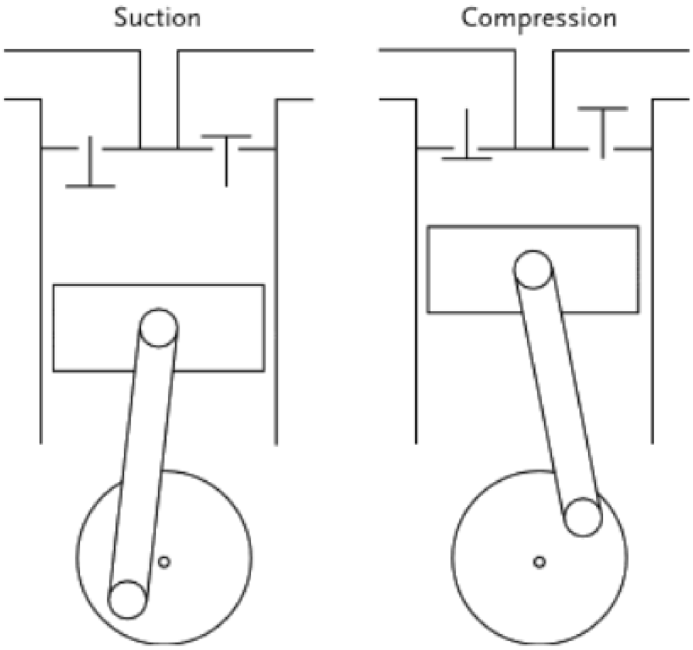

Figure 5.1: *Simple schematic of piston compression. [4]*

5.2.2 Diaphragm Compressor

A membrane-based compression has advantages compared to a piston based one. Especially that it is free of lubricants in the vicinity of the substance that is being compressed. This is very important when dealing with chemically pure or explosive gases. The principle is shown in figure 5.2. [4]

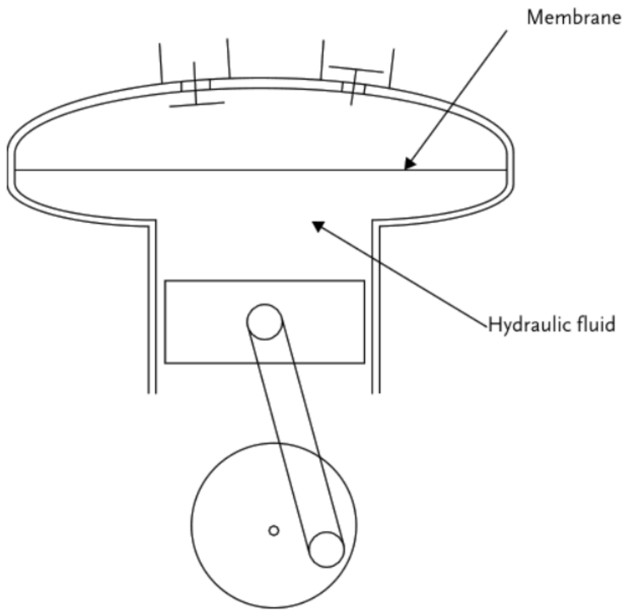

Figure 5.2: *Simple schematic of diaphragm compression. [4]*

5.3 Liquid Hydrogen

Another way to make hydrogen viable as an energy storage medium is through liquefaction. Hydrogen can be stored in liquid form which appropriate for larger volume transportation, or if liquid hydrogen is required by an end user. This is because such state conversion requires a lot of energy and is demanding to handle. One thing to note from table 5.2 is the small difference between the melting and boiling point of hydrogen. To achieve liquid hydrogen, it has to be cooled down to 20 K (1 atmosphere). [3, 4, 60]

Table 5.2: *Phase transition, hydrogen and water at 1 atm. [60]*

		Hydrogen	**Water**
Melting point	[°C]	-259.16	0
Boiling point	[°C]	-252.88	100

Liquid hydrogen has an energy density of 71 kg/m^3, which is substantially higher compared to compression at room temperature. The energy requirement to cool down hydrogen, is between 25-35 % of the original energy content of the hydrogen. [4]

The main issue in liquid hydrogen storage is evaporation. This could result in evaporation loss of 0.03-2% per day of the original volume. This is an important factor that has to be taken into account when comparing different storage alternatives. Systems that minimize the evaporation has to be deployed if liquid hydrogen storage is to be considered a viable alternative. [4]

5.4 Metal Hydride Storage

Metal hydride (MH) stores hydrogen atoms in a metal lattice structure. As a hydrogen storage technology it has some noticeable advantages. The metal hydride requires energy to release the hydrogen from the metal lattice, this means it's very stable and easy to handle. Additionally, due to the efficient absorption of hydrogen in the metallic lattice, the density of metal hydride storage is comparative to liquid hydrogen (≈ 70 kg/m^3), but at moderate pressure and temperature. The US DOE long term goals are a decomposition temperature between 60 and 120 °C for commercial use. The main challenges are the long absorption time, high total system weight and high cost. Studies indicate that improved kinetics and lower decomposition temperatures for the material used is feasible to improve. If the remaining challenges are solved, this method for storage could be feasible for commercial storage in multiple areas in the future. [67, 68]

The interaction between the MH and H-atoms is exothermic, and the desorption is endothermic. The process is illustrated in figure 5.3. [67]

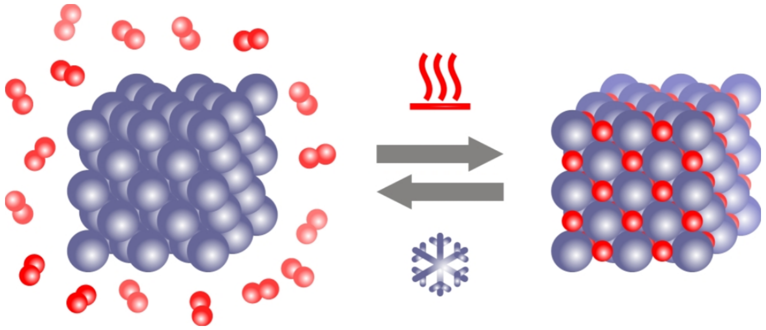

Figure 5.3: *The interaction between Metal Hydride and hydrogen atoms (red). [69]*

5.5 Chemical Storage

Chemical hydrogen storage usually refers to covalently bound hydrogen in solid or liquid form in compounds that have high hydrogen densities e.g. ammonia or methylcyclohexane. [70]

Ammonia contains over 17.6% hydrogen, based on weight. The hydrogen density in liquid, anhydrous ammonia at 25 °C and 10 bar is $\approx 107\text{kg/m}^3$. [3] The release of hydrogen, from the compound, is usually exothermic. This requires that the remaining dehydrogenated by-product has to be re-hydrogenated in a separate location and process. This will lead to an increase in the total system cost. Additionally, the by-product after the release of hydrogen could be challenging to use and handle. [70, 71]

One of the main advantages of using chemical storage is the high density of hydrogen that can be stored, relatively safe and in large volumes. Where pre-existing infrastructure is present, this could be a cost-efficient alternative and a way to bring down the carbon footprint in existing industry. [70, 71]

6 Alternative Energy Storage Systems

Due to the intermittent nature of many renewable energy systems (RES), such as solar and wind, power production might not follow the ideal consumption pattern. A transmission grid can be difficult and might not be economically feasible to extend to remote areas. In some situations, a microgrid or an off-grid system could be the only solution to have access to electricity.

To make an off-grid PV system reliable, an energy storage system (ESS) might be a viable solution for the intermittent production pattern. The surplus power can be stored and discharges when demand fluctuates. [72]

6.1 Battery Energy Storage System

There are several different battery technologies on the marked. The Lead Acid and the Lithium-Ion (Li-ion) battery is taken into consideration in this thesis.

The demand and innovation for Battery Energy Storage Systems (BESS), is rapidly evolving and prices are expected to drop in the following years. The costs are however relatively high in some regions, and may not be economically justifiable without subsidies or regulatory requirements. [73]

For a BESS there are several specifications to consider. The battery capacity is the total amount of energy that can be stored, given in kWh. While the power rating is how much energy that can be discharged at any moment in watts. The discharge rate is expressed as the C-rate, a C-rate of 1C will fully discharge a battery over one hour while C/8 over eight hours. By fully charge/discharging a battery the lifetime will rapidly decrease. Therefore a depth of discharge (DoD) limit is set, is the amount of energy cycled in the battery and is expressed as a percent of the battery capacity. Exceeding this limit would increase the degradation rate. [74].

Batteries naturally degrade over time. High battery cycle count and temperature has a potentially negative long term impact on a BESS, in terms of capacity degradation. Manufacturers provide a warranty for a certain capacity over the total lifetime or for a specific number of cycles. As the technology matures, improvement of the battery chemistry may increase. Leading to a longer lifetime of the BESS technologies [73, 75]. In table 6.1 key difference between lead acid and Li-ion batteries is presented.

Table 6.1: *Comparison between lead acid and lithium ion batteries.[74, 76]*

Parameters		**Lead Acid**	**Lithium Ion**
Specific energy	[Wh/kg]	35 - 40	150 - 180
Specific power	[W/kg]	250	800
Available capacity on the market		2-24 kWh	MW(s)
Efficiency	[%]	85	90
Life expectancy	[years]	15	10 - 15
Cost(battery only)	[$/kWh]	150 - 200	600 - 800
Installed system cost	[$/kWh]	400 - 600	1250 - 1500
Safety		Excellent	Issues to be resolved
Main usage		Residential	Commercial & Utility

6.2 Mechanical Energy Storage

Mechanical energy storage is a term that includes the storage technologies which utilize potential or kinetic energy. The best-known technologies are: pumped hydroelectric storage (PHS), compressed air energy storage (CAES) and flywheel energy storage (FES). The different energy storage systems are compared in table 6.2. The values are presented in min to max values for a thorough comparison. It is worth noting that there is a broad range for each storage system. [77]

Table 6.2: *Comparison between PHS, CAES and FES. [78, 79]*

		PHS	CAES	FES
Specific energy	[Wh/kg]	0.3 - 1.5	3.2 - 60	5 - 200
Energy density	[kWh/m^3]	0.5 - 1.5	0.4 - 20	0.25 - 424
Specific power	[W/kg]	0.007 - 0.117	2.2 - 24	400 - 30 000
Power density	[kW/m^3]	0.00761-0.117	0.04 - 10	40 - 2 000
Efficiency	[%]	65 - 87	40 - 89	70 - 96
Storage duration		hours - months	hours - months	sec - min
Self Discharge Rate	[%/day]	∼0	∼0	1.3 - 100
Lifespan	[year]	20 - 100	20 - 40	15 - 20
Scale	[MW]	10 - 8000	0.01 - 3000	0.001 - 20
Energy CAPEX	[USD/kWh]	1 - 291.2	1 - 140	200 - 150 000
Median Energy CAPEX	[USD/kWh]	33.00	11.88	900.00

6.2.1 Pumped Hydroelectric Storage

Pumped hydroelectric storage (PHS) is the most common form of large-scale energy storage in the world [77]. Figure 6.1 is an example of how a PHS-facility is designed.

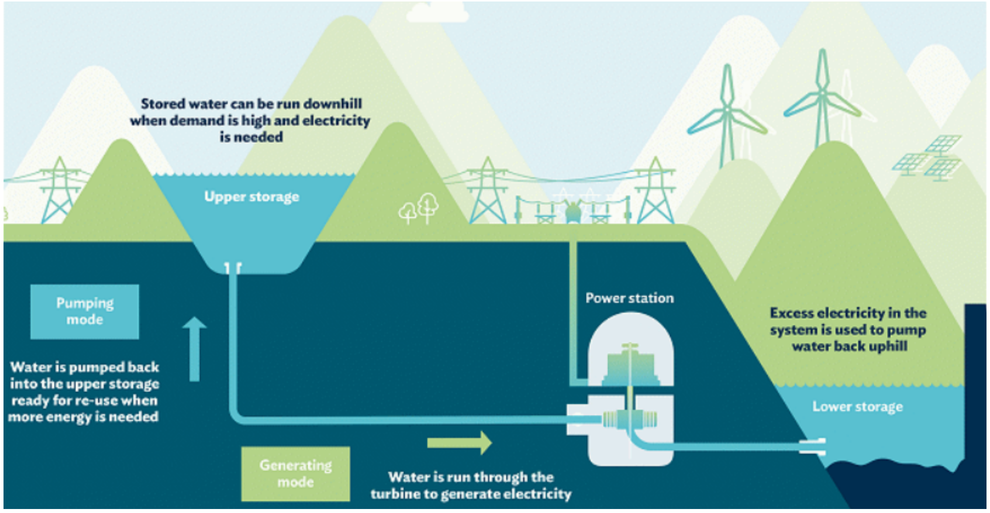

Figure 6.1: *Layout of a hydroelectric facility. [80]*

The reliability, flexibility, and simplicity of the system make it very attractive as an energy storage option. Traditionally PHS has been used to optimize high inertia load generation applications, additionally the system can function as a flood control and assist in irrigation, both upstream and downstream due to the predictable nature. Due to the large capacity and ability to store and supply on demand, it synergies well with intermittent renewable energy sources, such as wind and solar. [77]

PHS is not perfect in all aspects. It is often associated with high capital cost, development time, and long payback time. If the correct geographic conditions are not present, it is difficult to make such a project profitable. Large scale transmission might have to be built, to make such a facility effective and to be fully exploited. Environmental impacts of diversion of rivers and creation of artificial water bodies needs to be taken into consideration when constructing such a facility. [77]

6.2.2 Compressed Air Energy Storage

Compressed air energy storage is a viable technology for both large- and small-scale energy storage. All CAES systems have the three main steps in the cycle: compression, storage, and expansion. Electrical energy is converted into potential energy, in the form of pressurized air, and is released on demand to generate electricity with the help of gas turbines. Small systems (<100kW) often utilize tanks for storage. While larger systems often rely on natural or man-made caverns. Such as wells, hard rock/limestone mines, aquifers or salt caves. The layout of a system is shown in figure 6.2. [77]

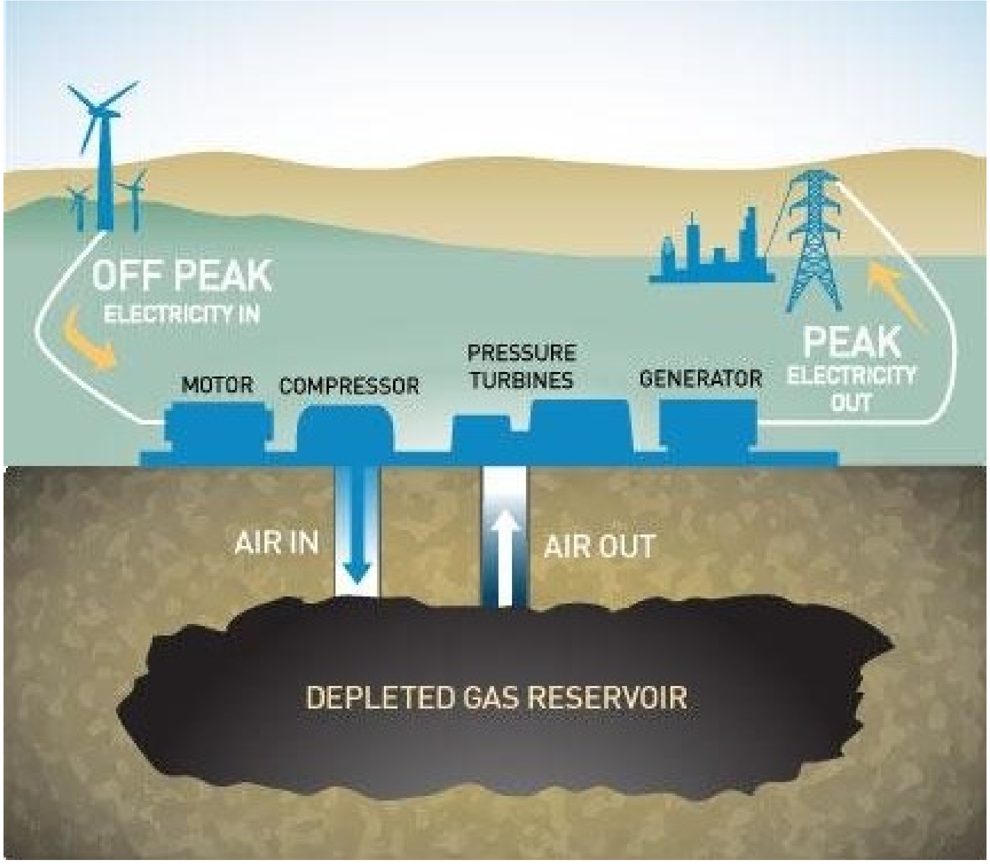

Figure 6.2: *The layout of a large scale CAES system. [81]*

The advantages of CAES shares some characteristics with PHS. High reliability, flexibility, long life expectancy, relatively low O&M costs compared to other technologies and low self-discharge rates. Additionally, CAES has better volumetric energy density and power outputs than PHS. By exploiting pre-existing, underground areas, it can have a low environmental impact. It would also be suitable for intermittent renewables energy sources, due to the flexibility of storage. [77]

The main challenge with CAES is the geological suitability. Especially for large scale storage, it is necessary to have suitable caverns for storage. There are multiple requirements for such an area to be feasible for storage: volume, minimal leakage and be able to handle thermal stress are important factors to make such a project economically feasible. These conditions are rare and make CAES difficult to implement in many regions of the world. [82]

6.2.3 Flywheel Energy Storage

The principle behind a flywheel is simple, it stores kinetic energy with the use of rotational mass. The main components subsystems are the flywheel, bearing, electrical generator, power converter, and chamber, shown in figure 6.3. [83]

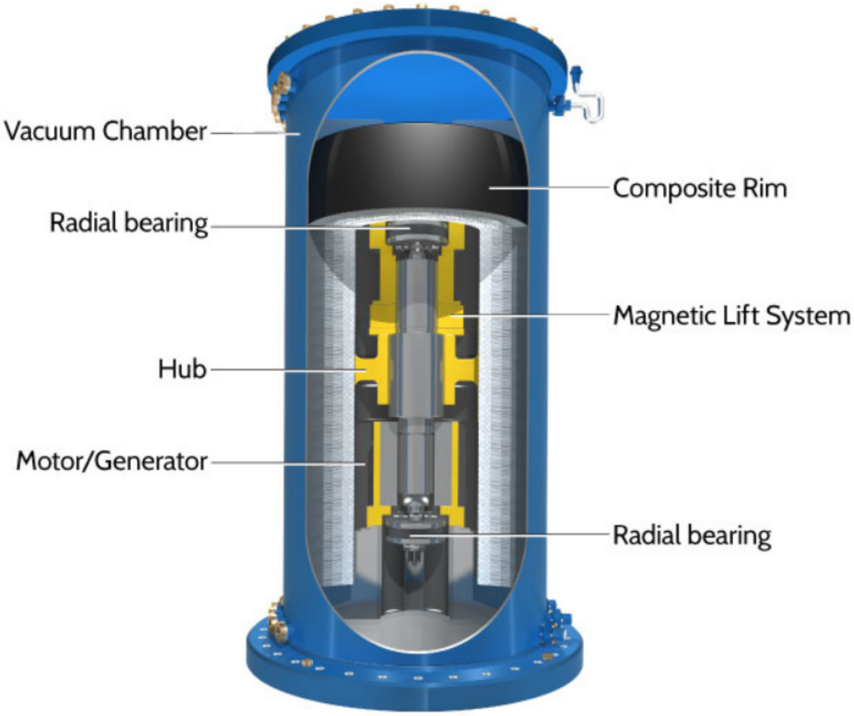

Figure 6.3: *Layout of a carbon fibre flywheel. [83]*

The reason why FES is attractive for energy storage is the high efficiency for short durations and negligible temperature fluctuations when discharging. The implementation of the system is also very flexible, and could be located independent of geography. [77, 84]

There are unfortunately some short-comings with the system: high self-discharge rates, continuous monitoring, and safety risks. The kinetic energy stored in the system puts extreme stress on the material. This could cause vibrations and material degradation, which could result in shattering of the rotor or material. Because of the high rotational speed a flywheel could be operating in (>100 000 rpm), this could result in projectiles with extremely high kinetic energy and could lead to the destruction of the imminent surroundings. This calls for continuous monitoring systems with rigorous safety routines, which would lead to higher costs. The discharge rate is mainly due to friction, which increases with the rotational speed. FES systems are usually deployed as a peak power supplier or for smoothing out rapid power fluctuations due to the limitations set by the discharge rate. [85, 77, 84]

7 Economics

In this section the economical terms used in this thesis will be explained, as well the background for the hydrogen prices used in the analysis.

7.1 Capital Expenditure

Capital expenditure (CAPEX) is the expense a company in the start-up phase or who is to expand its business has to spend. All expenses associated with new inventory, includes machinery and intellectual property is defined under CAPEX, different examples are listed below. [86]

- Acquisition of fixed assets.
- Preparation of acquired assets for suitable use.
- Upgrading assets.
- Adapting assets for different use.

7.2 Operating Expenditure

Operating expenditure (OPEX) is the expenses associated with the daily operations where raw materials are converted into products that are ready for sale. Examples are listed below. [86]

- Management expenses
- Insurance fees
- Property taxation expenses
- Fuel and maintenance
- Salary and wages
- Supplies and raw materials

7.3 Levelized Cost of Energy

Levelized cost of energy (LCOE) is used as an indication factor on whether a project will provide financial gain. LCOE takes into account fixed and variable costs as well as total energy production throughout the system lifetime. By estimating these costs and total energy produced, LCOE will provide a simple estimate of how much money must be made per unit of energy produced in order to break even. This value is obtained by utilizing equation 7.1. [87]

$$\text{LCOE} = \frac{\text{Total Lifetime Cost}}{\text{Total Lifetime Output Energy}} = \frac{\sum_{t=1}^{n} \frac{I_t + M_t + F_t}{(1+r)^t}}{\sum_{t=1}^{n} \frac{E_t}{(r+1)^t}} \tag{7.1}$$

I_t = Investment and expenditures for the year (t)
M_t = Operational and maintenance expenditures for the year (t)
F_t = Fuel expenditures for the year (t)
E_t = Electrical output for the year (t)
r = The discount rate
n = The expected lifetime of the system

Renewable energy sources often have expensive investment costs, some of which are compensated for by little or no fuel usage and carbon emissions, especially compared to fossil based energy sources. To make renewable energy more economically attractive, some countries have introduced tax credits and tax deductions and other subsidies to encourage renewable energy investments. [87]

7.4 Hydrogen Prices

Hydrogen prices are essential for the feasibility of a hydrogen electrolysis facility. The realistic end price of hydrogen will be determined by a multitude of factors. Such as the marketing strategies, underlying financial conditions, business model and competitive market. It's not unreasonable to expect unsustainable high prices in the beginning, as the local demand is low. The synergy between supply and demand will be a challenge that hydrogen suppliers will have to solve. [88]

The consumer price is especially important if the hydrogen is going to a fuel cell electrical vehicle (FCEV) consumer. From a consumer's perspective, the fuel price difference between an FCEV and other transport options is vital for the decision. High hydrogen prices will hold back the interest in the FCEV sector, and therefore make it less attractive for economical investment. [88]

In attachment G the U.S. Department Of Energy stated that the goal in 2015 was to produce hydrogen from an alkaline electrolyzer for 5.60 USD/kg H_2. This number is substantially lower than the 14 USD/kg H_2, that the California Energy Commission stated was the current price level in 2015. The difference in assumed values and the real-life value chain is something that needs to be taken into consideration when analyzing the economic feasibility of hydrogen production. [88, 89]

Mass production of electrolyzers and fuel cells, in combination with the need for energy storage and more research and development in the field. Could result in hydrogen, as an energy carrier, becoming a more cost-effective alternative in the future. According to NEL, due to highly tailored production methods today, standardized mass production of electrolyzers in the future, could decrease the cost of a module by 30% alone. [61]

The increase in the electrolysis plant capacity will also reduce cost per unit of energy, as shown in figure 7.1. This is because the cost of system monitoring, engineering, and operational cost will not increase in the same manner as the increased capacity. [90]

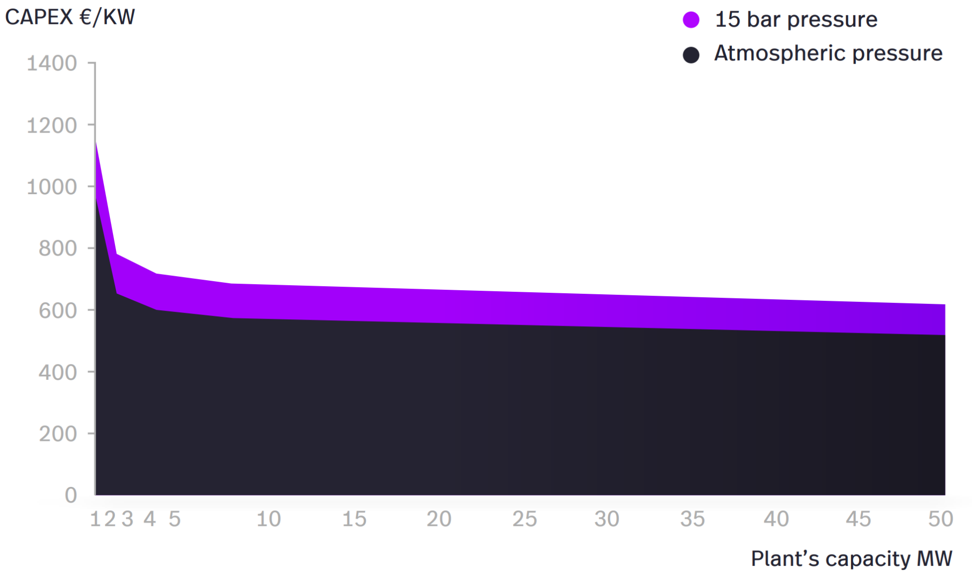

Figure 7.1: *CAPEX versus electrolyzer plant capacity. [90]*

Methods and Approach

In this section, the methods and approaches for obtaining the results will be presented. PVsyst, Matlab and Excel is used to carry out the simulations, calculations, and analysis, respectively. Autocad was used for various graphical representations. We choose a time-frame of 25 years for the system.

The overarching structure is listed below:

1. PV-simulations	PVsyst
2. Power consumption	Matlab
3. Hydrogen production	Matlab
4. Economical analysis	Excel

In figure 7.2 the system simulated in the thesis is illustrated.

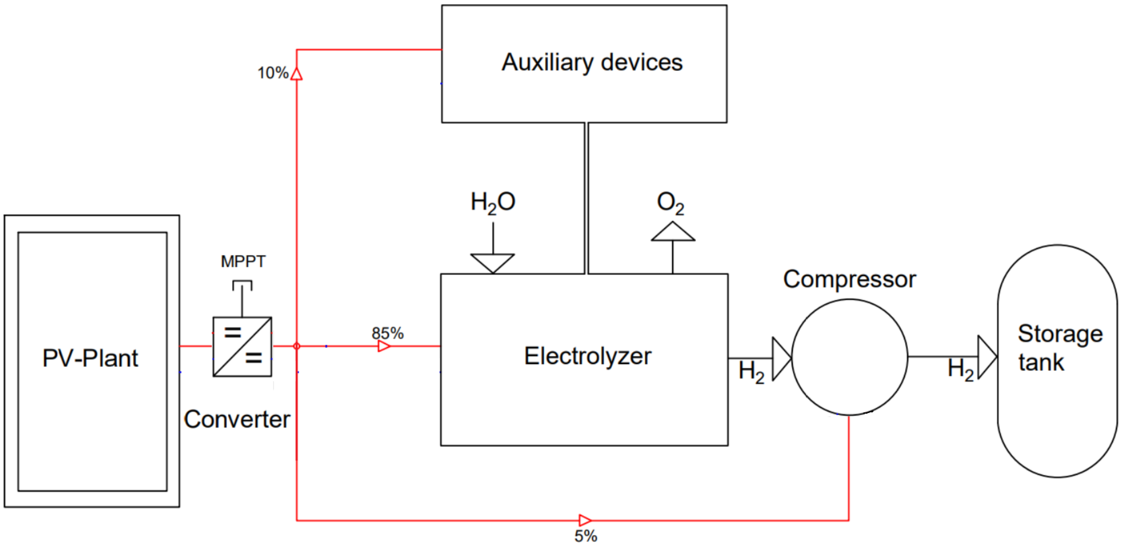

Figure 7.2: *Visual representation of the system simulated in the thesis.*

8 Photovoltaic

This section explains the method and approach used to simulate and calculate the different parameters regarding the PV-module component of the system.

8.1 PVsyst

PVsyst is a software program, used to model the PV-system in this thesis. The software is suitable for designing and scaling a PV-system, by combining weather data with specific PV-modules from different manufacturers. This combination gives an approximation of the power production for a complete PV-system.

The coordinates for Chililabombwe's location is added to PVsyst. From this, PVsyst could obtain different meteorological data such as solar irradiation, temperature, wind velocity, relative humidity. The meteorological data source chosen for this project is Metronome 7.1.

The nominal installed power was set in the thesis description (1 MW). The other system design parameters are chosen based on literature review, mail correspondence and preliminary simulations. A poly-crystalline PV-module from Canadian Solar Inc (CS3U-345p-FG) with 17.39% efficiency is chosen, as well as two 500 kW generic DC/AC inverter from the PVsyst database. All simulations are done in 5 year intervals for 25 years. The values between the intervals is calculated with linear interpolation. Options for soil loss, degradation due to aging and thermal loss due to wind are chosen in PVsyst. Shading of nearby PV-modules is not taken into account in PVsyst simulations.

PVsyst is unable to simulate a DC off-grid system due to an error in the software. The simulated production is conducted with a DC/AC inverter, which may have some impact on the final result since the electrolyzers uses DC-current. In table 8.1 the different input parameters added to conduct the simulation are presented.

Table 8.1: *Specific design inputs for the PVsyst simulations.*

Input	Value
Coordinates	12 to 13 °S and 27 to 28 °E
Nominal power	1000 [kW]
Specific PV-module	Canadian Solar Inc, 345 Wp 33 Volt, SI poly CS3U-345P-FG
Inverter	Generic 500 kW, 320-700V, LFTr 50Hz, 500kW AC x 2
Configuration	Fixed tilt & Single-axis tracking system
Soil loss	2%

8.2 Land Coverage and PV-Orientation

Based on the literature review, different PV-orientations where examined. Fixed tilted angle in the east-west axis and an additional single-axis tracking system in the north-south axis is examined as possible configurations.

To determine the orientation of the PV-module, several simulations were conducted to find the optimal angle for the fixed tilt (18°east-west axis). This angle was then used in further simulations when determining which range the additional single-axis tracking system should operate in. Data from the initial simulations was imported to Matlab for processing.

Because the simulations done in PVsyst did not take shading into account, additional land coverage required to prevent shading on nearby panels is calculated.

This was done by sketching in Autocad and applying geometric calculations in Matlab, to determine the optimal fixed tilted angle and the tracking systems maximum angle in the north-south axis. The sketch and geometric equations are presented in appendix E. Values for the land coverage was calculated as a percentage increase of the module area and graphically presented with its respective annual power production.

Due to the shading of nearby PV-modules and the effect this had on the increase of land coverage, for the tracked configuration a range limit in the north-south direction was set (± 60°). In order not use the excessive area for the PV-plant. The loss in efficiency due to the shading that occurs for steeper angles than ± 60° is not taken into account in the thesis.

The simulated power production is uploaded to Matlab. To obtain a representative plot for the production, an average production time of 12 hours per day is used in the calculations. The sum of the power production over the 25 years was done by numerical integrating the plotted result. This is done for both fixed tilt and fixed tilt with a tracking system.

8.3 PV Price Estimate

The CAPEX for the PV-system is based on NREL's system cost benchmark [45]. The prices in that report was based on PV-systems above 5 MW. By extrapolation, the prices for a fixed tilt and single-axis tracking system is estimated for the 1 MW system. The CAPEX is calculated with equation 8.1.

$$\text{CAPEX} = C_{est} \cdot P_{nom} \tag{8.1}$$

C_{est} = Cost estimate [\$/Wp dc]
P_{nom} = Nominal Power [Wp]

The OPEX for the PV-system is found in the literature review to be 0.8% of the CAPEX [91]. The 0.8% is also used for the single-axis tracking system. A discount rate of 5% is used in the the LCOE calculation.

$$\text{OPEX} = \text{CAPEX} \cdot 0.008 \tag{8.2}$$

9 Electrolyzer System

This section explains the method and approach used to calculate the hydrogen output regarding the electrolyzer component of the system.

Because of the intermittent energy source and the small scale of the system, MCWE and SOWE electrolyzers are deemed not feasible and are excluded from further simulations and analysis in the report. The main challenge for high-temperature electrolyzers is the day/night cycle regarding solar power. This means that the electrolyte must be re-heated daily to reach ionic conductivity. Which will be detrimental for the overall system efficiency. Additionally, MCWE and SOWE are regarded as less mature than AWE and PEMWE.

The electrolyzer values are based on NELs PEMWE-module (M-series) and AWE-module (A-series). Datasheet is found in appendix A and B for the PEMWE-module and the AWE-module respectively. The numeration indicates the volumetric capacity in Nm^3 H_2/h. The M100 and M200 equals 500 and 1000 kW stack size respectively. Due to the A-series having higher efficiency than the M-series, the A100 and A200 has some deviations from the 500 and 1000kW stack size. This was deemed to be in an acceptable range for calculations according to NEL. The M-series is upgradable in 250 kW increments, which is also assumed to be true for the A-series. [61]

9.1 Power Consumption

The electrolyzer parameters that are investigated through Matlab is presented in table 9.1.

Table 9.1: *Simulation parameters used for the electrolyzer in Matlab modelling.*

Simulation parameters	
Electrolysis technology	AWE & PEMWE
Installed stack size [kW]	250, 500, 750 and 1000
Dynamic range (PEMWE)	0-100% of installed capacity
Dynamic range (AWE)	15-100% of installed capacity

According to NEL the system could be simplified in order to estimate the final electrolyzer system range. Different sub components where regarded as auxiliary devices, it was found to be 10% power consumption of the electrolyzer stack size. This was based on the datasheet for the M-series in appendix A, and assumed to be true for the A-series. The M-series has an outlet pressure of 30 bar and the A-series 1 bar. The difference in outlet pressure between the two electrolyzers has not been taken into account, and a 5% power consumption for compression was added to both AWE and PEMWE. This gave the total system consumption range, presented in table 9.2.

Table 9.2: *Electrolyzer system range used in Matlab modelling.*

System range	
System range (PEMWE)	15-115% of stack size
System range (AWE)	30-115% of stack size

The power consumption is calculated by comparing the power output from the PV-inverter to the system range for each stack size. The energy outside the system range is regarded as surplus energy. The lower system corresponds to when the electrolyzers is able to produce hydrogen. The system power consumption was plotted over one week to illustrate how the electrolyzers respond to the fluctuating power input.

The energy required to have continuous operation throughout the year is calculated as the electrolyzer capacity. The system energy consumption was divided on the full electrolyzer capacity to get the capacity loss. This indicates if the electrolyzer is under- or over-dimensioned according to the PV-energy produced.

9.2 Hydrogen Production

There is a difference in the efficiency in the technologies. For AWE the production rate is 42.3-48.9kWh/kg H_2 and for PEMWE 47.5-55.0 kWh/kg H_2.The hydrogen production rate also varies throughout the dynamic range for the electrolyzers. By applying equation 9.1 and 9.2 the power consumption was calculated for the AWE and the PEMWE. By using equation 9.3 the hydrogen production was calculated.

$$\dot{P}_{AWE} = 48.9 - 7.765\left(1 - \left(\frac{P}{P_{El}}\right)\right) \tag{9.1}$$

$$\dot{P}_{PEMWE} = 55 - 7.5\left(1 - \left(\frac{P}{P_{El}}\right)\right) \tag{9.2}$$

$$m_{H_2} = \frac{P}{\dot{P}} \tag{9.3}$$

$\dot{P}$ = Power consumption $[\frac{kWh}{kg}]$
P = Power input [kW]
P_{El} = Installed stack size [kW]
m_{H_2} = Hydrogen produced [kg]

To further improve the hydrogen production calculations, the stacks degradation is taken into account. Specific data given by Norconsult said that the AWE cell stack should be replaced when reaching 20% degradation.

Based on literature review and information given by Norconsult, the lifetime of an AWE was set to 87 600 hours (10 years) and the PEMWE to 20 000 hours (≈ 2.3 years) of continuous operation. Based on this, the AWE is set to reach 20% degradation after 87 600 operating hours and the PEMWE is set to reach 20% degradation after 20 000 operating hours. Stack replacement was simplified for the PEMWE to be every 5 years, since this corresponds to the five year interval from the PV output and is about the time when the PEMWE reaches 20 000 operational hours.

Since the feasibility study is for a PV-supplied electrolyzer-system, the equation for AWE 9.4 and PEMWE 9.5 is made to give degradation per hour. The hours of operation is calculated by counting all values, that is inside the dynamic range. The equations are applied from year one, and applied every five years consecutively, assuming that degradation between the five-year interval is linear. The possible degrading effect of a variable power input will have on the electrolyzers or the standby degradation has not been taken into consideration, due to the scope of this project.

$$\eta_{AWE} = 1 + \frac{0.02}{8760} \cdot h \cdot y \tag{9.4}$$

$$\eta_{PEMWE} = 1 + \frac{0.0876}{8760} \cdot h \cdot y \tag{9.5}$$

η = Degradation rate
h = Total Operational time [h]
y = Year

The degradation rate is multiplied with the power consumption to account for the increase in energy demand by the stack throughout the years.

10 PV-Hydrogen System

This section explains how the complete system analysis is conducted. Assumptions made to produce the economic analysis are mentioned in this section.

The peak power output from the PV is set to 1 MW. The analysis is done with the SI poly CS3U-345P-FG module, with fixed tilt of 18° in the east-west axis and a ±60° north-south axis tracking configuration. CAPEX used for the PV-system is 1.62USD/W DC and OPEX is 0.8% of the CAPEX.

Based on the literature review, chemical conversion, liquefaction and metal hydride where excluded as storage options for further economic analysis in the thesis. The suggestion from NEL was steel tanks for storage and a generic compressor, that could compress hydrogen to 300 bar. The values for the tank and compressor used in the system analysis are shown in table 10.1. [61]

Table 10.1: *Storage tank and compressor values used in the simulations. [61]*

Parameters		**Value**
Tank Size	[m^3]	6
Tank weight	[kg]	13 000
Hydrogen weight	[kg]	120
Tank pressure	[bar]	300
Tank Cost	[USD]	92 915
Compressor Size	[kWh]	37.5
Compressor cost	[USD]	114 930

CAPEX for electrolyzer and compressor is given by NEL and is presented in table 10.2. [61]

Table 10.2: *CAPEX for electrolyzer and compressor combined, given by NEL.[61]*

	A100	**A200**	**M100**	**M200**
CAPEX[million NOK][61]	10.0	13.0	14.0	19.5
CAPEX[million USD][a]	1.15	1.49	1.61	2.24
CAPEX[$/kW]	2300	1490	3220	2240

[a] *Converting price with 0.1149 USD/NOK at May 5th.*

The O&M cost for the 500 kW AWE stack including storage tanks is found to be 3.33% of the CAPEX, with a discount rate of 5%, suggested by Norconsult [92]. This was assumed to be appropriate for all stack sizes. The cost is presented in table 10.3. The O&M cost for the compressor was suggested by NEL to be 1-2 % of the CAPEX. In the economic analysis 1.5 % (1724 USD) is used.[61]

Table 10.3: *0&M cost for electrolyzer and tanks combined, the first year, given by Norconsult.*

	A100	**A200**	**M100**	**M200**
O&M [USD] [92]	34 479	45 972	40 226	56 028

The CAPEX and OPEX for the 250 kW and 750 kW stack size are calculated by extrapolating and interpolating values from table 10.2 and 10.3. The LCOE is calculated by using equation 7.1 and the following assumptions:

- Neglected lye cost[a].
- No O&M escalator.
- No cost associated with transportation and distribution.
- No down-time due to maintenance.
- Feed water cost is not included.
- Resale value of the system is not included.
- No engineering cost.

[a] Only applies to AWE.

10.1 Hydrogen Price Estimate

The economic analysis is based on the accumulated cost of the total system and the accumulated income from the hydrogen produced. The hydrogen value range used in the analysis is based on the estimated hydrogen fuel prices and values from the literature review. The hydrogen fuel price is estimated by comparing fuel cost and vehicle range with values from the USA and Zambia.

In table 10.4 the range for a Conventional Gasoline Vehicle (CGV) and a Fuel Cell Electrical Vehicle (FCEV) is presented.

Table 10.4: *Vehicle range CGV and FCEV. [88]*

	Range
CGV	11.5 km/L gas
FCEV	106.2 km/kg H_2

The national average gasoline prices in January 2019, for both Zambia and the USA, is described in table 10.5.

Table 10.5: *Gasoline prices USA and Zambia. [93, 94]*

	Price of Gasoline
USA	0.75 USD/L
Zambia	1.66 USD/L

For the analysis, the upper bound was decided to be the estimated FCEV fuel price in Zambia, this was calculated to be 15 USD/kg H_2. The calculation is shown in appendix G.

As a lower bound, 5 USD/kg H_2 was decided to be appropriate, due to the U.S. Department Of Energy stated that the goal in 2015 was to produce hydrogen from an alkaline electrolyzer at 5.60 USD/kg H_2 G.

Based on initial simulations and prices given for the different electrolyzer stack sizes.

The final economical system analysis is done with a 750 kW stack for both AWE and PEMWE, and assuming that 100% of the hydrogen is sold.

10.2 Additional Energy Storage System

To improve the hydrogen output from the PV-Hydrogen system, an additional energy storage system is considered in the thesis.

Matlab is used to calculate the surplus energy for all stack sizes. The peak surplus energy is considered to be the capacity requirement for an additional energy storage system. The cost of an additional energy storage system coupled with the associated surplus energy for each stack size is going to be estimated.

Due to the time limitations of this thesis, an analysis of the hydrogen production with a realistic additional storage system is not going to be conducted. Instead, the PV-Hydrogen system is going to assume that an ideal storage system is deployed (100% efficiency and storage capabilities). This is done to examine the possible gain in hydrogen production, with an additional storage system.

Results

All results obtained by PVsyst, Matlab and excel will be presented in this chapter.

11 Photovoltaics

The results from solar irradiation to the inverter power output will be presented in this section.

11.1 PVsyst Simulation

For the simulation in this thesis a solar panel of ”SI-poly CS3U-345P-FG” from the manufacturer Canadian Solar Inc. is used (data sheet is presented in appendix D), and two 500kW DC/AC generic inverter from PVsyst’s database. Due to a software error, PVsyst was unable to perform off-grid DC/DC simulations. By analyzing figure 3.7 and 3.6 similarities between AC/DC and DC/DC characteristics lead to the assumption that AC/DC inverter could be used without major deviations compared to a DC/DC converter. The PV-module layout used for the simulation was 13 modules in series and 223 strings, which equals 2 899 PV-modules. This gave the nominal power of 1 000kW.

11.1.1 Solar Irradiation

The global horizontal irradiation varies throughout the year due to the climatic variations as seen in figure 11.1. The Zambian rain season stretches from October to April, where GHI peaks, but have a lower average GHI, mainly due to cloud formation. From May to September the dry climate causes a relatively stable average GHI as seen in table 11.1.

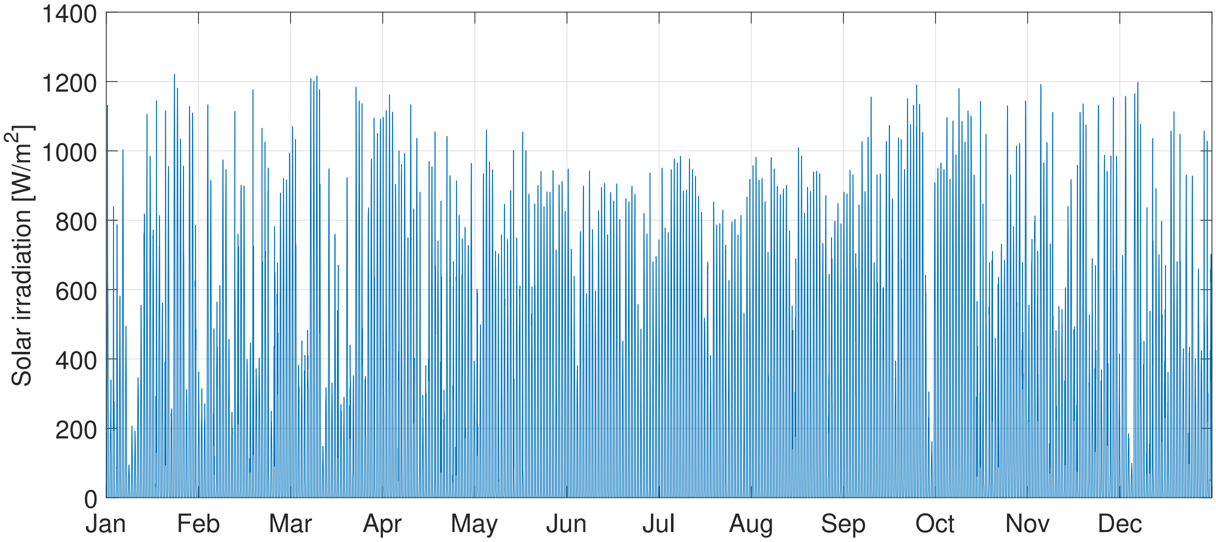

Figure 11.1: *Global horizontal irradiation in Chililabombwe, Zambia.*

Table 11.1: *Average GHI in Chililabombwe, Zambia.*

Month	**Average GHI [W/m^2]**
January	207.5
February	213.8
March	223.8
April	235.4
May	238.8
June	233.8
July	244.6
August	266.2
September	270.8
October	265.4
November	238.3
December	215.0
First year total	1.982 [MW/m^2]

11.1.2 Fixed Tilt vs Tracking System

The optimal fixed tilt angle for the east-west axis was found to be 18°. This gives a 5.2% increase in the module area (5 752m^2). Which results in a total land coverage of 6 051m^2. The first year power production for fixed tilt was found to be 1 740 MWh. The simulations results can be seen in figure 11.2.

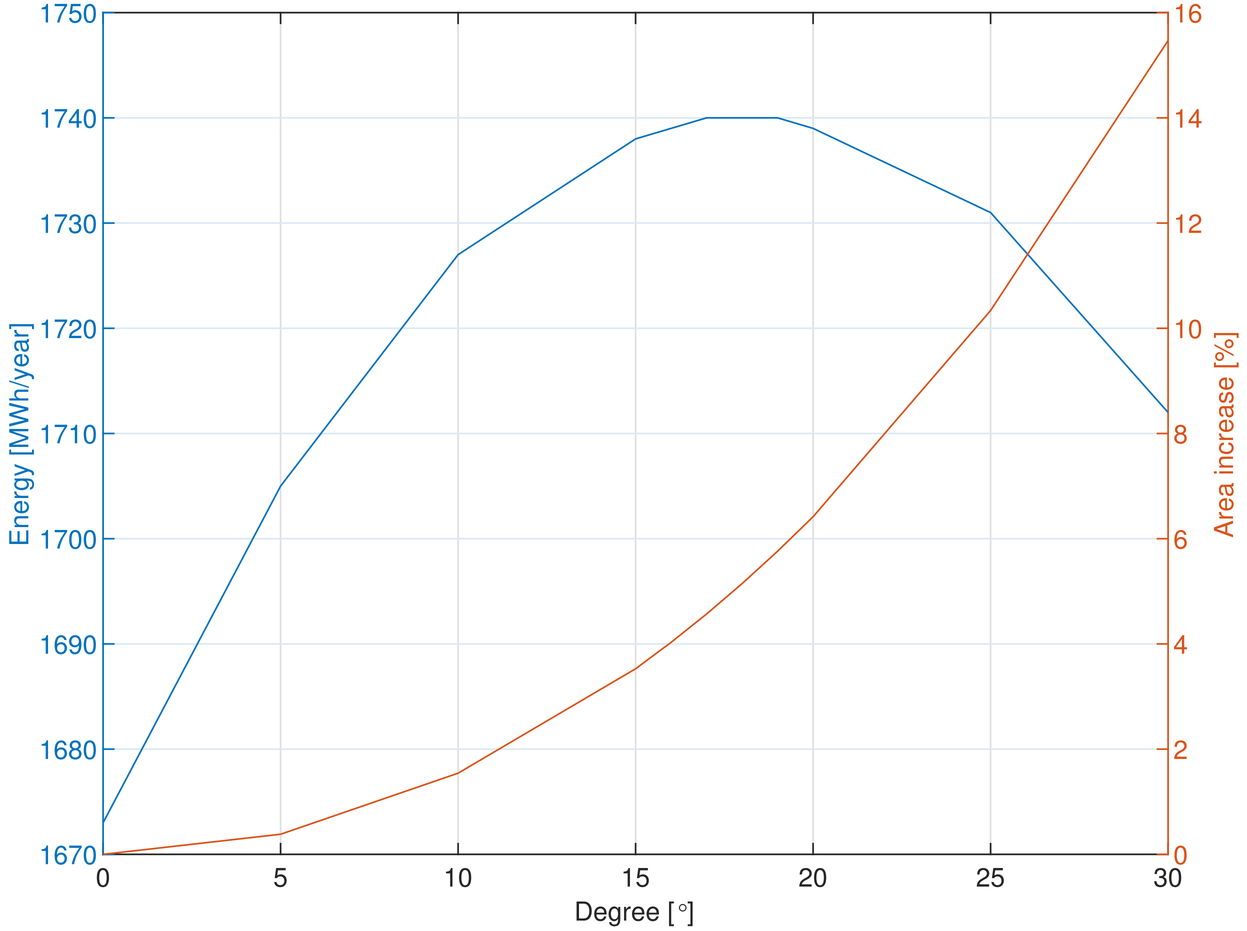

Figure 11.2: *Power output versus land coverage with East-west tracking.*

The range for the north-south axis tracking system was found to be optimal at ± 80-90°. This range gave an unjustifiable increase in area. Therefore further simulations was done with ±60°. This configuration resulted in a first-year production of 2 238 MWh. The total land coverage increase, with the 18°fixed tilt and a tracking system, was found to be

110.4%. This equals a total module area of 12 102m^2. The simulation results are presented in figure 11.3.

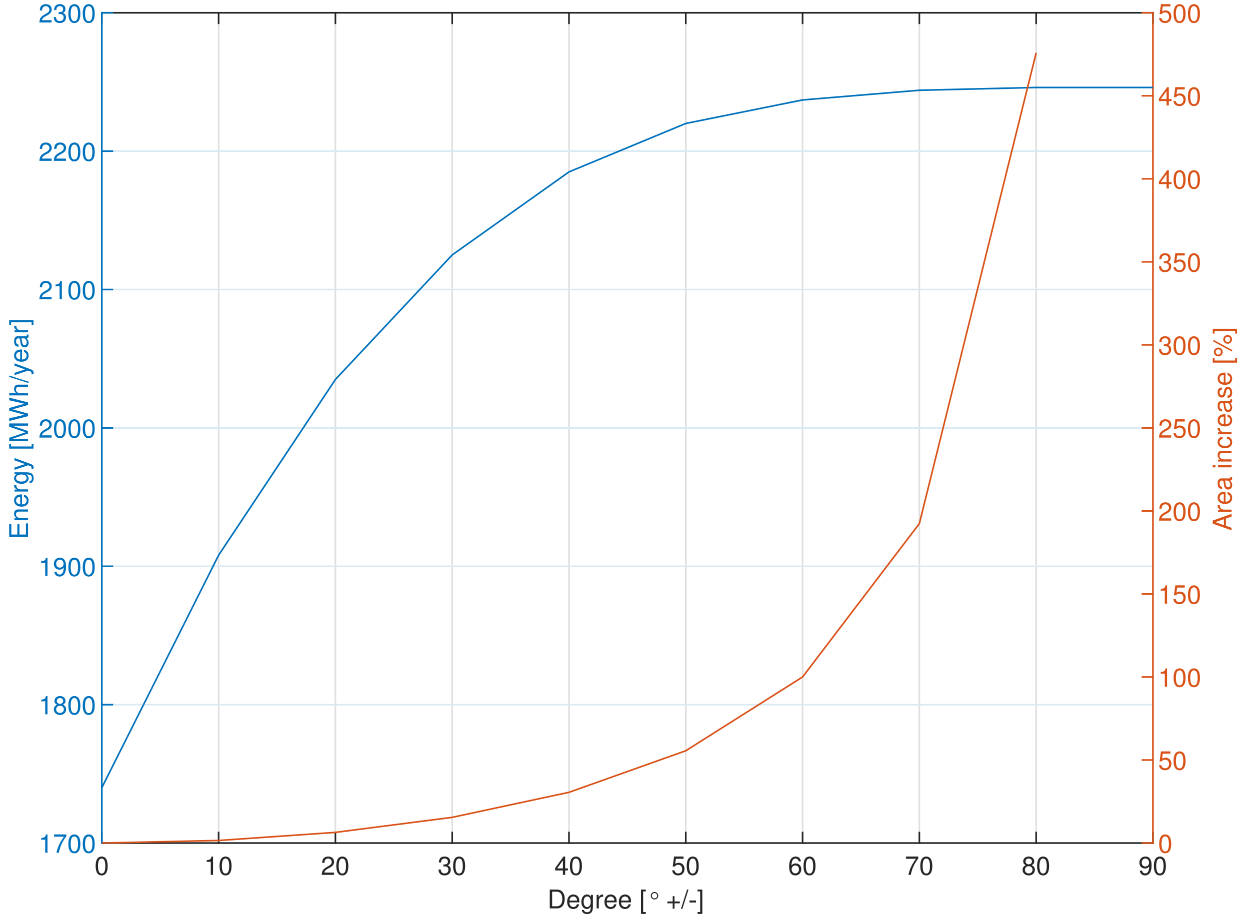

Figure 11.3: *Power output versus land coverage with north-south tracking.*

A summarize and comparison between module orientation, for fixed tilt and a tracked configuration, can be seen in table 11.2.

Table 11.2: *Summarized results after module orientation simulations.*

Output		**Fixed tilt**	**Tracking configuration**
Module area	[m^2]	5 752	5 752
Total area increase	[%]	5.2	110.4
Land coverage	[m^2]	6 051	12 102
1st year power production	[MWh]	1 740	2 237

In appendix E a visual display of the PV-module land coverage, due to shading with a single-axis tracking system is illustrated. The simulation in this project has not taken into account the shading that occurs in the early morning or late evening due to the sun's position.

11.1.3 Power Production

The PV-system produces power 4 023 h/year due to the day/night cycle and variations in climatic conditions. The mean power production with a single-axis tracking system ranges from 499.1± 90.5kW/h in the Zambian rain season to a relatively stable mean production in the winter, 656.5± 6.6 kW/h. With fixed tilt, the production varies from 373.9 ± 65.3 to 490.0±24.1 kW/h, in the rain season and winter. The mean power production each month for a fixed tilt and tracking system is presented in figure 11.4.

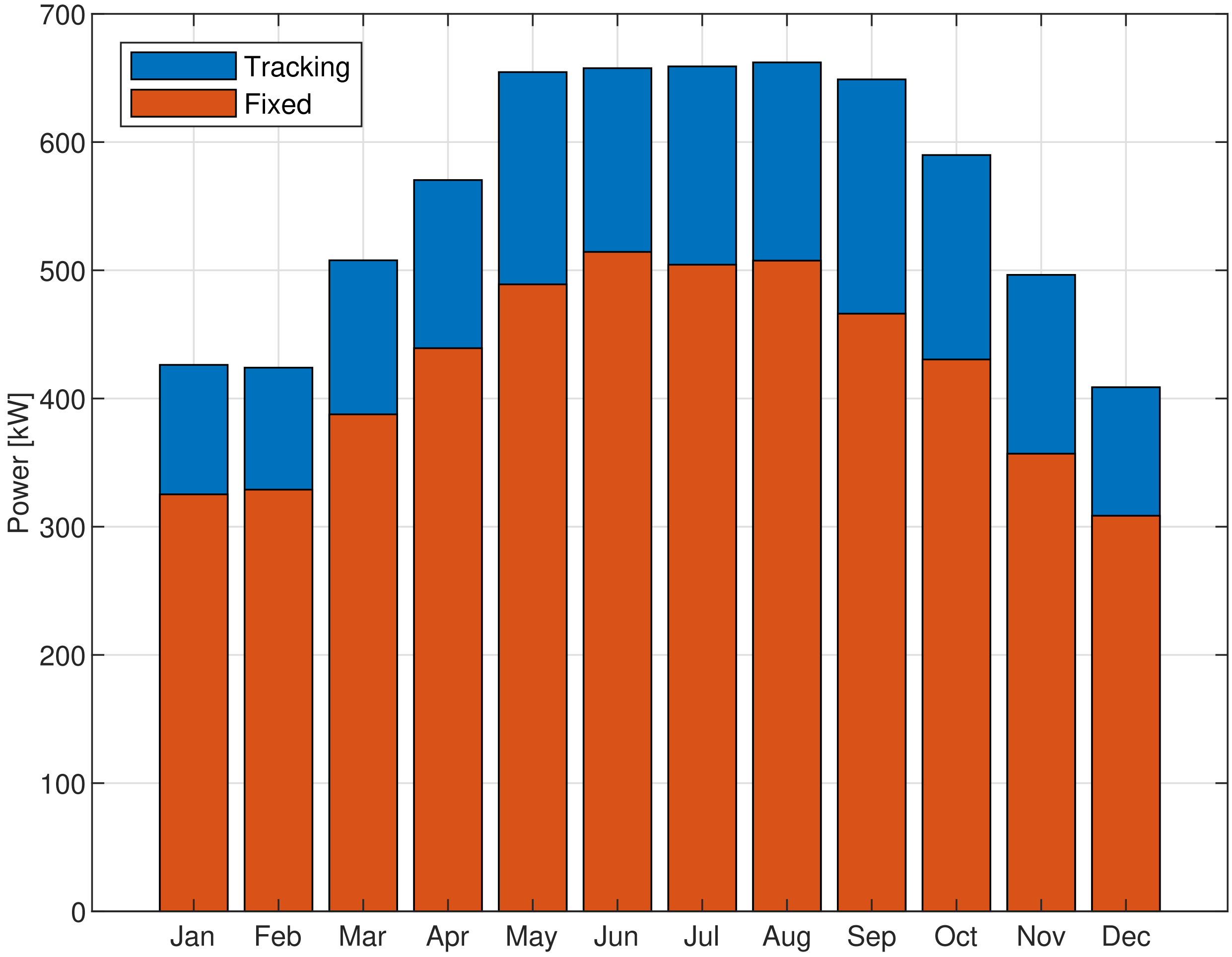

Figure 11.4: *Fixed versus tracking, mean monthly power production.*

Figure 11.5 shows the difference in power output for the PV-plant between the tracking configuration and fixed tilted, on an hourly time scale for the first week in January.

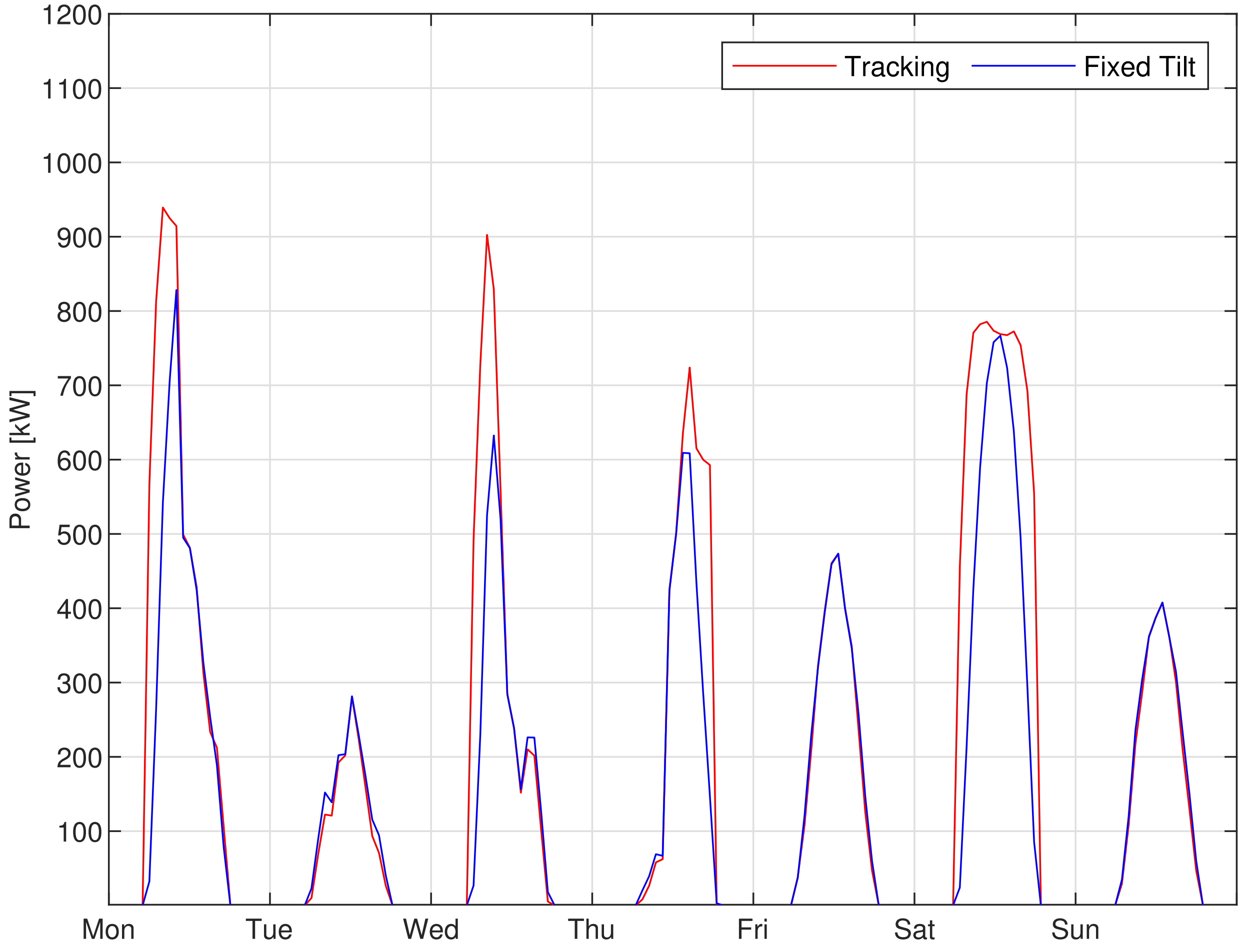

Figure 11.5: *Fixed versus tracking, daily power output, first week in January.*

According to PVsyst, degradation and increasing mismatch in the PV-modules leads to an efficiency loss of 14.7% over 25 years. The 25th year production is down to 1 491 MWh/year and 1 919 MWh/year for fixed tilt and tracking system, respectively. This relationship is presented in figure 11.6.

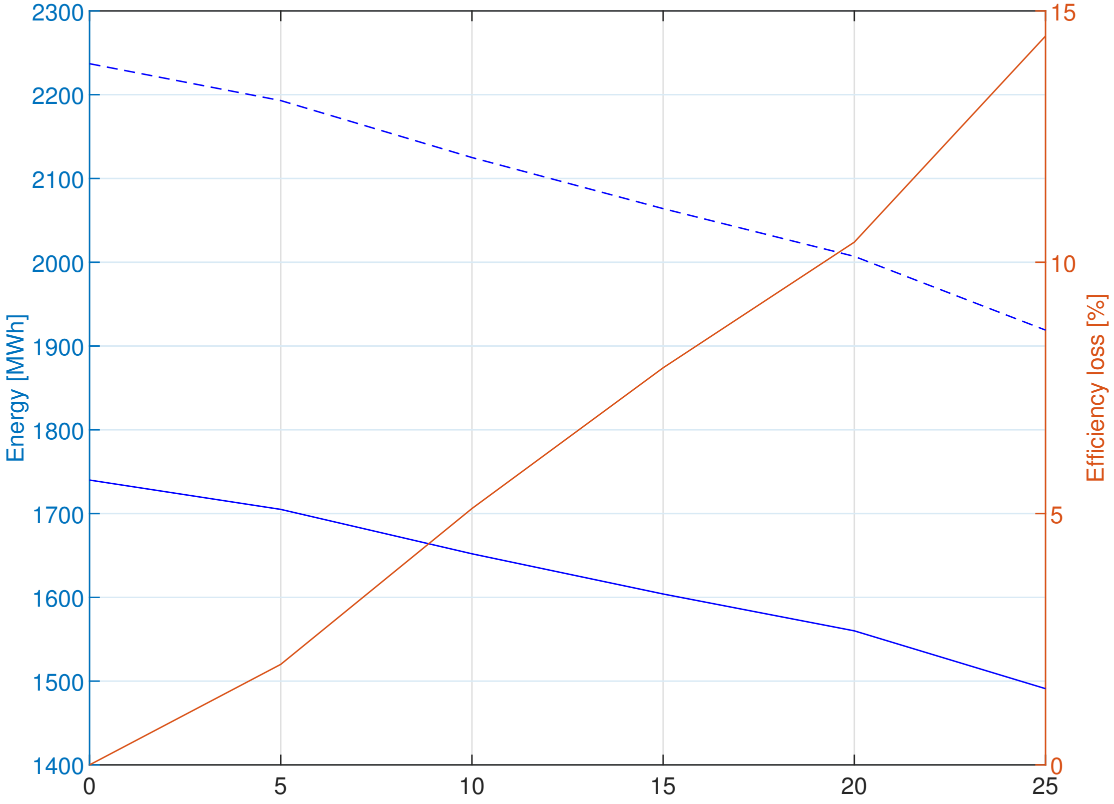

Figure 11.6: *Effect of PV degradation on annual power production, continuous line represents tracking and dotted line fixed tilt.*

The first year energy production increases with 28.6% when using a single-axis tracking configuration compared to only having the fixed tilt. Table 11.3 displays the annual energy production every five years, from the simulations.

Table 11.3: *Annual power production from the PV-system.*

Year	Fixed [MWh]	Tracked [MWh]
1	1 740	2 237
5	1 705	2 193
10	1 652	2 125
15	1 604	2 064
20	1 560	2 007
25	1 491	1 919
Total	40 683	52 335

11.2 Economics

For a 1MW fixed tilted system one can expect to pay approximately 1.5 USD/W DC, while for single-axis tracking system prices increases 8% to 1.62 USD/W DC. This is shown in figure 11.7. The CAPEX is approximately 1.5 million USD for fixed tilt and 1.62 million USD for a single-axis tracking system. The OPEX was found to be 0.8% of the CAPEX, 12 000 and 12 960 USD for fixed tilt and tracking, respectively. Based on equation 7.1 the levelized cost of energy for fixed tilted system was calculated to 0.072 USD/kWh and decreasing with 15.3% to 0.06 USD/kWh for single-axis tracking.

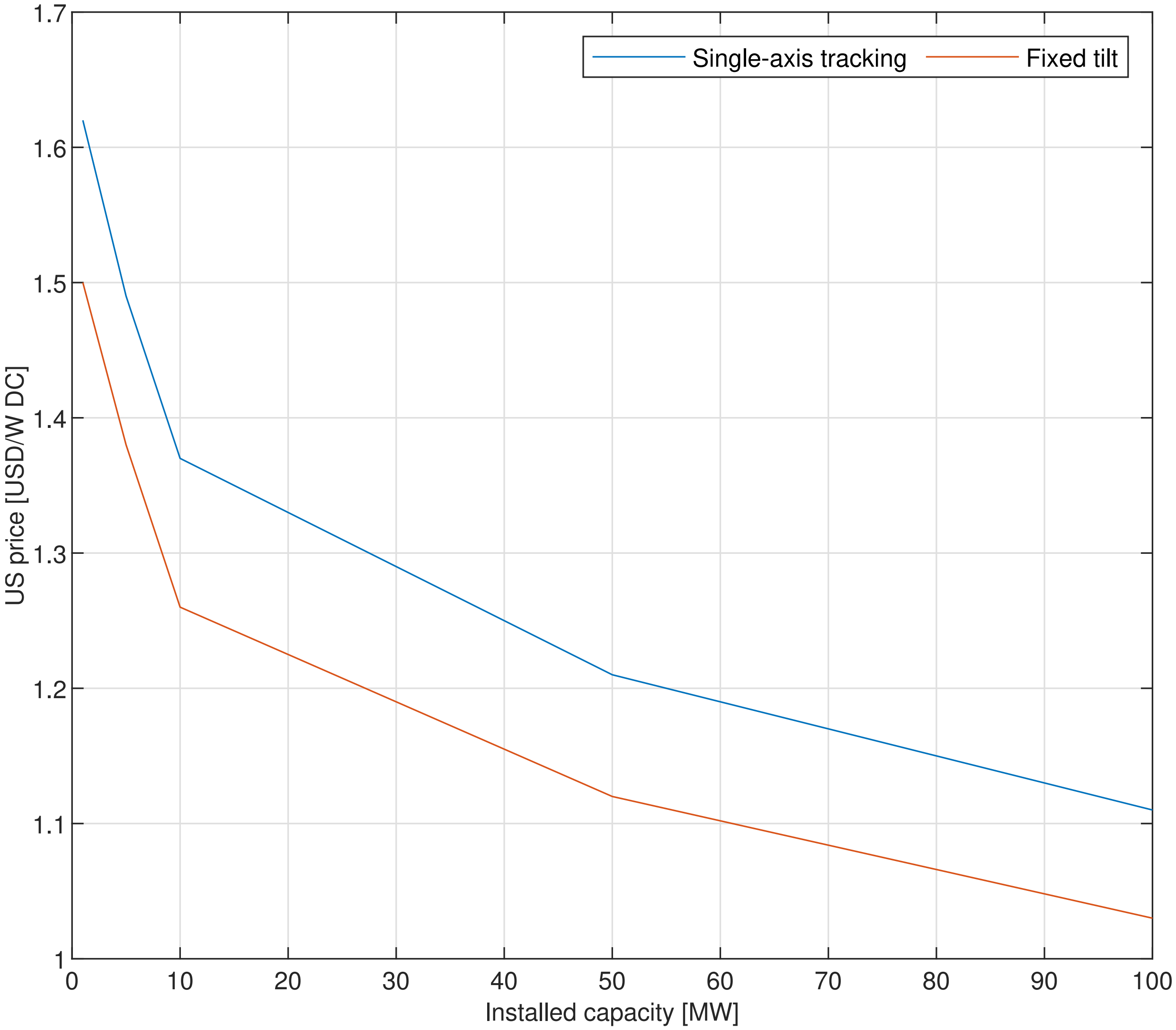

Figure 11.7: *Extrapolated prices for PV-modules, based on NREL system cost benchmark.*

12 Alkaline Water Electrolyzer

This section contains the results with an AWE, obtained from Matlab and excel calculations. Energy production from PV with a single-axis tracking system used as a reference. The AWE module in this paper is based on NELs A-series, the datasheet is found in appendix B. NELs M-series (PEMWE) is upgradeable in 250 kW increments, which is assumed to be true for the A-series as well.

12.1 Power Consumption

The total power consumed by the electrolyzer system is dependent on the stack size, support equipment, and compression. The dynamic stack range for the A-series is 15-100% with a DC power consumption ranging from 3.8-4.4kWh/Nm^3 H_2 (42.3-48.9kWh/kg H_2). For the electrolyzer system range, an additional 15% is added. This is based on the assumption that the support equipment equals 10% and the compression 5% of the power consumption. Table 12.1 contains the limits used for further calculations.

Table 12.1: *System and stack ranges for Alkaline Water Electrolysis for different installed capacities.*

Stack size [kW]	**Dynamic range [kW]**	**System range [kW]**
250	37.5 - 250	75 - 287.5
500	75 - 500	150 - 575
750	112.5 - 750	225 - 862.5
1 000	150 - 1 000	300 - 1 150

Figure 12.1 and 12.2 shows the variation in daily energy consumption compared to the PV energy available throughout the first year. The difference between PV output and electrolyzer consumption is the surplus energy available.

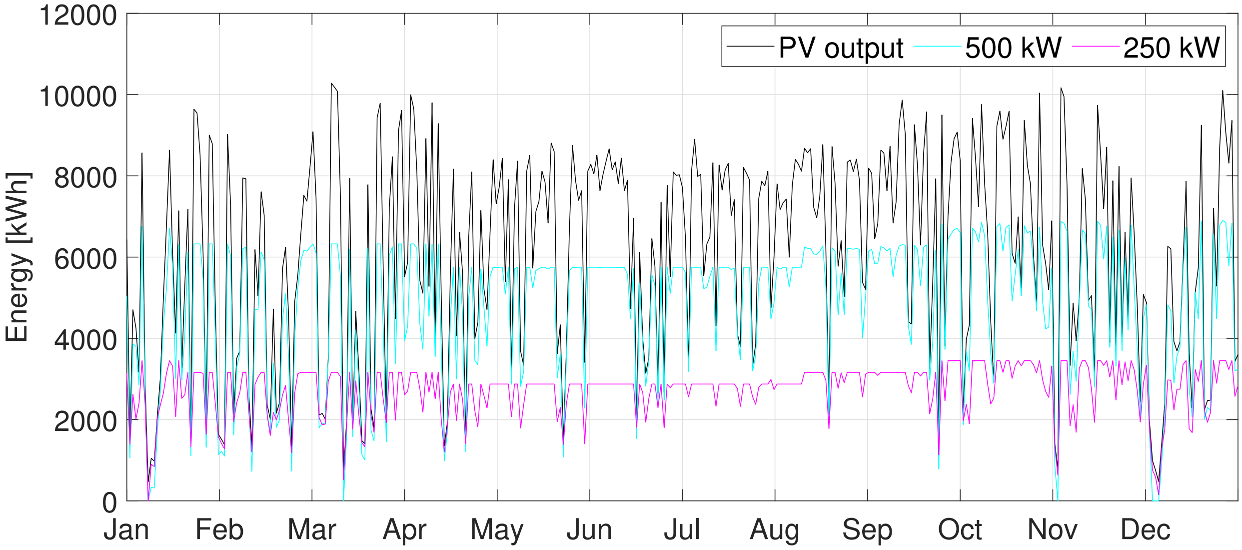

Figure 12.1: *Daily energy consumption by electrolyzer versus PV energy available, 250 kW and 500 kW, AWE.*

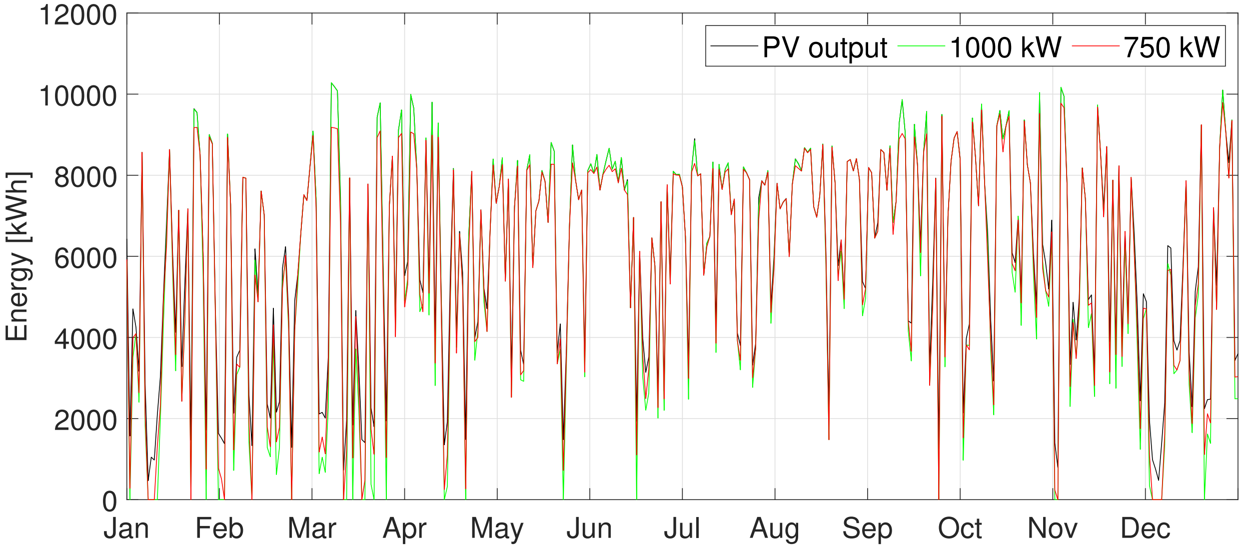

Figure 12.2: *Daily energy consumption by electrolyzer versus PV energy available, 750 kW and 1000 kW, AWE.*

Figure 12.3 and 12.4 shows the variation in hourly power consumption compared to the PV power available for the first week in January.

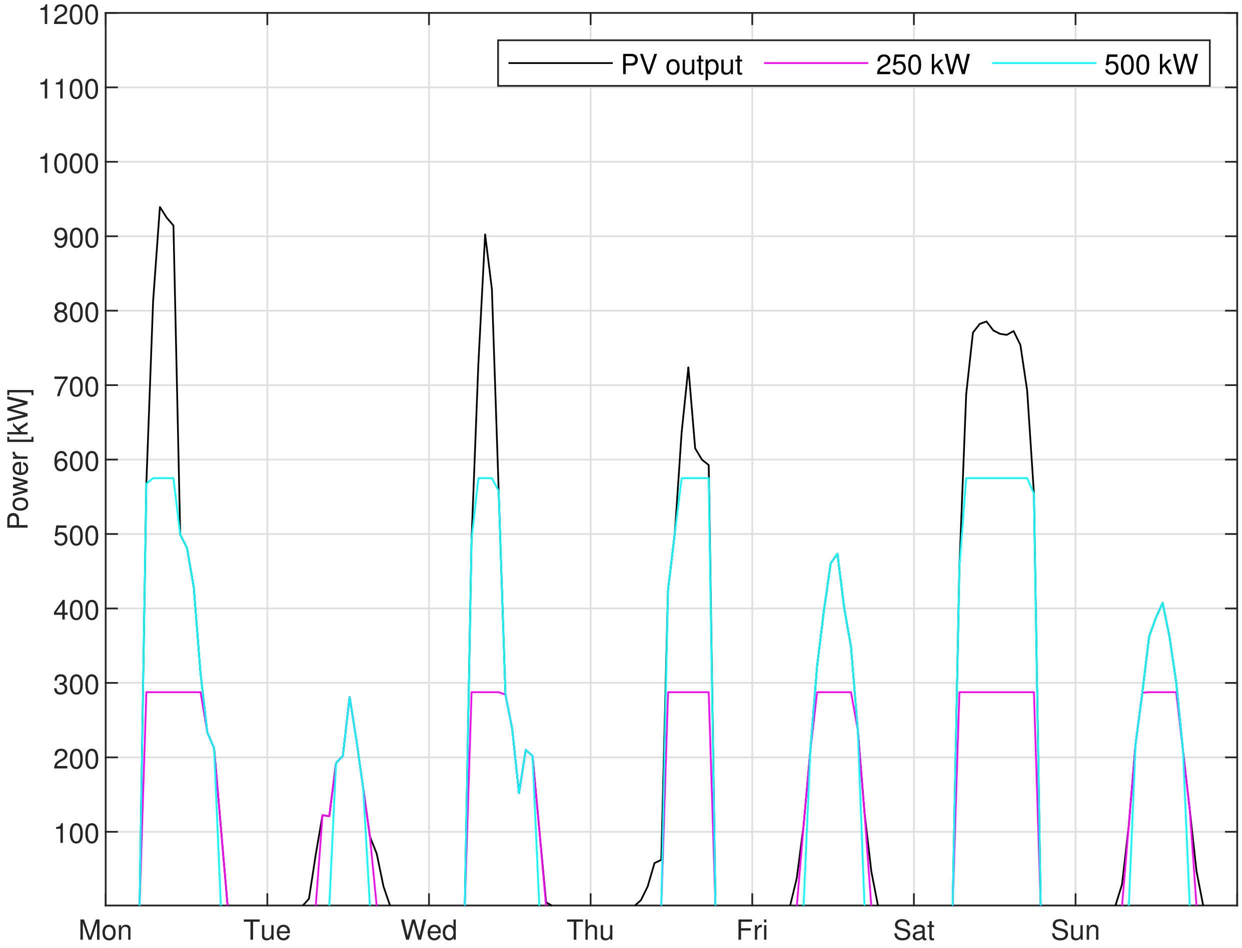

Figure 12.3: *Hourly power consumption by the electrolyzer versus PV power available, 250 kW and 500 kW, first week in January, AWE.*

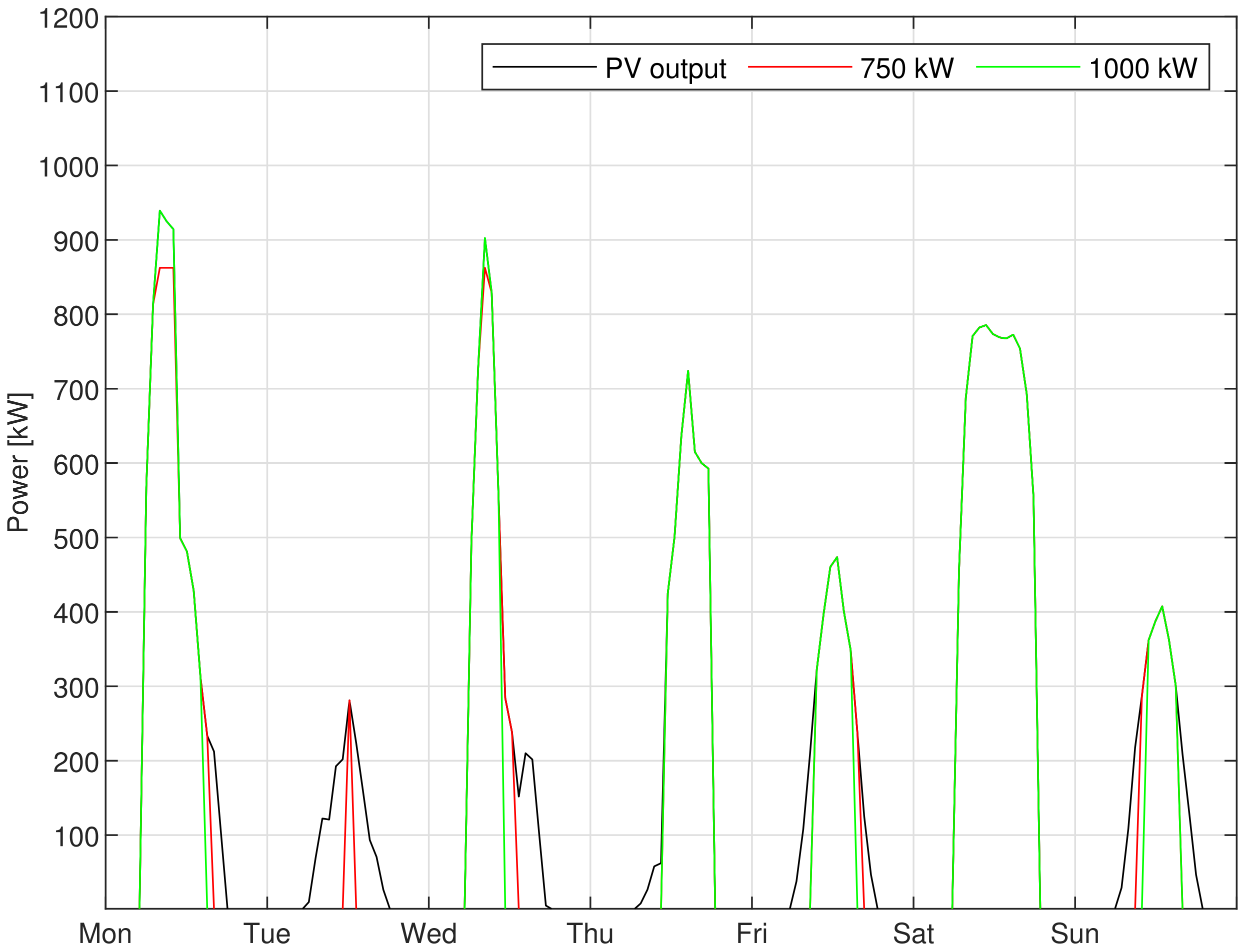

Figure 12.4: *Hourly power consumption by the electrolyzer versus PV power available, 750 kW and 1000 kW, first week in January, AWE.*

As the stack size increases the difference in system consumption and surplus energy becomes less significant. Although the 1 000kW modules maximum system range (1 150kW) is above the PV-systems nominal power of 1 000kW. The yearly consumption, surplus energy and the energy loss for the evaluated stack sizes can be seen in table 12.2.

Table 12.2: *First year hydrogen electrolyzer system consumption and solar surplus energy, AWE.*

Stack size [kW]	**System consumption [MWh]**	**Surplus energy [MWh]**	**Energy loss [%]**
250	994.7	1 242.7	55.6
500	1 734.6	502.9	22.5
750	2 126.1	111.3	5.0
1 000	2 103.4	134.1	6.0

By comparing the first year system consumption to the full capacity of the electrolyzer (24h/day), the 250 kW stack consumes 39.5% of its available capacity. The capacity loss increases with increasing stack size. The yearly production time for the different stack sizes decreases due to the system range seen in table 12.1. All values are presented in table 12.3.

Table 12.3: *First year performance, in terms of capacity, capacity loss and up time, AWE.*

Stack size [kW]	**Electrolyzer capacity [a] [MWh]**	**Capacity loss [b] [%]**	**Operational hours [c] [h/year]**
250	2 518.5	60.5	3 706 (92.1%)
500	5 037.0	65.6	3 475 (86.4%)
750	7 555.5	71.9	3 227 (80.2%)
1 000	10 074.0	79.1	3 031 (75.3%)

[a] *Continous production throughout the year.*

[b] *System consumption in table 12.2 compared to the full capacity of the electrolyzer stack size.*

[c] *Percent value is production time compared to the available power produced by PV (4023 hours 1st year).*

12.2 Hydrogen Production

Hydrogen production fluctuates close to the same manner as the PV-power production. The deviations from the power production is due to the power needed for the support equipment and compression. With the 250 and 500 kW stack, the hydrogen production is relatively stable, as seen in figure 12.5. Fluctuation is expected due to the highly variable power input. As the stack size increases to 750 and 1000 kW, the hydrogen production becomes rather unstable. The difference between the 750 and 1 000 kW electrolyzer is minor, as seen in figure 12.6. In figure 12.7 the monthly production from the different electrolyzers is compared.

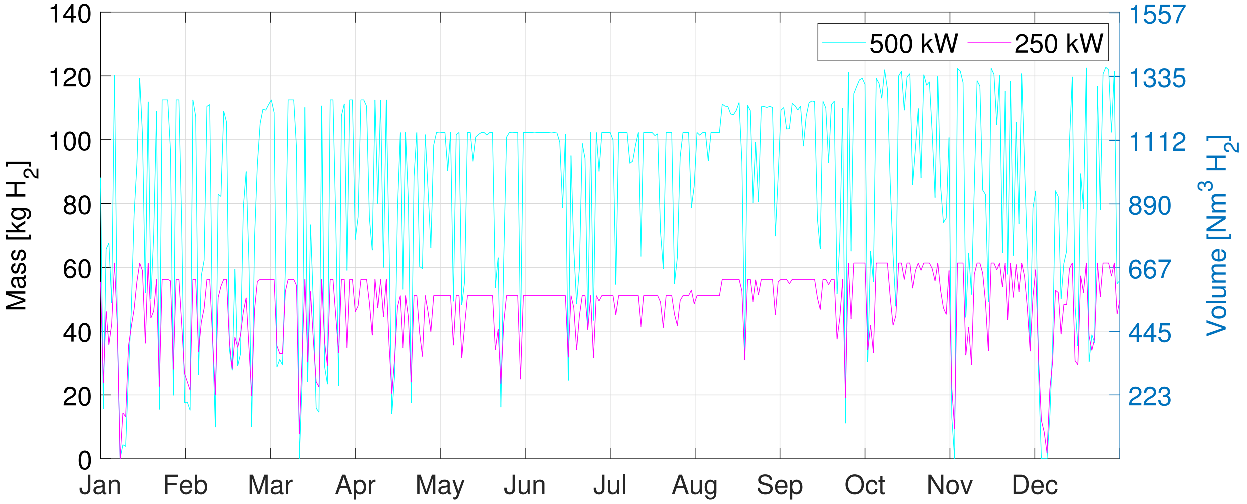

Figure 12.5: *Daily hydrogen production the first year, 250kW & 500kW, AWE.*

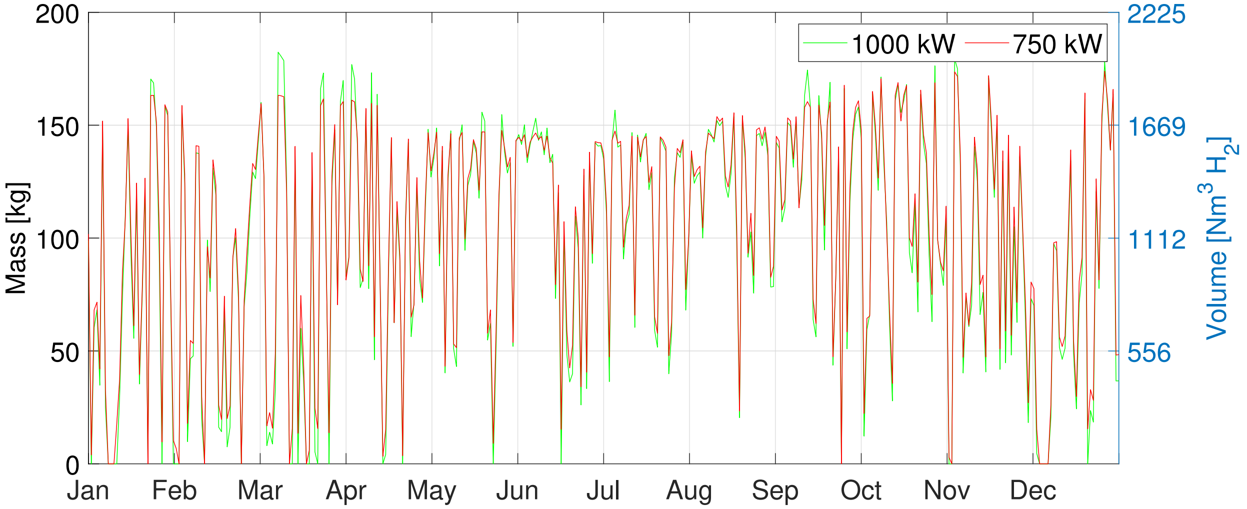

Figure 12.6: *Daily hydrogen production the first year, 750kW and 1000kW, AWE.*

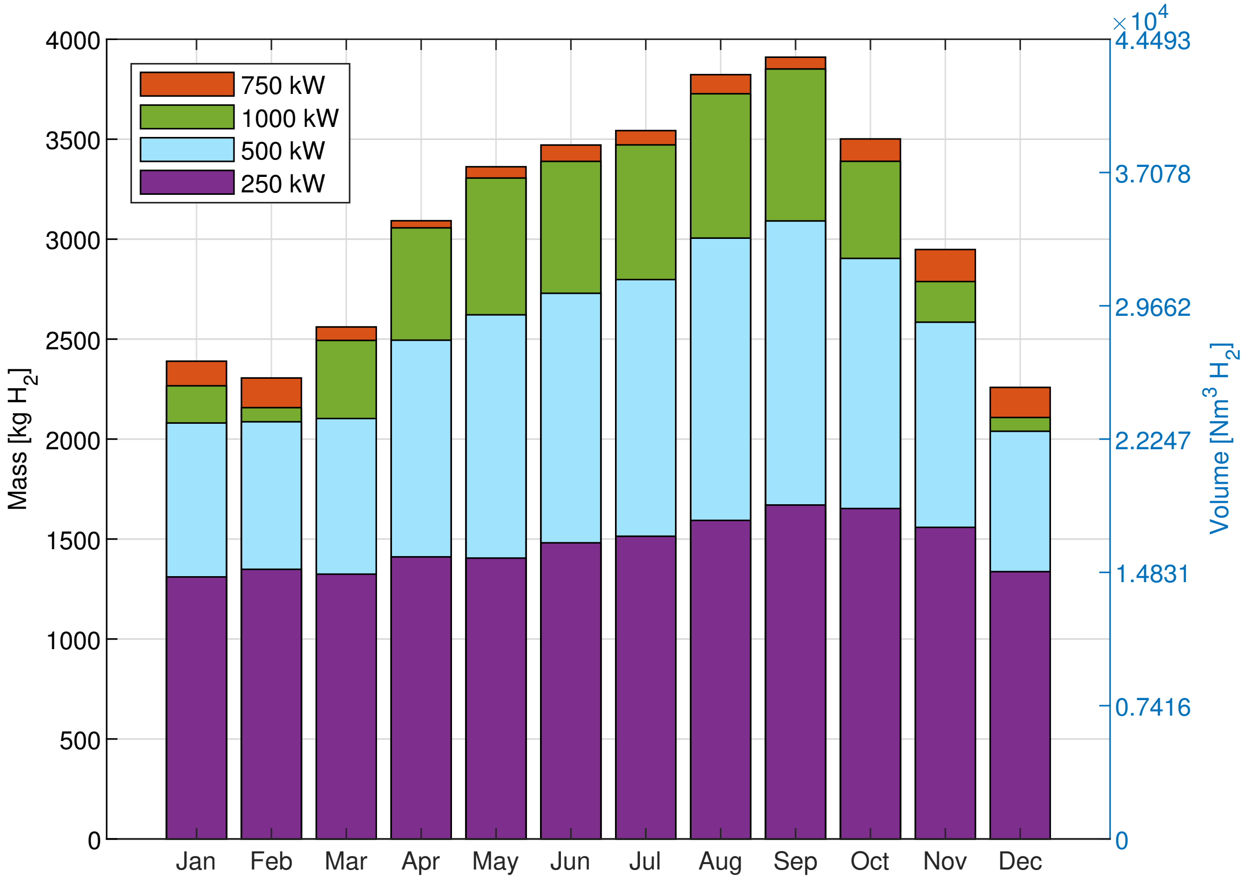

Figure 12.7: *Monthly hydrogen production, the first year, AWE.*

The 250, 500 and 750kW stacks reaches the maximum hydrogen production potential. The 1000kW stack has a maximum production of 17.8 kg H_2/h where the maximum potential is 20.4 kg H_2/h. The difference in production is largest between 250 and 500kW, and the increase in production seems to taper off after the 750kW stack size. Table 12.4 shows the first year the production for both the PV-Hydrogen system and an Ideal Electrolysis System.

Table 12.4: *First year hydrogen production, AWE.*

Stack size	**Max production**		**Production**[b]	**Production capacity**[c]
[kW]	**[kg H_2/h]**	**[Nm^3 H_2/h]**	**[kg H_2 /year]**	**[kg H_2 /year]**
250	5.1	56.7	17 607	44 676
500	10.2	113.5	30 537	89 352
750	15.3	170.2	37 166	134 028
1000	17.8[a]	198.0	36 004	178 704

[a] *Maximum production potential for a 1000kW stack is 20.4kg H_2/h or 226.9Nm^3/h.*
[b] *Hydrogen production from the PV-module.*
[c] *Max production 8 760 hours/year*

The hydrogen production declines due to degradation from both cell stack and PV-system, the effect of degradation is presented in figure 12.8. The expected lifetime for the AWE PV-hydrogen system is about 25 years of operation (≈ 87 600 hours), which equates to about 20% degradation [92].

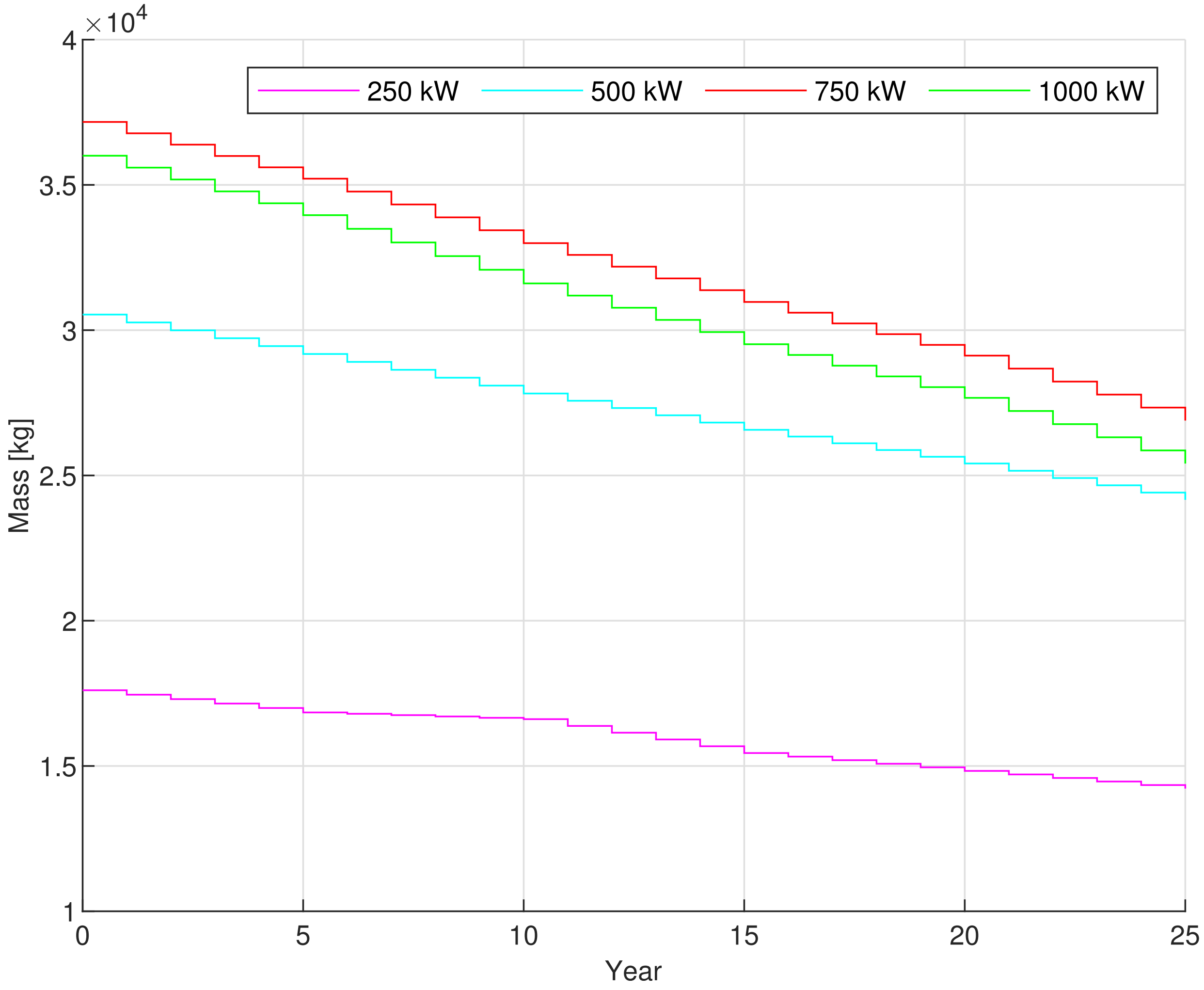

Figure 12.8: *Hydrogen production over 25 years, AWE. The decrease is due to degradation.*

Over 25 years the 250kW stack has degraded to 20.9% while the 500, 750 and 1000kW stacks is sub 20% as presented in table 12.5.

Table 12.5: *Hydrogen production and stack degradation over 25, AWE.*

Stack size [kW]	25 Year Production [kg]	Stack degradation[a] [%]
250	399 925	20.9
500	684 836	19.4
750	806 796	17.8
1000	772 595	16.5

[a] *Degradation after 25 years (20% degradation = 87 600 operational hours).*

12.3 Hydrogen Compression and Storage

NEL suggested that a storage capacity of seven days, before further transportation would be reasonable. NEL also recommended using tanks that could hold 120 kg of hydrogen at 300 bar. The number of tanks is based on the maximum hydrogen production, from figure 13.9. The total number of tanks with this capacity is presented in table 12.6.

By compressing hydrogen from 1 to 300 bar, the compressor size was considered to be 5% of the electrolyzer stack size, this was given by Norconsults supervisor. Values are presented in table 12.6.

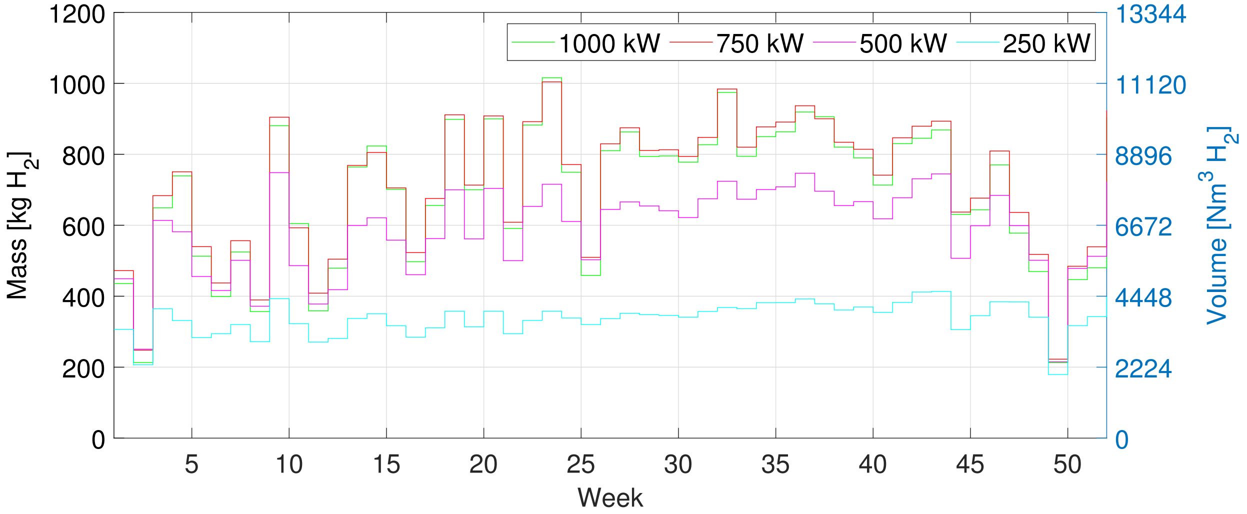

Figure 12.9: *Hydrogen production the first year, with a weekly interval, AWE.*

Table 12.6: *Compressor and tank size for each evaluated stack size, AWE.*

Stack size [kW]	**Compressor size [kW]**	**Mass [kg H_2]**	**Number of tanks**[a]
250	12.5	414.0	$3.5 \approx 4$
500	25.0	748.0	$6.2 \approx 7$
750	37.5	1004.0	$8.4 \approx 9$
1000	50.0	1016.0	$8.5 \approx 9$

[a] *Roundup value.*

12.4 Economics

For the system including the PV, AWE, compression, and storage the CAPEX was found to range from 2.97-3.95 million USD. The calculated values are presented in table 12.7.

Table 12.7: *Total CAPEX and OPEX, and the LCOE including the PV-system with tracking and AWE.*

Stack size [kW]	**CAPEX [USD]**	**OPEX [USD/year]**	**LCOE [USD/kg H_2]**
250	2 968 565	43 416	15.5
500	3 419 705	49 162	10.4
750	3 777 930	54 909	9.7
1000	3 950 325	60 656	10.8

In figure 12.10 the accumulated cost of the total system over 25 years, using a 750 kW AWE is shown. The accumulated cost is presented by the blue line and is increasing due to O&M. The other lines represent the accumulated income generated by hydrogen sales. After $\approx$ 11 years, the project reaches it payback period with the 15 USD/kg H_2 value. After $\approx$ 23 years, the project reaches it payback period with the 10 USD/kg H_2 value. The 5 USD/kg H_2 value will not accumulate enough income to make the project economical viable during the 25 year lifetime.

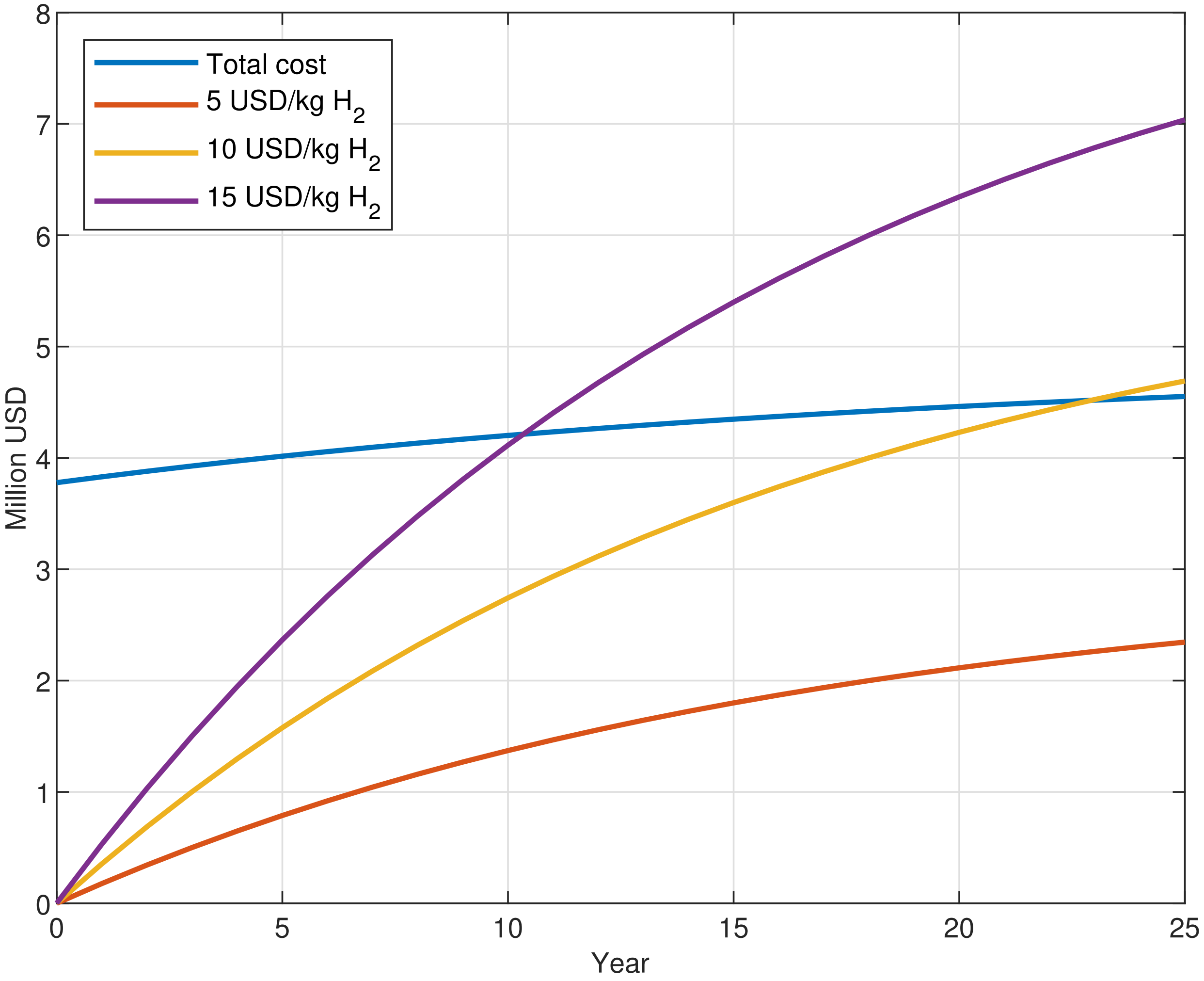

Figure 12.10: *The accumulated system cost and income for variable hydrogen prices, AWE.*

13 Proton Exchange Membrane Water Electrolysis

This section contains the results with a PEMWE, obtained from Matlab and excel calculations. Energy production from PV with a single-axis tracking system used as a reference. The PEMWE module is based on NELs M-series, the datasheet is found in appendix A. The results for the PEMWE deviate only by a small amount compared to the AWE result, the major difference is in the economical aspect.

13.1 Power Consumption

The total power consumed by the electrolyzer system is dependent on the stack size which contains the stack, support equipment, and compression. The dynamic stack range for the M-series is 0-100%. With a DC power consumption ranging from 4.3-4.9kWh/Nm^3 H_2 (47.5-55.0 kWh/kg H_2). For the electrolyzer system range, an additional 15% is added. This is based on the assumption that the support equipment equals to 10% and the compression to 5% of the power consumption. Table 13.1 contains the limits used for further calculations

Table 13.1: *System and stack ranges at different installed capacities, PEMWE.*

Stack size [kW]	**Dynamic range [kW]**	**System range [kW]**
250	0 - 250	37.5 - 287.5
500	0 - 500	75 - 575
750	0 - 750	112.5 - 862.5
1000	0 - 1000	150 - 1150

Figure 13.1 and 13.2 shows the variation in daily energy consumption compared to the PV energy available throughout the year. The difference between PV output and electrolyzer consumption is the surplus energy available.

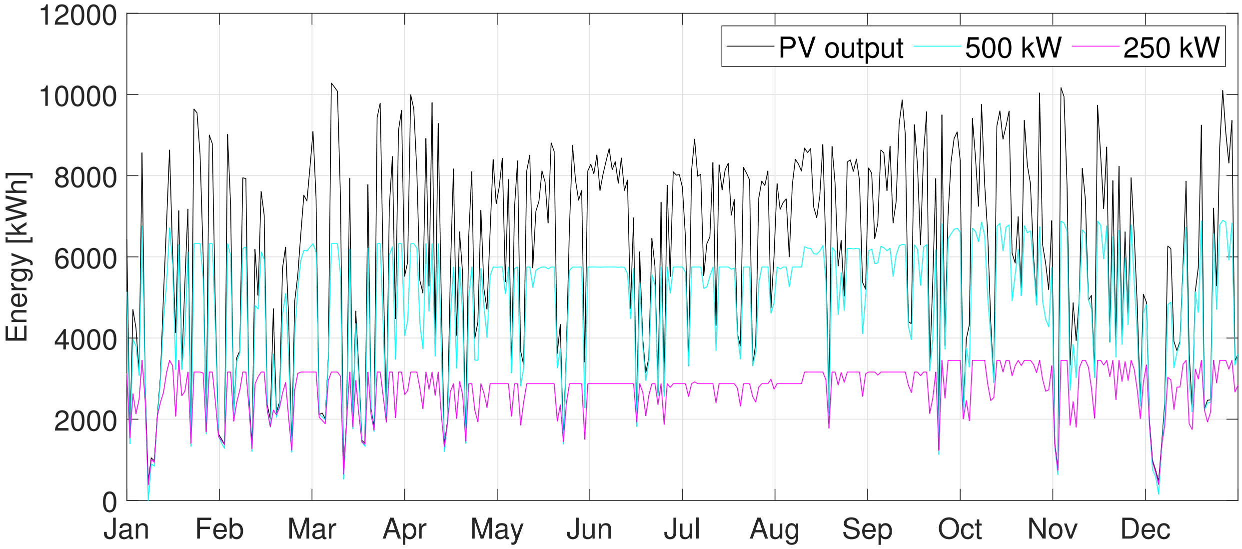

Figure 13.1: *Daily energy consumption by electrolyzer versus PV energy available, 250 kW and 500 kW, PEMWE.*

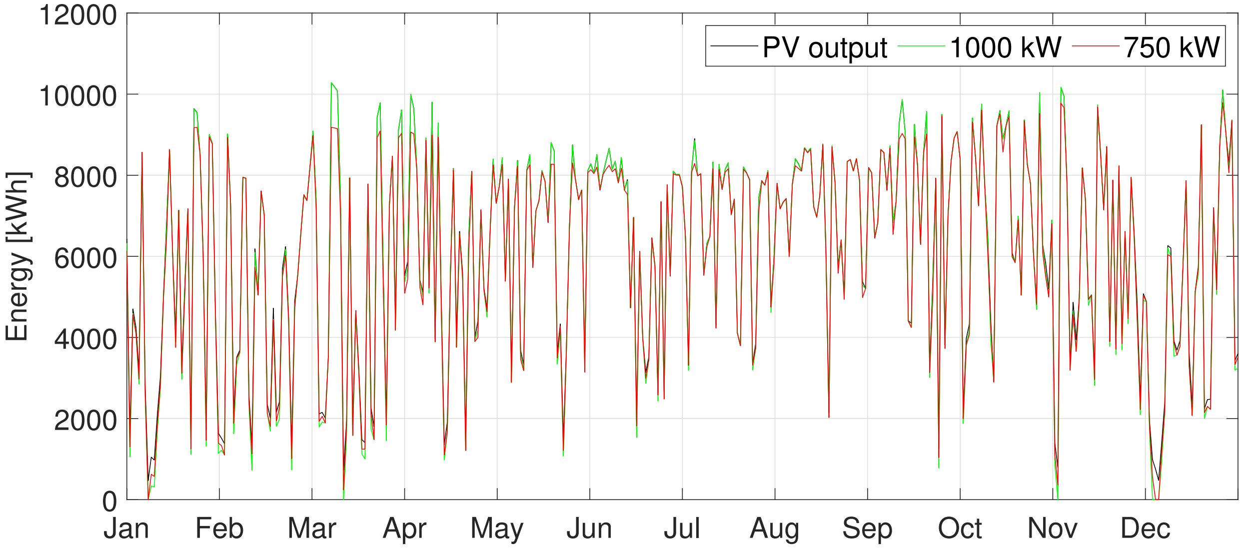

Figure 13.2: *Daily energy consumption by electrolyzer versus PV energy available, 750 kW and 1000 kW, PEMWE.*

Figure 13.3 and 13.4 shows the variation in hourly power consumption compared to the PV-power available for the first week in January.

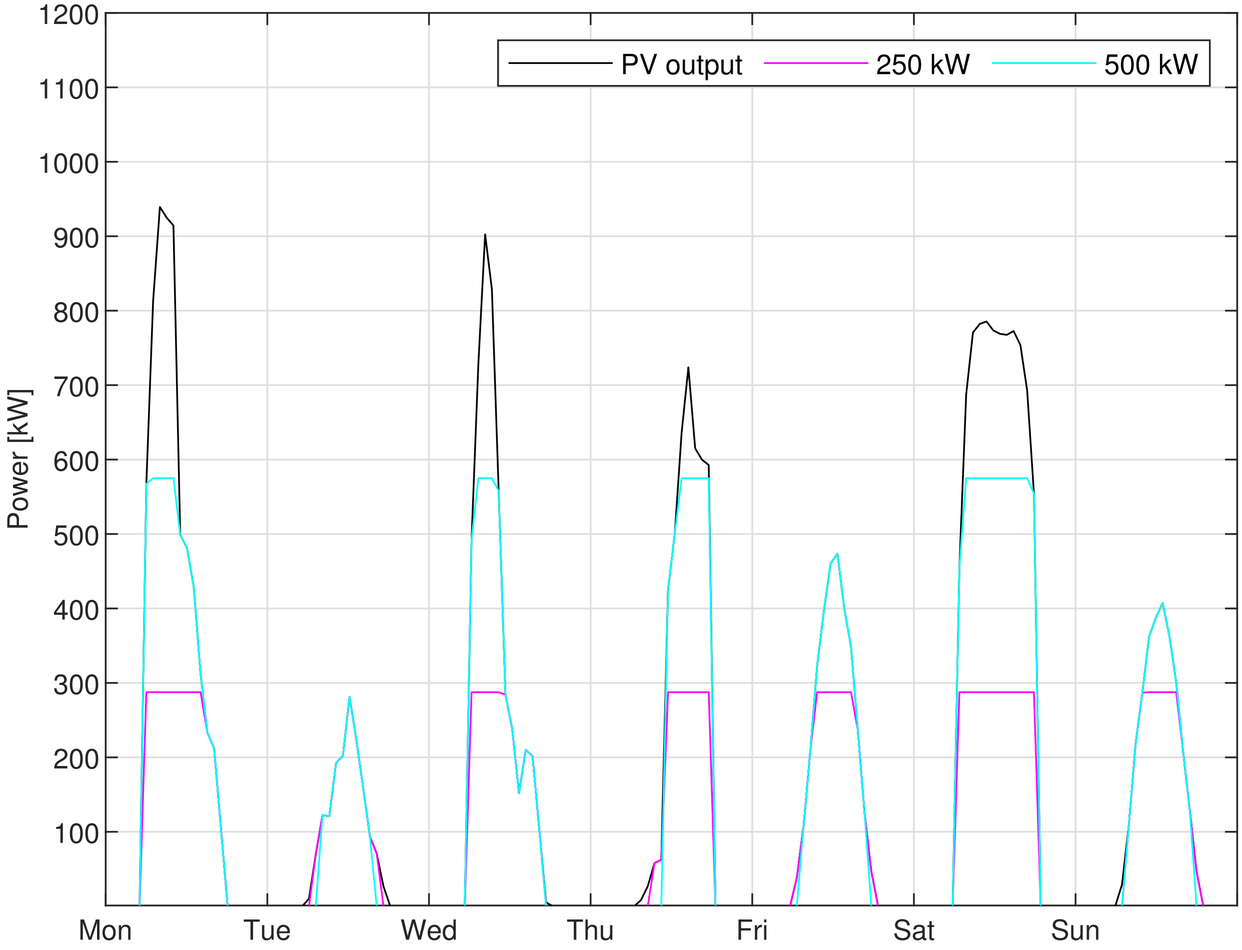

Figure 13.3: *Hourly power consumption by the electrolyzer versus PV power available, 250kW and 500kW, PEMWE.*

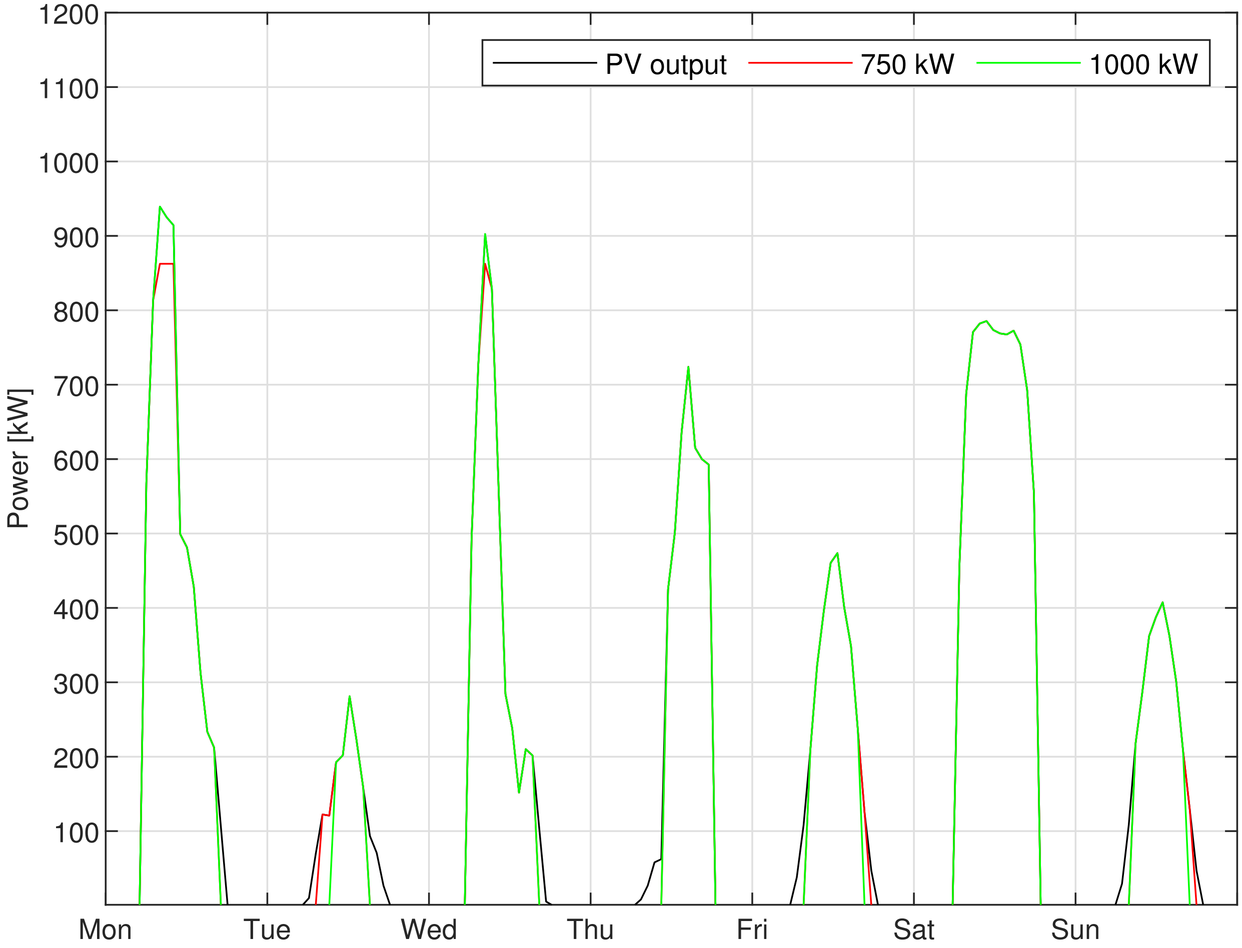

Figure 13.4: *Hourly power consumption by the electrolyzer versus PV power available, first week in January, 750kW and 1000kW PEMWE.*

As the stack size increases the difference in system consumption and surplus energy becomes less significant. Although the 1 000kW modules maximum system range (1 150kW) is above the PV-systems nominal power of 1 000kWp. The yearly consumption, surplus energy and energy loss for the evaluated capacities can be seen in table 13.2.

Table 13.2: *First year hydrogen electrolyzer system consumption and solar surplus energy, PEMWE.*

Stack size [kW]	**System consumption** [MWh]	**Surplus energy** [MWh]	**Energy loss** [%]
250	1002.3	1235.1	55.2
500	1760.0	477.4	21.3
750	2186.8	50.7	2.3
1000	2201.5	36.0	1.6

By comparing the first year system consumption to the capacity of the electrolyzer (24h/day), the 250 kW module consumes 39.8% of its available capacity. The capacity loss increases with increasing stack size. The yearly production time for the different stack sizes decreases due to the system range seen in table 13.1. All values is presented in table 13.3.

Table 13.3: *First year performance, in terms of capacity, capacity loss and up time, PEMWE.*

Stack size [kW]	**Electrolyzer capacity** [a] [MWh]	**Capacity loss** [b] [%]	**Operational hours** [c] [h/year]
250	2518.5	60.2	3841 (95.5%)
500	5037.0	65.1	3706 (92.1%)
750	7555.5	71.1	3582 (89.0%)
1000	10074.0	78.2	3475 (86.4%)

[a] *Maximum system power consumption limit multiplied with 8760 [h/year]*
[b] *System consumption in table 13.2 compared to the full capacity of the electrolyzer stack size.*
[c] *Percent value is production time compared to the available power produced by PV (4023 hours 1st year).*

13.2 Hydrogen Production

Hydrogen production fluctuates close to the same manner as the PV-power production. The deviations from the power production is due to the power needed for the support equipment and compression. With the 250 and 500 kW stack, the hydrogen production is relatively stable, as seen in figure 13.5.

Fluctuation is expected due to the highly variable power input. As the stack size increases to 750 and 1000 kW, the hydrogen production becomes rather unstable. The difference between the 750 and 1 000 kW electrolyzer is hardly noticeable, as seen in figure 13.6. In figure 13.7 the monthly production from the different electrolyzers is compared.

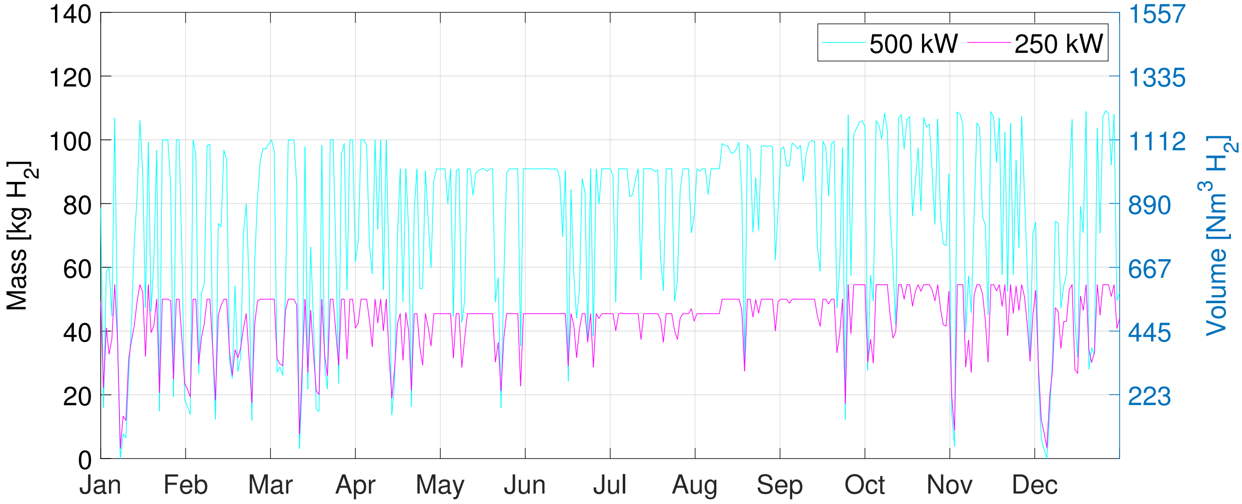

Figure 13.5: *Daily hydrogen production the first year, 250kW and 500kW, PEMWE.*

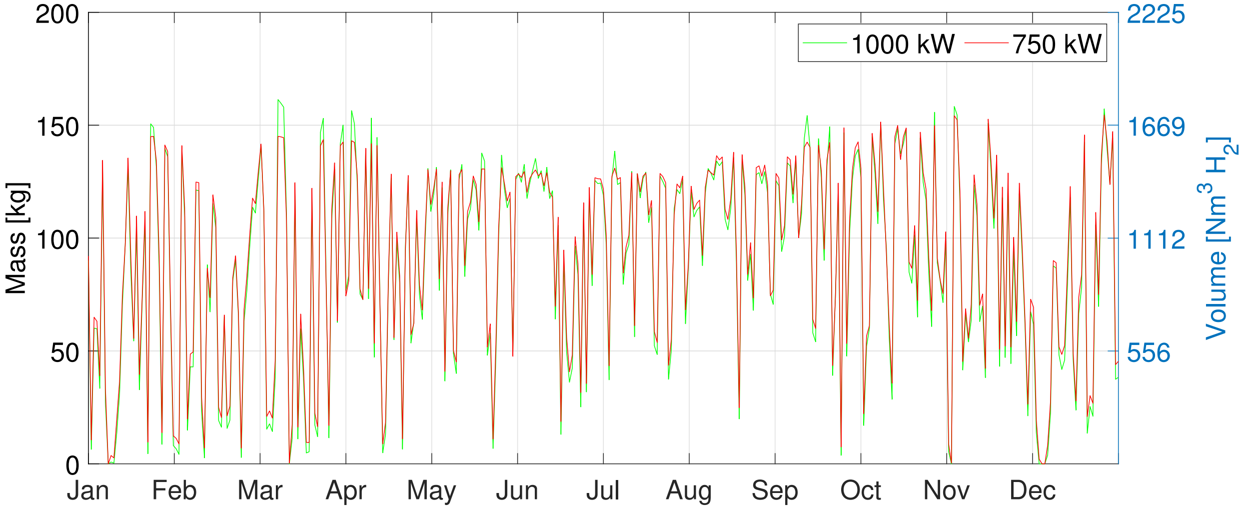

Figure 13.6: *Daily hydrogen production the first year, 750kW and 1000kW, PEMWE.*

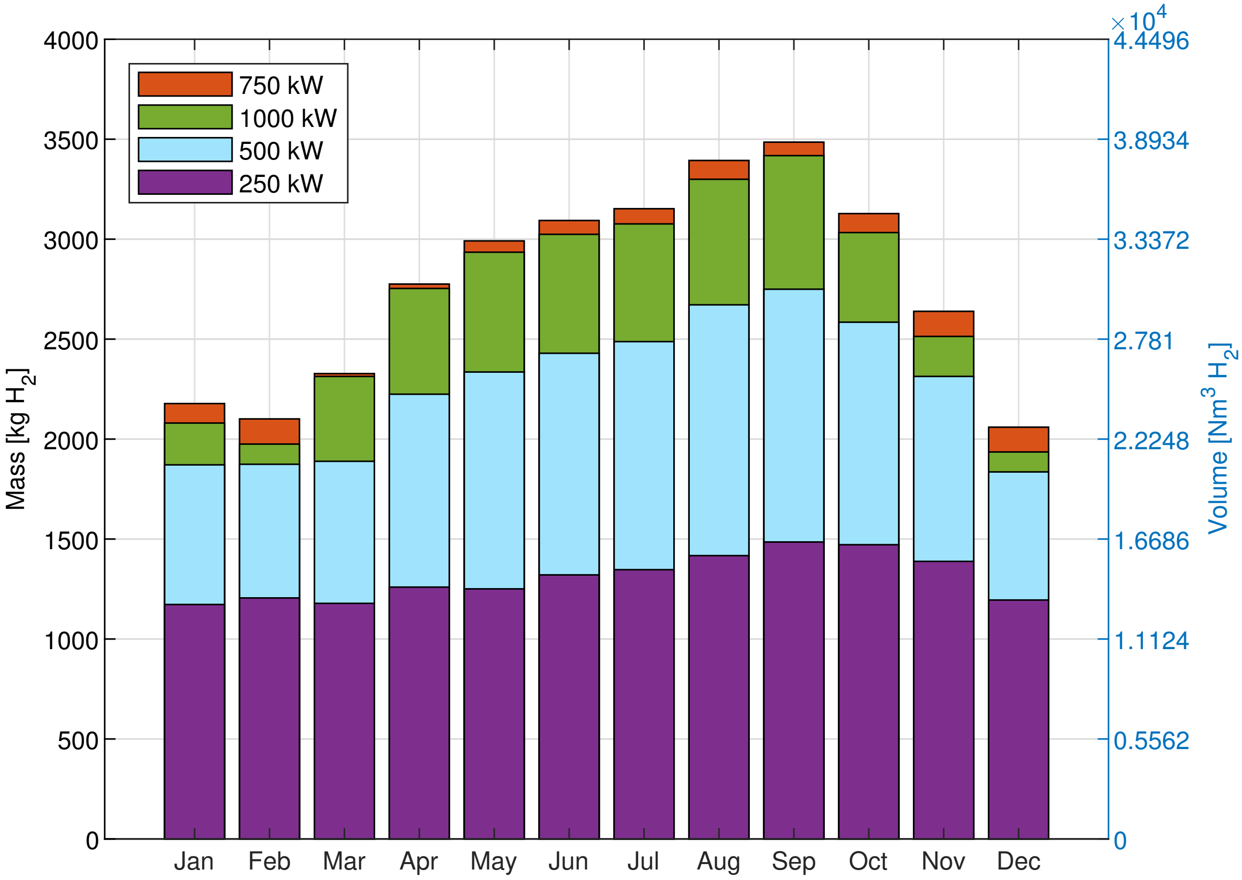

Figure 13.7: *Monthly hydrogen production, the first year, PEMWE.*

The 250, 500 and 750kW stacks reaches the maximum hydrogen production potential. The 1000kW stack only reaches a production of 15.8 kg H_2/h, the maximum potential production is 18.2kg kg $_2$/h. The difference in production is largest between 250 and 500kW, and the increase in production seems to taper off after the 750kW stack size. Table 13.4 shows the first year production for both the PV-hydrogen system and the production capacity electrolyzer system.

Table 13.4: *First year hydrogen production, PEMWE.*

Stack size	**Max production**		**Production**[b]	**Production capacity**[c]
[kW]	**[kg H_2/h]**	**[Nm^3 H_2/h]**	**[kg H_2 /year]**	**[kg H_2 /year]**
250	4.6	50.6	15 692	40 296
500	9.1	101.1	27 266	79 716
750	13.6	151.7	33 324	119 136
1000	15.8 [a]	175.5	32 357	159 432

[a] *Maximum production potential for a 1000kW stack is 18.2kg H_2/h or 202.2 Nm^3/h.*

[b] *Hydrogen production from the PV-module.*

[c] *Max production 8 760 hour/year.*

The hydrogen production declines due to degradation from both the cell stack and the PV-system, the effect of degradation is presented in figure 13.8. The calculated lifetime of a PEMWE is about 5 years of operation ($\approx$ 20 000 hours), which equates to about 20% degradation [92]. The time before a stack is replaced is approximately 5 years, as seen in 13.8.

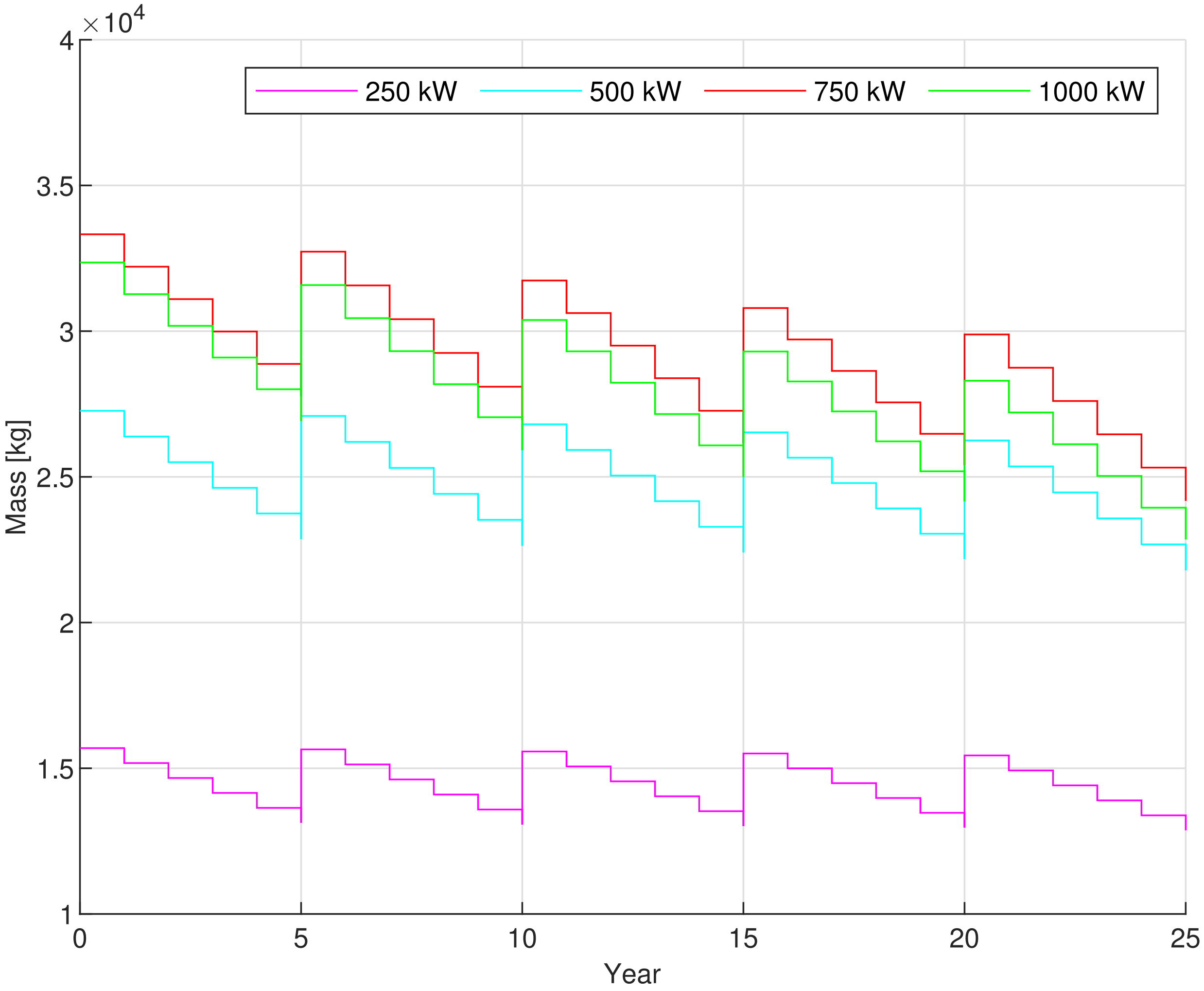

Figure 13.8: *Hydrogen production over 25 years, PEMWE. The production fluctuation is due to membrane degradation and replacement.*

After 5 years the 250, 500, 750 and 1000kW stacks is sub 20% as presented in table 13.5.

Table 13.5: *Hydrogen production and stack degradation over 25 years, PEMWE.*

Stack size [kW]	25 Year Production [kg]	Stack degradation[a] [%]
250	363 671	19.15 ± 0.5
500	625 555	18.40 ±1.0
750	736 251	17.75 ± 1.5
1000	705 463	17.15 ± 1.5

[a] *Degradation after 5 years (20% degradation ≈ 20 000 operational hours).*

13.3 Hydrogen Compression and Storage

NEL suggested that a storage capacity of seven days, before further transportation would be reasonable to assume, and that using tanks that could hold 120 kg of hydrogen at 300 bar. The number of tanks is based on the maximum hydrogen mass, produced with a seven day interval over the first year, using values from figure 13.9. The total number of tanks with this capacity is presented in table 13.6.

By compressing hydrogen from 1 to 300 bar, the compressor size was considered to be 5% of the electrolyzer stack size, this was given by Norconsults supervisor. Values is presented in table 13.6.

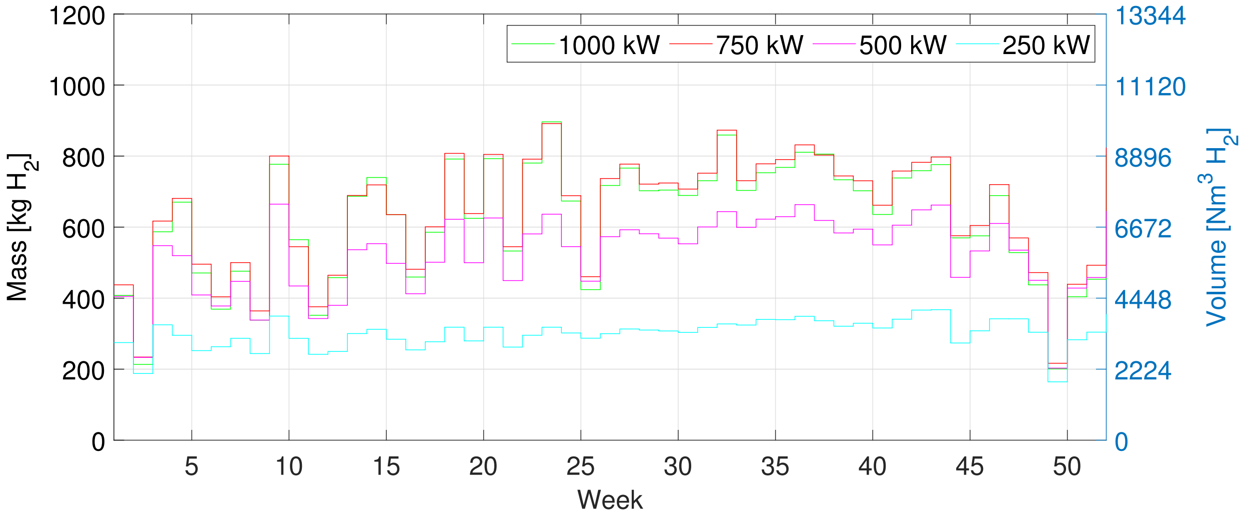

Figure 13.9: *Hydrogen production the first year, with a weekly interval, PEMWE.*

Table 13.6: *Compressor and tank size for each evaluated stack size, PEMWE.*

Stack size [kW]	Compressor size [kW]	Mass [kg H_2]	Number of tanks[a]
250	12.5	368.0	$3.1 \approx 4$
500	25.0	665.0	$5.5 \approx 6$
750	37.5	892.0	$7.4 \approx 8$
1000	50.0	896.0	$7.5 \approx 8$

[a] *Roundup value.*

13.4 Economics

For the system including the PV, PEMWE, compression, and storage, the CAPEX was found to range from 3.28 - 4.70 million USD. OPEX for the PV-system was assumed to be 0.8% of its OPEX based on literature. OPEX for the PEMWE system was estimated to be 2.5% of its CAPEX. With a discount rate of 5%. The calculated values is presented in table 13.7.

Table 13.7: *Total CAPEX and OPEX, and the LCOE including the PV-system with tracking and PEMWE.*

Stack size [kW]	CAPEX [USD]	OPEX [USD/year]	LCOE [USD/kg H_2]
250	3 284 623	47 008	21.3
500	3 879 425	54 909	14.7
750	4 381 313	62 811	14.0
1000	4 697 370	70 712	16.0

In figure 13.10 the accumulated cost of the total system over 25 years, using a 750 kW PEMWE is shown. The accumulated cost is presented by the blue line and is increasing due to O&M and stack replacement. The other lines represent the accumulated income generated by hydrogen sales. Only the 15 USD/kg H_2 is economically feasible, and the sufficient income will be generated after ≈ 20 years. The other hydrogen values will no generate enough income to make the project economical sustainable during the 25 year project time.

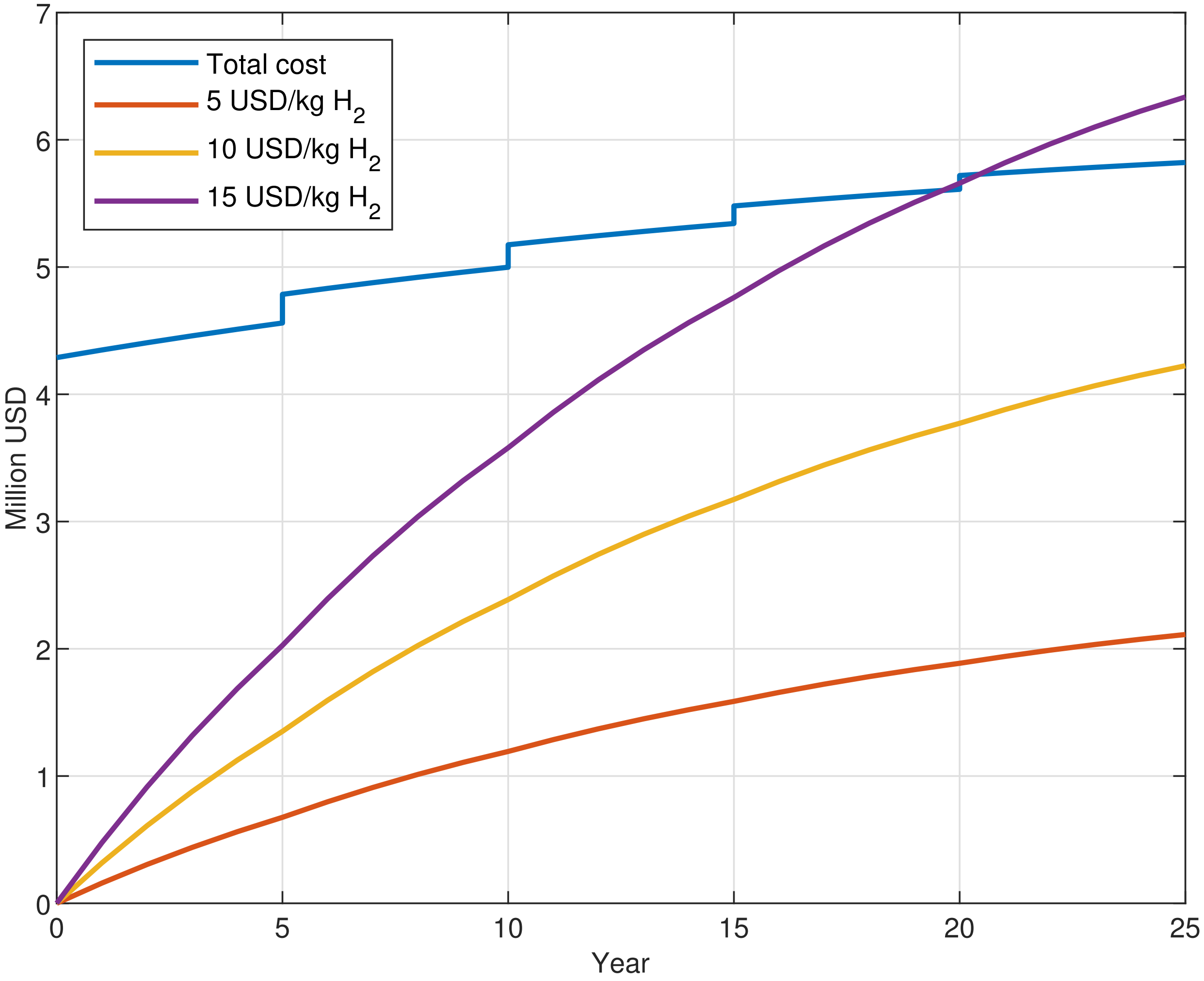

Figure 13.10: *The accumulated system cost and income for variable hydrogen prices, PEMWE.*

14 Surplus Energy

In this section, the amount of surplus energy from the Matlab calculations will be presented. How an ideal storage system will affect hydrogen production and the investment cost regarding storage of the surplus energy for an AWE will be presented.

The surplus energy produced each day is highly variable due to climatic conditions affecting the PV-plant output. Figure 14.1 and 14.2 shows the surplus energy produced each day throughout the year.

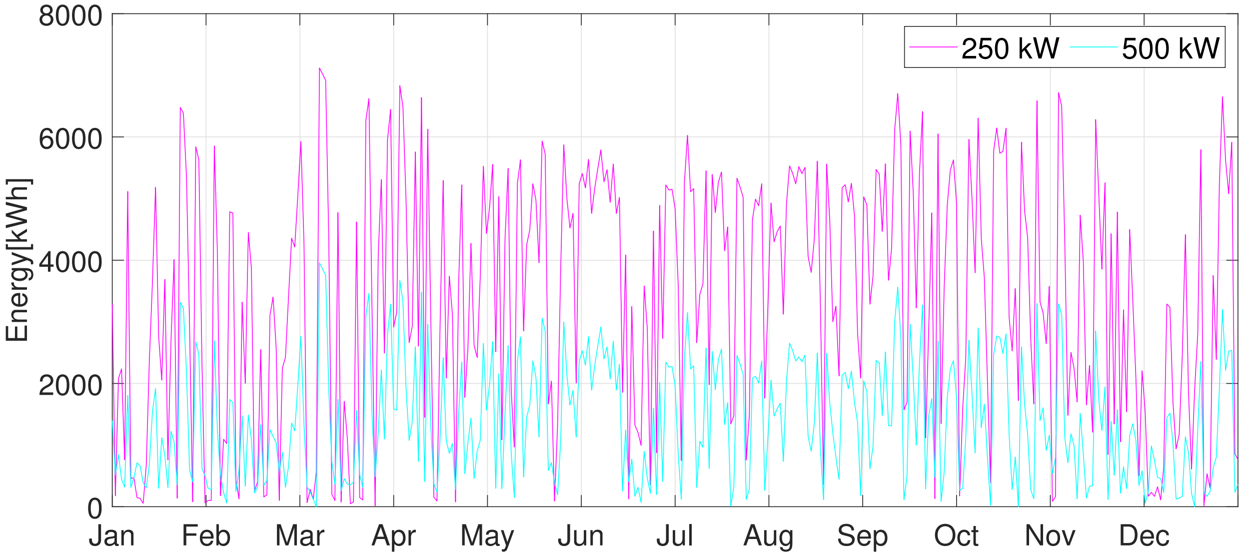

Figure 14.1: *Daily surplus energy, 250 kW and 500 kW, AWE.*

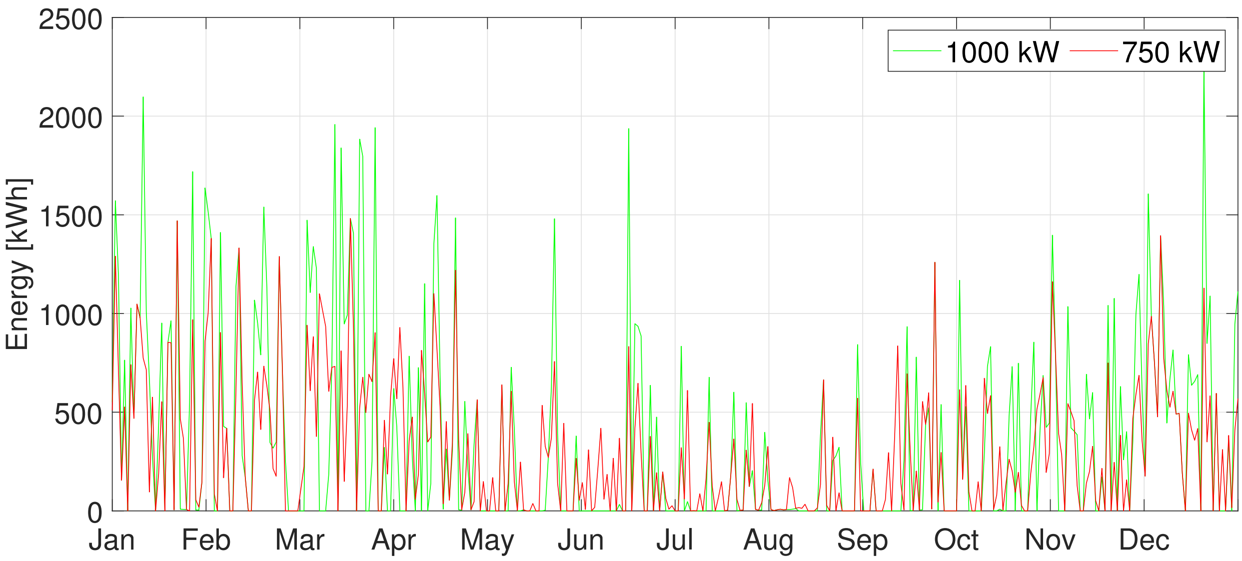

Figure 14.2: *Daily surplus energy, 750 kW and 1000 kW, AWE.*

Table 14.1 shows a comparison of how much surplus energy each cell stack will have, and maximum daily surplus energy.

Table 14.1: *Surplus energy of the system, relative to the electrolyzer stack size, AWE.*

Stack size [kW]	**Mean surplus energy [kWh/day]**	**Maximum surplus energy [kWh/day]**
250	3 404.7	7 118.6
500	1 377.8	3 956.1
750	305.0	1 481.3
1 000	367.3	2 242.8

14.1 Ideal Energy Storage

Figure 14.3 shows the energy consumption with an ideal secondary energy storage system for the 250 and 500kW stack size. The 750 and 1000kW stack plot is not presented as the energy loss is assumed to be insignificant.

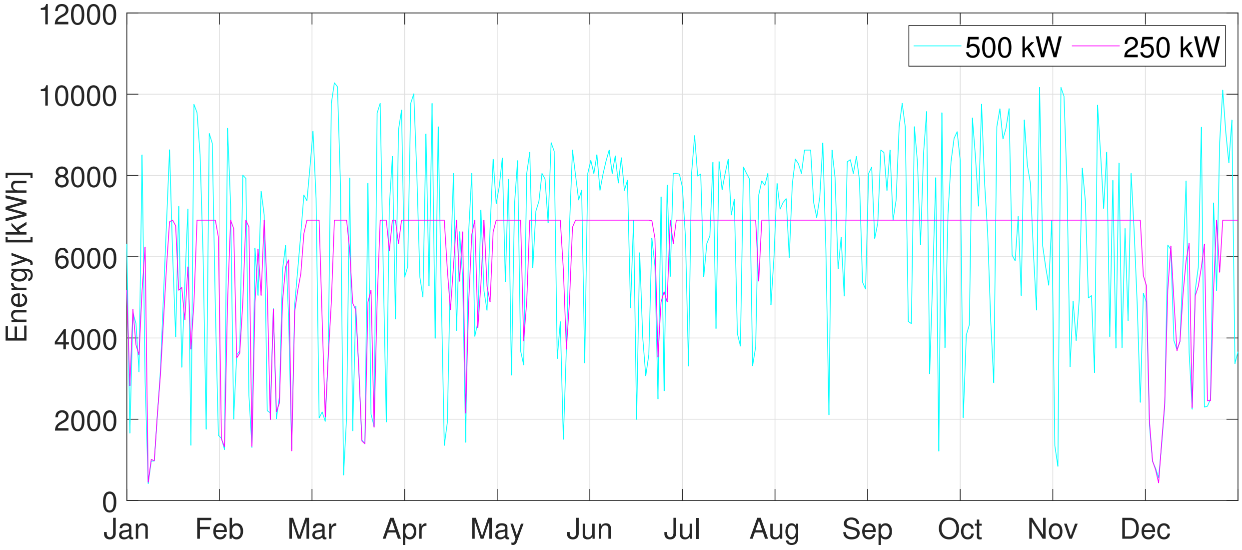

Figure 14.3: *Energy consumption with an ideal secondary energy storage system, 250 kW & 500 kW, AWE.*

Figure 14.4 shows the variation in power consumption throughout the 1st week in January with an ideal ESS.

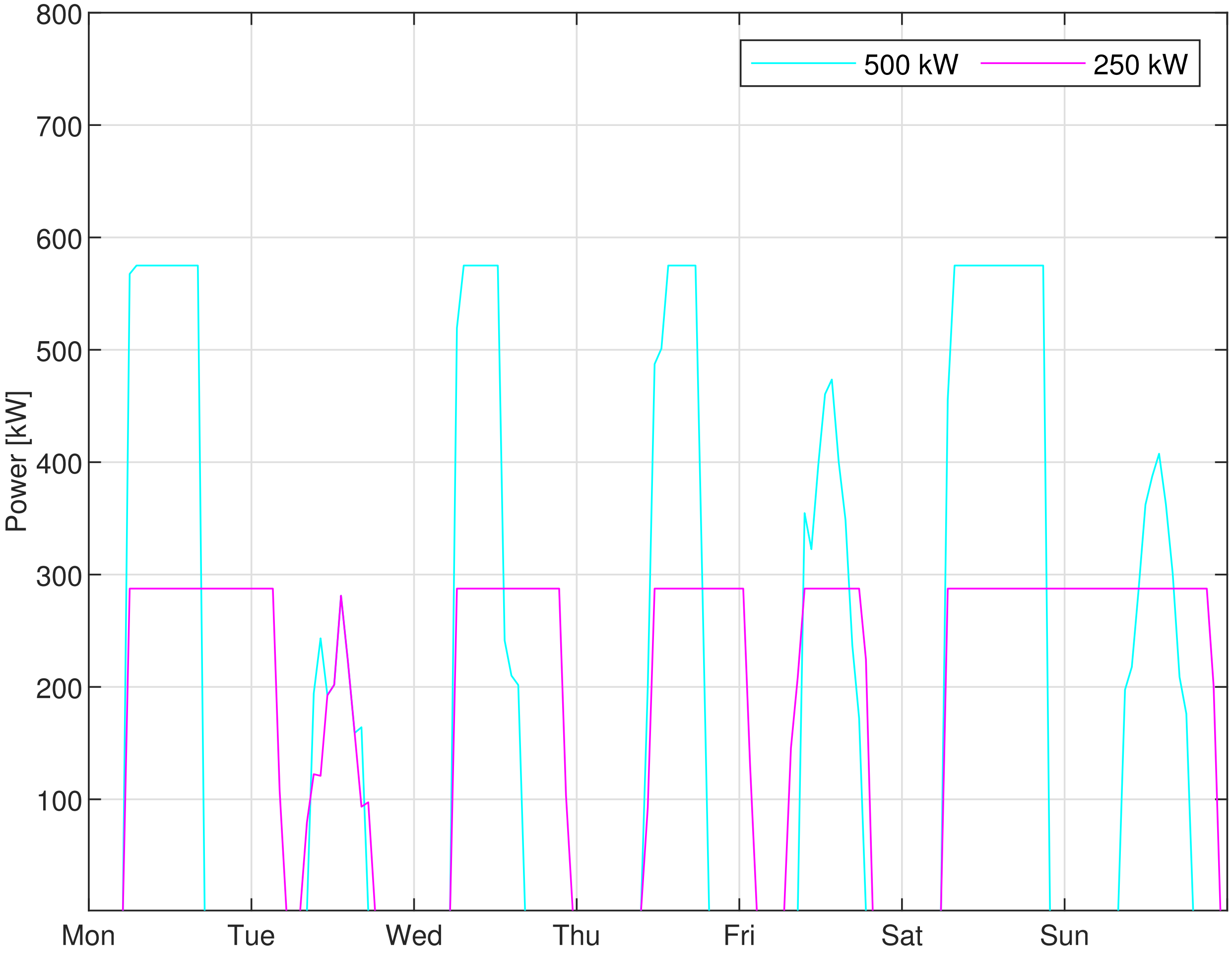

Figure 14.4: *Hourly power consumption with an ideal secondary energy storage system. First week in January, 250 kW & 500 kW, AWE.*

Table 14.2 shows the increase in hydrogen production with an additional Ideal ESS (100% efficiency and unlimited capacity).

Table 14.2: *Hydrogen production with an Ideal Energy Storage System, AWE.*

Stack size [kW]	**Production with ESS [kg H_2]**	**Increased H_2 production [%]**	**Operational time [h/year]**
250	39 639	125.1	7 882
500	39 433	29.1	4 382
750	39 006	5.0	3 447
1000	38 125	5.9	3 293

14.2 Economics

Table 14.3 shows the cost to store the maximum surplus energy from table 14.1, with different storage systems. The cost per kWh for batteries is from table 6.1, the average price for an installed system is used in the calculations (500 USD/kWh for lead acid and 2125 USD/kWh for Lithium Ion). The cost per kWh for mechanical storage is from table 6.2, and the *Median Energy CAPEX* value is used.

Table 14.3: *The CAPEX for an additional energy storage system to store the maximum surplus energy for different stack sizes, values in USD.*

	250 kW	**500 kW**	**750 kW**	**1000 kW**
Lead acid	3 559 300	1 978 050	740 650	1 121 400
Lithium ion	15 127 025	8 406 713	3 147 763	4 765 950
PHS	234 914	130 551	48 883	74 012
CAES	84 569	46 998	17 598	26 644
FES	6 406 740	3 560 490	1 333 170	2 018 520

Discussion

This segment provides the final analysis of the obtained results and discusses which factors will affect the feasibility of the project. The thesis main goal is to examine the feasibility of producing hydrogen from a 1 MW PV-system, in Zambia. The practical challenges regarding implementing such technologies in the region will be taken into consideration.

15 Zambia

The Zambian economy is quite vulnerable to fluctuations in international copper prices. This is because approximately three-quarters of the national export product is copper. Investment in a hydrogen infrastructure could help strengthen the economy and make it more flexible. Hydrogen as a resource can be used in multiple areas such as fuel in the transport sector, as a chemical component in the industry, and the storage medium in the power sector. The investment in hydrogen infrastructure could contribute to increased international trading, job creation and electrification.

The current power sector in Zambia is highly dependent on the seasonal rainfall in the region, due to the reliance on the installed hydropower capacity. Diversification of the energy sources could help strengthen the energy sector. This could lead to reduced loss associated with load shedding and energy shortage in the industry. Flexible energy storage, such as hydrogen, could be a viable alternative to assist in the electrification of the nation.

Grid connection is usually considered the most reliable power supply available in the industrialized world, this is due to frequency regulation and the potential of diversified energy sources available. This might not be the case in Zambia. Where load-shedding is a major tool to combat energy shortage. Places where a steady power supply is critical, diesel generators often supply the remaining energy demand. Alternative energy sources could be implemented, to increase reliable access to electricity.

The electrification of the rural population in Zambia is demanding. The majority of the population does not have access to electricity. The existing grid in large parts of the region is also lackluster, especially in rural areas. The pre-existing road infrastructure is not well suited to support electric expansion in large parts of the nation either. The investment capital to expand and improve the transmission grid is lacking, especially in the public sector, where foreign debt is a major issue.

The current expansion in the transmission is happening in the north-south corridor through Zambia, where the southern hydro capacity is connected to the main mining industry load in the north. This expansion is heavily incentivized due to the increased demand for power from the mining industry. The corridor already has a high-voltage transmission and with acceptable road connectivity.

In many cases, despite high investment costs, grid connections could be favorable, Due to high capacity, flexibility, and longevity. In regions where the transmission is lackluster or non-existing, alternatives could be considered. Off-grid facilities that could function as micro-grids for small cities or villages could eliminate the need for new or upgrading existing transmission lines.

16 Photovoltaics

PV is regarded as an established technology and is deployed to residential, commercial and utility scale. The Zambian power industry is already investing in multiple large scale PV-plants, where multiple international actors are involved. This provides a promising outlook when considering future PV-facilities in the region. The Zambian government has also proclaimed PV-development to be a focus of attention in the energy sector, to help combat the current energy shortage in the region.

The solar irradiation in Zambia is high, because of the position relative to the equator. The climatic drawbacks of the region are the high average temperature and the rain season, these factors could lead to a loss in efficiency. Although the temperature is high, it is still inside the acceptable range for solar-modules. It was not considered necessary to have any additional cooling system for the PV-system, but it could prove to be beneficial by increasing the efficiency.

The main concerns when choosing the PV-modules are price, efficiency, and reliability. The most common technology deployed in the industry is crystalline silicon. This is because of higher efficiency and longevity compared to e.g. thin film. Which are two important criteria for this study. The experience in the field makes the technology relatively easy to implement compared to hydrogen electrolysis.

According to ZESCO, the acquisition of land is not an issue in Zambia. This impression was further solidified after the field trip and the literature review. Because of the population- and elevation distribution, large areas of grassland remain unused. These areas could be used for large scale PV-facilities in the future.

This is the main reason for choosing a poly-crystalline module instead of a mono-crystalline. Poly-crystalline has lower efficiency per m^2 but is cheaper, which would lead to an overall lower investment cost. The module chosen for the simulations is the CS3U-345P-FG, from Canadian Solar Inc, due to having a high power output and considered to be a reliable module, with a 30-year warranty.

16.1 Inverter

Choosing the correct inverter/converter for the PV-system was not emphasized due to the scope of this project. PVsyst has a function for simulating an off-grid DC PV-system, but due to a software error, this was not possible. The simulation is therefore conducted with two 500 kW generic DC/AC inverters from the PVsyst database. Some research indicated that the efficiency difference between the DC/AC inverter and DC/DC converter is not substantial ($\approx$5%) at max load. Similarities in the transient characteristics are also present. From this, an assumption is made that this did not have a substantial impact on the final results of either cost or power production. From the literature review, it is found that a DC/DC converter with an MPPT is a preferable choice.

16.2 Fixed Tilt and Tracked Configuration

The main differences between fixed tilted and a single-axis tracking system are the increase in annual energy output from the PV and the cost associated. A tracking system with a range of ± 60 ° in the north-south axis and a fixed tilt of 18° in the east-west axis, increases the 1st year energy production by 28.6% compared to only having a fixed tilt of 18°in the east-west axis. The tracking system also contributes to stabilizing the power output and achieving higher power output in the early mornings and late evenings. This is preferable when having a load that demands continuous supply to function optimally.

The PVsyst simulation did not take into account the shading effect on nearby PV-panels. This is solved by calculating the shading effect a module had, and increase the total area accordingly.

For the fixed tilt a 5.2% increase of the area in the north-south direction with equal spacing between the PV-panels would be sufficient to ensure that the panels would stay clear of the shading. Although it would be preferable to adjust the fixed tilted angle approximately 2-4 times a year to maximize the power output and minimize the land coverage, due to the zenith angle changes throughout the year. This adjustment has not been taken into account in the simulation or analysis.

For the single axis tracking system a 110.4% total increase in area and an equal spacing between the rows in east-west direction is deemed to be sufficient to prevent shading on nearby modules. The shading that occurs at early mornings and late evenings will affect the power output of the PV-plant, as the tracking stops at ±60° and the sun has a theoretical positioning of ±90°. This shading has not been taken into consideration in the simulations. Therefore the realistic output is most likely lower than the simulated result.

The increase in the total occupied area for the tracking system is deemed acceptable. The geographic conditions coupled with a relative large urbanization percentage in Zambia results in large uncultivated areas that are suitable for hosting large scale PV-plants.

16.3 PV Economics

The production cost of PV-modules has been steadily decreasing in the later years and this trend is likely to continue. Increased attention towards the technology will contribute to the increase in development and competition, which could help drive the prices further down.

The total CAPEX in USD/W DC for the PV-system is obtained from NRELs "U.S Solar Photovoltaic System Cost Benchmark: Q1 2017". The cost of a 1 MW PV-system is extrapolated to 1.5 USD/W DC and 1.62 USD/W DC respectively for fixed tilt and with a tracking configuration. By considering the extrapolation and regional dependency, the CAPEX can be expected to deviate from the prices in Zambia.

According to Hilton M. Fulele, from the Copperbelt Energy Corporation, the 1 MW PV-plant constructed in Kitwe, has an estimated CAPEX of 1.3 million USD, and that future project could have a CAPEX of 1.1 million USD, due to improved logistics. Other than the nominal output, system specifics of the facility that Mr. Fulele referred to, is unknown. The CAPEX used in the thesis analysis is substantially higher, at 1.5 million USD for fixed tilt and 1.62 million USD for tracked configuration. A lower overall system cost will contribute to the economical feasibility of a PV-hydrogen system.

The increase in CAPEX for a tracked configuration relative to only having a fixed tilt is found to be 8%. Due to the cost and maintenance of the mounting and gear system, the OPEX of a tracked configuration is also higher, this is not takin into consideration in the thesis. The results showed that a tracking system is preferable due to the lower LCOE. Tracked configuration resulted in 0.060 USD/kWh, compared to the fixed tilted system at 0.072 USD/kWh. The overall cost per kWh decreases with approximately 15.3% the first year when choosing a tracked configuration rather than fixed tilt only.

17 Electrolyzer Module

Values for the electrolyzer modules in this thesis are based on NELs M-series (PEMWE) and A-series (AWE). The results indicates that the A-series is the better option, due to higher efficiency and lower overall system cost.

17.1 Electrolyzer Technology

In a situation where the amount of power will fluctuate predictably on a day/night cycle, and an electrolysis cell will have to be turned off daily, a high-temperature electrolyzer would not be optimal. The amount of energy and time used to re-heat a SOWE or MCWE daily would be detrimental for the overall efficiency of the facility. These types of electrolyzer cells will also have to be closely monitored due to the high operating temperatures, which would increase the OPEX. If the heat is supplied by heat-intensive industries, the high-temperature cell could prove to be a viable option, due to the high overall efficiency that could be achieved.

Another challenge is the quick changes in power output from an intermittent energy source. This is problematic due to the fluctuations of the cell-voltage in the electrolyzer cell. If there are no modifications done to the system, a PEMWE would be better suited. Due to the membrane in a PEMWE limits gas-crossover which can occur with rapid voltage fluctuations. There is also no delay due to inertia, as it would be with a liquid electrolyte.

These short-term fluctuations could most likely be mitigated through quick responsive small scale storage, such as batteries or flywheels. This storage system would only be responsible for supplying power in the amount of time these fluctuations occur, with the main purpose to avoid unnecessary stress on the electrolyzer.

The main differences between an AWE and a PEMWE cell can be summarized in three parameters: cost, efficiency, and flexibility. PEMWE is more expensive due to the material used in the membrane, and has lower efficiency, but is more flexible due to the design. The opposite is true for an AWE. The choice between the modules is, therefore, a choice between the amount of hydrogen produces and the investment cost of the cell. Even though the PEMWE utilizes more of the solar power and has a wider system range, the AWE produces more hydrogen due to higher efficiency. The results indicated that AWE will be the better choice, due to lower overall system cost and higher efficiency. The design advantages with PEMWE has not been taken into consideration in the simulations.

17.2 Electrolyzer Stack Size

The main problem with an electrolyzer that is only supplied with electricity from a solar cell, is the fluctuating power-input. Electrolyzer-modules functions best with a continuous and stable electricity supply. Rapid fluctuations will result in deterioration of the electrolyte and electrodes. The day/night cycle will result in sub-optimal power input during the day and daily start/stop of the electrolyzer. This means low yearly hydrogen production, and loss associated with reheating the electrolyte.

Another problem is the surplus energy generated when the electrolyzer stack size is below the power output of the PV-plant. The surplus energy could either be considered as 100% loss, stored in short-term ESS, stored in long-term ESS or be sold directly to the transmission grid, if available. Additional short-term and long-term energy storage technologies could be considered, to shift the surplus solar energy into periods where there is possible to produce hydrogen. This will enable the electrolyzer to produce more hydrogen but will increase the overall system cost.

The cost of an electrolyzer will increase with size, as seen in table 12.7 and 13.7. For both AWE and PEMWE, the same trend in stack size and associated hydrogen production is the same.

As the stack size increases the difference between the PV-power output and the energy demand of the electrolyzer decreases. Because of this, the fluctuations in hydrogen production increases with the stack size. The highly variable power input could result in undermining the structural integrity of the electrolyzer. Even though the effect of a highly variable power input has not been taken to into consideration, it is worth noting for an extended continuation of this thesis.

The smaller stack sizes have a more stable hydrogen production compared to the larger stack sizes, due to the electrolyzer system range is within the PV-output more of the time. Despite having an unstable hydrogen production, the bigger stack sizes produce more hydrogen, due to the wider system range. The upper system range limit for the 1000 kW stack, exceeds the nominal power output of the PV system, which indicates that a 1000kW electrolyzer is oversized for a 1000 kW PV-plant. The results support this since the 750kW stack produced more hydrogen than the 1000kW stack in the Matlab calculations.

The operational time of the electrolyzer decreases when the stack size increases. This is because the lower system range limit increases, resulting in less time where the system is able to produce hydrogen. This reduces stack degradation in the simulations since the degradation rate is based on operational time.

Although the energy consumption is highly variable on a daily basis, the 750 kW produces the most hydrogen of the evaluated stack sizes. The PV output is mostly within the system range, which results in the least loss of surplus energy. This system is far from optimal, compared to the potential hydrogen production from the electrolyzer stack size.

17.3 Electrolyzer Degradation

The degradation has not been thoroughly investigated due to the scope of this thesis. The impact of the variable power input, temperature fluctuations and the degradation on standby has on the cell stack is not simulated. Instead, the degradation is assumed to have a linear relationship over the operational lifetime that is selected for the AWE and PEMWE.

The AWE stack is found to have a lifetime of approximately 87 600 hours (10 years) of continuous operation before replacement. Due to the intermittent power supply, the different AWE electrolyzers reach 20% degradation after approximately 25 years. The 250 kW stack exceeded the 20% limit (20.9%), but the larger stacks are still below 20% at the end of the 25 evaluated years. Replacement of the 250 kW AWE stack is deemed to be unreasonable economically, so close to decommissioning.

PEMWE is found to have a lifetime of approximately 20 000 hours ($\approx$ 2.3 years) of continuous operation, which is substantially lower than the AWE. After reaching 20 000 hours of continuous operation, it is assumed that the degradation is 20% for the PEMWE. In the simulations, a 5-year interval before replacement is assumed, due to simplicity. However the degradation is found to vary more dependent on stack size than assumed, and none of the stack sizes reached 20% degradation before replacement. A more precise replacement time could have positively affected the economic feasibility.

It is difficult to predict the lifetime of a cell stack, as the estimated lifetime is often given in wide intervals and deviate between different sources. The stack should preferably be replaced when the loss in income exceeds the cost of a new stack, this would be closely monitored in an actual system. Finding a reliable source where the electrolyzer had been supplied from a variable power input at this scale is without success, and should get more attention in a potential future project.

17.4 Hydrogen Transformation and storage

This thesis includes different hydrogen transformation and storage methods, including compression, liquefaction, metal hydride absorption, and chemical conversion. Only mechanical compression is analyzed due to this was deemed to be the most cost-effective option.

Hydrogen electrolysis delivers hydrogen in a gaseous state, with low volumetric energy density compared to other fuels. For any practical application, it is necessary to increase the volumetric energy density.

Mechanical compression is a well tested, common technology that is widely used for multiple applications. For stationary storage and on-site usage, compression is often deployed due to volume constraints not being the limiting factor. Pressurized hydrogen can be stored for long periods, and has a negligible self-discharge. For this scale and situation, compression and pressurized storage seem to be the best option.

Liquid hydrogen has a high energy density volumetrically ($\approx$ 70 kg/Nm^3). The method is generally deployed where there are volumetric constraints or the end-user requires liquid hydrogen. Liquid storage is considered unfit for a system that is only being supplied by an intermittent energy source. Liquid hydrogen transformation and storage do not justify the increased investment in both cost and energy expenditure for this particular system. There are also multiple challenges associated with long term liquid hydrogen storage, especially the boil-off, which reduces the overall efficiency of the process significantly.

Metal hydride storage is a promising candidate for future commercial hydrogen storage. This is due to the safety advantage and high volumetric energy density. The long absorption time is not ideal when having a high production rate. This mismatch between storage time and production rate will lead to the need for either additional hydrogen storage or solar energy storage. Metal hydride will most likely not be an ideal option for hydrogen storage at the production site. The high system weight is most likely not a major problem regarding stationary storage, but the high CAPEX would not justify the investment.

Hydrogen used as a chemical component is the most common way of handling hydrogen today. Compounds that carry hydrogen is therefore well known in the hydrogen industry. These compounds usually have a high volumetric hydrogen density.

Producing pure hydrogen from electrolysis and binding it with other compounds for either transport purposes or as a chemical compound is an interesting opportunity. The process plant that is required to do such a conversion safely on a large scale is however costly. Where existing infrastructure that handles these hydrogen carrying compounds (ammonia, methane) is present, this could be a relatively cost-effective and safe method to distribute and handle large scale hydrogen production.

From the literature review and conversation with NEL, compression storage seemed to be the most fitting option for this system. Liquefaction of hydrogen would most likely require a substantial amount of energy from the PV, and therefore limit the hydrogen production rate. Metal hydride is assumed to be too expensive and ill-suited to store the volume of hydrogen produced. Chemical conversion is probably not a cost-effective option for this facility, due to the scale and additional investment cost associated. The storage option selected is based on price, efficiency, and simplicity. Hydrogen compressed to 300 bar and stored in steel tanks is deemed to be the cheapest practical alternative available. A generic mechanical compressor that could handle compression from 0 to 300 bar is chosen, based on recommendations from the industry.

18 Surplus Energy Storage System

The following section will evaluate the feasibility of an additional energy storage system for the PV-Hydrogen system.

Due to the surplus energy generated and the power fluctuations produced by the PV-Hydrogen system. The power production does not follow an ideal consumption pattern for the electrolyzer. The function of a secondary energy storage system is to shift the surplus energy into periods where the electrolyzer can produce hydrogen or to mitigate rapid power fluctuations.

With an ideal energy storage system, the increase in hydrogen production is substantial for the 250 kW stack size. The hydrogen output increased by 123.1% by taking advantage of the surplus PV-energy. It is also worth noting that operational time increased from 3 706 to 7 882 hours per year. To invest in an additional energy storage system for the smaller stack sizes could be cost-effective if the gain in hydrogen production outweighs the increased cost. It is worth emphasizing that the results are for an ideal energy storage system. A realistic storage system will have efficiency loss related to the storage cycle.

The alternative energy storage system evaluated in the thesis is divided into two groups, batteries, and mechanical storage. The batteries evaluated are Lead Acid and Lithium-Ion batteries. Mechanical energy storage consists of Pumped Hydroelectric Storage (PHS), Compressed Air Energy Storage (CAES) and Flywheel Energy Storage (FES).

The most important parameters considered in the thesis regarding an additional energy storage system that is going to be compatible with the PV-Hydrogen system are response time, cost/kWh and efficiency.

18.1 Battery Energy Storage System

Batteries are suitable for the PV-Hydrogen system in many aspects; they have fast response time, low self-discharge rate and high efficiency. This makes them ideal to mitigate the rapid fluctuations in power output from the PV. A stable power input could help decrease the degradation of the electrolyzer.

The investment cost associated with the battery capacity required to shift the surplus energy generated is substantial. The investment cost seems to outweigh the income that could be generated by the additional hydrogen produced.

18.2 Pumped Hydroelectric Storage

PHS is relatively cost-effective compared to the other storage systems, especially batteries and flywheel energy storage. It is an interesting option in Zambia, due to the number of hydroelectric power plants installed. If there are areas where the geographical conditions are met for PHS, this could be an interesting way of utilizing and optimizing the nation's hydropower. Reliability, flexibility and low cost of storing a large amount of energy are some of the reasons why this is an attractive option for optimizing the PV-Hydrogen System. The PHS can shift the surplus energy into periods when PV-energy is unavailable or the system range is not optimal for the input.

The construction of new PHS-systems is often associated with high investment costs. The geographical conditions must be met for these projects to economical feasible, large scale transmission lines might have to be built, agriculture and environmental impacts needs to be accounted for. The cost of constructing a new PHS-system for the sole purpose of optimizing the PV-Hydrogen system is difficult to justify. Especially on the system scale relevant in this thesis.

If there is a pre-existing, large scale PHS-facility available, an additional PV-Hydrogen system could be an interesting hybrid solution.

18.3 Compressed Air Energy Storage

The optimization of the PV-Hydrogen system could be feasible with CAES. Due to the fast response time, scalability and low self-discharge rate. If pre-existing underground areas are available, this system could have a low environmental impact and overall investment cost.

CAES is suitable for both large- and small-scale energy storage. Smaller systems (<100kW) are more flexible than large scale systems, due to the utilization of pressure tanks, which are not geographic dependable. Large scale systems require increased storage volumes, such as underground caverns, to be practical and economically feasible.

There are multiple requirements for underground caverns to be suitable for energy storage: sufficient volume, minimal leakage and ability to handle thermal stress. These conditions have to be met and will limit the locations where a CAES-system can be implemented. The research of suitable CAES locations in Zambia has not been conducted due to the scope of this thesis.

18.4 Flywheel Energy Storage

An FES-system could be suitable for mitigating the rapid fluctuations in power output from the PV to the electrolyzer. This is due to the high efficiency for short duration storage, low response time, and high capacity. The FES-system can also be located independent of geographical conditions. Safety risks associated with the amount of kinetic energy that could be released due to shattering is something that must be taken into consideration when implementing the system.

The high self-discharge rate and investment cost are factors that make FES less suited for shifting the surplus energy produced by the PV-Hydrogen system. The gain in increased hydrogen production is most likely less than the additional capital cost of the total system.

19 System Economics

In the current economic and political landscape in Zambia, there are many challenges to face. Fortunately, a large part of the international community is committed to the development and implementation of renewable energy. This could help projects that would not be economically feasible in the short to medium term, to receive subsidies and be realized.

The prices given by NEL is a rough estimate, and the price of an electrolyzer will vary dependent on the region, energy source, scale, and production requirement. In this thesis, the overnight investment cost for this particular system scale and production is taken into account. By increasing the system scale, the overall cost per unit produced would most likely decrease due to the economy of scale.

The CAPEX for an electrolyzer module is quite high, but it is expected to decrease in the following years. The need for energy storage and more research and development in the field could make hydrogen as an energy storage alternative more economically attractive in the future. According to NEL, due to highly tailored production methods today, standardized mass production of electrolyzers in the future, could decrease the cost of a module by 30% alone.

The LCoE calculation for the PV-Hydrogen system is found to vary, due to the mismatch between power output from the PV and the electrolyzer system input. For the 250 kW stack size, the PV-system seemed to be over-dimensioned, which results in a relatively stable hourly/daily hydrogen production, but a large surplus energy quantity, this results in the highest LCoE for all of the calculated stack sizes. By increasing the stack sizes, the LCoE decreased up to the 750 kW stack size. The 1000 kW stack is calculated to have a higher LCoE compared to 750 kW, due to lower hydrogen production and higher CAPEX.

PEMWE has a significantly higher LCoE than AWE for all the evaluated stack sizes, due to the higher CAPEX and lower efficiency relative to AWE. This could indicate that the electrolyzer stack size should be in the vicinity of 750 kW, for an off-grid PV-system with the selected configuration in this thesis, and that an AWE could be the optimal technology.

The payback time of approximately 11 years for the 750 kW AWE electrolyzer, is based on the assumption that the hydrogen could be sold for 15 USD/kg. The hydrogen price is based on the equivalent fuel price for driving an FCEV and CGV in Zambia. However, the current investment cost for an FCEV could be higher than for a CGV, which would have to be taken into account when considering investing in a hydrogen vehicle.

20 Assumptions and Limitations

In the final economical analysis, it is assumed that 100% of the hydrogen is sold. This assumption is made to see the possible amount of income that could be generated by the hydrogen produced. In reality, this number would most likely be lower, and the market price of hydrogen could fluctuate. The marked price fluctuations could both be beneficial and unfavorable for the economic sustainability of the project. The hydrogen prices do not include the additional cost associated with transportation and distribution of the hydrogen. Which would most likely increase the overall cost for the end consumer.

The calculations are based on stack size and the DC power consumption from NELs datasheet for the A-series and the M-series. The calculated values deviate from the numerical indications of the specific modules. The output in Nm^3 H_2/h from the 500 kW AWE used in the simulations is slightly higher than it would be for an A100. Since the price estimate from NEL is a rough estimated value, this deviation is deemed to be insignificant, and therefore would not affect the final economic analysis.

The cost for the 250 and 750 kW stack size was not specified by NEL and is acquired by interpolation and extrapolation. These values is deemed to be an acceptable approximation since it was stated that the stack size where upgradeable in 250 kW increments.

The complete system LCoE calculation is limited to 25 years. As the PV-module has a 30 year warranty a mismatch between the PV and electrolyzer module is unavoidable, to make up for this mismatch the systems residual value should have been subtracted from the CAPEX, with a present value at the end of the 25th year. There is not found any way to determine the residual value of a PV system in Zambia, therefore the residual value is assumed to cover the decommissioning cost.

Since the PEMWE has a significantly higher CAPEX than the AWE, approximately 32-50% higher, dependent on the electrolyzer capacity. This directly impacts the electrolyzer OPEX, since it is directly calculated from the electrolyzer CAPEX. The electrolyzer OPEX is also expected to cover the O&M cost of the storage tanks. These estimates is based on correspondence with Norconsult for the AWE 500 kW and assumed to be true for the economic calculations of all stack sizes, for both AWE and PEMWE. This adds to the inaccuracy of the analysis.

The increased CAPEX of the PEMWE is mainly due to the rare earth metals used in the PEMWE stack. The accumulated cost of the PEMWE increases throughout the 25 years, due to the relatively low life of the PEMWE stack. The expected lifetime of the stack is calculated from the operational hours per year with an estimated linear characteristic. Degradation at the 25th year varies between the stack sizes, due to the difference in operational hours. The degradation at standby has not been taken into consideration due to the scope of this project. The degradation rate could be higher, due to corrosion at standby and the fluctuating power input.

A stack should realistically be replaced when the loss of income exceeds the cost of a new stack. This economic evaluation has not been considered, due to the lack of an established hydrogen infrastructure and hydrogen market price in Zambia. This particular analysis is therefore considered outside the scope of this thesis.

Estimated CAPEX given by NEL for the electrolyzer modules includes a compressor. The compressor cost is a fixed amount ($\approx$ 115 000 USD) and is added to the price estimate for all of the electrolyzers. In reality, as the hydrogen production rate increases/decreases the compressor capacity and cost will vary. This is not taken into account as the CAPEX given for the electrolyzer and compressor is already a rough estimate.

The O&M cost is based on the CAPEX and is a fixed amount. The increase in O&M cost throughout the years due to increased wear and tear has not been taken into consideration. In reality, the stress on the system will accumulate and different components will most likely need replacement or more maintenance over its lifetime.

Any additional lye cost is not considered in the analysis. This is due to the assumption that the cost related to lye is included in the OPEX of the AWE.

Additional cost regarding the feed water and cooling system has not been taken into account, due to the scope of this thesis. The cost regarding this will be highly regional dependent.

Downtime due to maintenance is not expected to affect the production hours, due to the intermittent energy source leaves a maintenance window during the night. If prolonged maintenance is required, this would negatively affect the overall hydrogen production.

Storage systems come in a wide range of capabilities, price, and appliances. The large intervals they often are depicted in, make a comparison of storage methods difficult. This results in an inaccurate CAPEX calculation. The values calculated in the result section are therefore used for a rough comparison only.

During the literature review and field trip, the attempt was made to get information about the transmission and electricity consumption pattern in the region. The companies and government agencies in Zambia were reluctant to share this information. Therefore the simulations and calculations is done without considering this.

Conclusion

The energy sector in Zambia is heavily reliant on hydropower to serve the energy demanding mining industry, which consumes over half the electricity produced in the nation. Hydrogen production and storage systems, supported by PV-plants, could contribute to solving the electrification and energy-related challenges in Zambia. The implementation of alternative energy production and storage capabilities would also diversify and reinforce the current energy mixture. This thesis assessed the economic and technological aspects of implementing a hydrogen production and storage system, supported by a 1MW PV-plant.

By simulating and examining different configurations for an off-grid 1MW PV-plant. The conclusion is that a 750 kW AWE system is the most beneficial solution. The system has an LCOE of 9.7 USD/kg H_2 for the projected 25-year lifetime. This system would utilize 27.8% of the hydrogen production capacity.

If the power from the PV-system is fully exploited. With an ideal energy storage system, the results indicate that the 250 kW AWE is the better choice. By fully exploiting the power delivered from the PV, the system will utilize 88.6% of the hydrogen production capacity.

Based on the literature review and the result analysis, the conclusion is that a PV-Hydrogen System is technologically feasible, but not very efficient compared to the potential hydrogen production achievable.

Additional energy storage and power sources should be implemented to increase the total hydrogen production, and not have the system rely on a single intermittent energy source. The PV-Hydrogen system seems to only be economically feasible for use in the existing industry, rather than for commercial electrification. Incentives and subsidies would contribute towards the economic feasibility for commercial use.

21 Future Work

In the thesis description, the nominal power of the PV plant was limited to 1 MW. It would be recommended to tailor the PV-output to fit the electrolyzer size instead. Also emphasize the 3D-modeling of the PV-plant in PVsyst, to improve the accuracy of the power production, due to nearby shading of the PV-module.

Research the system auxiliary components in detail and analyze how the corrosion, standby degradation, and power fluctuation input, will impact the electrolyzer performance.

Include losses for an additional ESS in Matlab script, for an improved hydrogen production accuracy. And evaluate the LCoE calculation with ESS costs.

It is recommended to upgrade the system scale to improve the economic factor, due to the economics of scale.

Gain improved knowledge about Zambian incentives and subsidies, as well as for Norwegian foreign investments.

Economic analysis of the potential hydrogen marked in Zambia and potential hydrogen importers in neighboring countries.

Analyze the consumption and load pattern in the Zambian power sector.

References

[1] Dominguez C. and Foster V. Zambia's infrastructure: A continental perspective. http://siteresources.worldbank.org/INTAFRICA/Resources/Zambia-Country_Report_03.2011.pdf, 2010. Accessed: 2019.

[2] Zambia energy. http://www.zambiainvest.com/energy, 2017. Accessed: 2019.

[3] Klima og miljødepartementet og Olje-og energidepartementet. Produksjon og bruk av hydrogen i norge. https://www.regjeringen.no/contentassets/0762c0682ad04e6abd66a9555e7468df/hydrogen-i-norge---synteserapport.pdf, 2019. Accessed: 2019.

[4] Walter Jehle Agata Godula-Jopek and Joerg Wellnitz. Hydrogen storage technologies: New materials, transport, and infrastructure. https://ebookcentral.proquest.com/lib/ntnu/detail.action?docID=966171, 2005. Accessed: 2019.

[5] Central Intelligence Agency [US]. The world factbook, zambia. https://www.cia.gov/llibrary/publications/the-world-factbook/geos/za.html, 2019. Accessed: 2019.

[6] United Nations. Zambia's infrastructure: A continental perspective. http://worldpopulationreview.com/countries/zambia-population/, 2018. Accessed: 2019.

[7] Kalipeni Ezekiel Zulu-Leo. Moise, Imelda. Analyzing geographical access to hiv sentinel clinics in relation to other health clinics in zambia. https://www.researchgate.net/figure/Spatial-distribution-of-Zambias-rural-and-urban-population-2002_fig4_254372232, 2002. Accessed: 2019.

[8] Central Intelligence Agency [US]. The world factbook, world. https://www.cia.gov/library/publications/the-world-factbook/geos/xx.html, 2019. Accessed: 2019.

[9] Central Intelligence Agency [US]. The world factbook, norway. https://www.cia.gov/library/publications/the-world-factbook/geos/no.html, 2019. Accessed: 2019.

[10] World Bank. Gdp per capita (current us$). `https://data.worldbank.org/indicator/NY.GDP.PCAP.CD?view=chart`, 2019. Accessed: 2019.

[11] PopulationPyramid.net. Population pyramids of the world from 1950 to 2100. `https://www.populationpyramid.net/zambia/2017/`, 2017. Accessed: 2019.

[12] World Bank Group. Esmap zambia solar modeling report. `http://documents.worldbank.org/curated/en/259231467986245030/pdf/98030-ESMAP-P145271-Box391499B-PUBLIC-WBG-ESMAP-Zambia-Solar-Modeling-Report-2014-11-26.pdf`, 2014. Accessed: 2019.

[13] Rita Kesselring. The electricity crisis in zambia: Blackouts and social stratification in new mining towns. `https://www.sciencedirect.com/science/article/pii/S2214629617301858`, 2017. Accessed: 2019.

[14] SSB. Power stations, by type. maximum output. number. mw. `https://www.ssb.no/en/energi-og-industri/statistikker/elektrisitet/aar`, 2017. Accessed: 2019.

[15] Energy Regulation Board. Energy sector report 2014. `http://www.erb.org.zm/reports/EnergySectorReport2014.pdf`, 2014. Accessed: 2019.

[16] Energy Regulation Board. Electricity tariff determination guidelines for retail customers. `http://www.erb.org.zm/downloads/eregulation/guidelines/electricityTariffDeterminationGuidelines.pdf`, 2008. Accessed: 2019.

[17] H. Walimwipi. Investment incentives for renewable energy in southern africa: Case study of zambia. `http://www.into-sa.com/uploads/download/file/365/Renewable_Energy_Incentives_in_Zambia__2012_.pdf`, 2012. Accessed: 2019.

[18] Freedom to create. Policy report on the electricity sector in zambia. `http://www.freedomtocreate.com/ftc/wp-content/uploads/2017/06/FTC_Electricity_Sector_in_Zambia.pdf`, 2016. Accessed: 2019.

[19] Peter Engbo Rasmussen African Development Bank. African economic outlook 2019. `https://www.afdb.org/fileadmin/uploads/afdb/Documents/Publications/2019AEO/AEO_2019-EN.pdf` , 2019. Accessed: 2019.

[20] Industrial Development Corporation. About idc. `http://www.idc.co.zm/about-idc`, 2018. Accessed: 2019.

[21] Enel. Enel and idc sign 34 million us dollar financing agreement with ifc and eib for solar project in zambia. `https://www.enel.com/media/press/d/2018/06/enel-and-idc-sign-34-million-us-dollar-financing-agreement-with-ifc-and-eib-for-solar-project-in-zambia`, 2018. Accessed: 2019.

[22] Zambia Reports. Lungu commissions 54mw solar power plant. `https://zambiareports.com/2019/03/11/lungu-commissions-54mw-solar-power-plant/`, 11.03.2019. Accessed: 15.05.2019.

[23] The African Hydrogen Partnership Association. African hydrogen partnership. `https://docs.wixstatic.com/ugd/6a6d83_96270178f3fc4c4f88a40a4b068df0a4.pdf`. Accessed: 2019.

[24] Kailyn Stenhouse Brodie Yyelland Bethel Afework, Jordan Hanania and Jason Donev. Photovoltaic cell. `https://energyeducation.ca/encyclopedia/Photovoltaic_cell`, 2018. Accessed: 2019.

[25] Lynn Billman Gary Cook and Rick Adcock. Photovoltaic fundamentals. `https://www.nrel.gov/docs/legosti/old/16319.pdf`, 1995. Accessed: 2019.

[26] Solargis. Solargis solar resource database. `https://solargis2-web-assets.s3.eu-west-1.amazonaws.com/public/doc/8e24dda319/Solargis-database-description-and-accuracy.pdf`, 2016. Accessed: 2019.

[27] NREL. Solar resource glossary. `https://www.nrel.gov/grid/solar-resource/solar-glossary.html`. Accessed: 2019.

[28] Ecosmart. Pv system performance: Ghi to poa. `https://ecosmartsun.com/pv-system-performance-3/pv-system-performance-ghi-to-poa/`. Accessed: 2019.

[29] NREL. Basic photovoltaic principles and methods. `https://www.nrel.gov/docs/legosti/old/1448.pdf`, 2017. Accessed: 2019.

[30] Electrical4U. Solar cell. `https://www.electrical4u.com/solar-cell/`, 2018. Accessed: 2019.

[31] Solar Nation. What does the rated power of a pv module actually mean? `http://www.solar-nation.org/what-does-the-rated-power-of-a-pv-module-actually-mean`. Accessed: 2019.

[32] A. Rezaee Jordehi. Maximum power point tracking in photovoltaic (pv) systems: A review of different approaches. `https://www.sciencedirect.com/science/article/pii/S1364032116303811`, 2016. Accessed: 2019.

[33] Boris P. DUMNIC Zoltan J. CORBA, Vladimir A. KATIC and Dragan M. MILICEVIC. In-grid solar-to-electrical energy conversion system modeling and testing. `https://www.researchgate.net/publication/260350341_In-grid_solar-to-electrical_energy_conversion_system_modeling_and_testing`, 2012. Accessed: 2019.

[34] Alternative Energy Tutorials. Solar photovoltaic panel. `http://www.alternative-energy-tutorials.com/solar-power/pv-panel.html`. Accessed: 2019.

[35] Samlexsolar. Solar (pv) cell, module, array. `https://www.samlexsolar.com/learning-center/solar-cell-module-array.aspx`. Accessed: 2019.

[36] RECOM. Recom power rec15e-z series dc/dc converters. `https://no.mouser.com/new/recom-power/recom-rec15e-z-converters/`. Accessed: 2019.

[37] PV Performance. Cec inverter test protocol. `https://pvpmc.sandia.gov/modeling-steps/dc-to-ac-conversion/cec-inverter-test-protocol/`. Accessed: 2019.

[38] Mathias Aarre Maehlum. Mono- vs. polycrystalline vs. thin film. `http://energyinformative.org/best-solar-panel-monocrystalline-polycrystalline-thin-film/`, 2018. Accessed: 2019.

[39] Tom Schoder. Monocrystalline cells vs. polycrystalline cells: What's the difference? `https://www.civicsolar.com/support/installer/articles/monocrystalline-cells-vs-polycrystalline-cells-whats-difference`, 2018. Accessed: 2019.

[40] The Ecoexperts. The life expectancy of solar panels. `https://www.theecoexperts.co.uk/solar-panels/life-expectancy`. Accessed: 2019.

[41] Dirk C. Jordan and Sarah R. Kurtz. Photovoltaic degradation rates — an analytical review. `https://www.nrel.gov/docs/fy12osti/51664.pdf`, 2012. Accessed: 2019.

[42] William H. Brune. Start at the source: Earth rotating around the sun. `https://www.e-education.psu.edu/meteo300/node/681`. Accessed: 2019.

[43] Altitude & azimuth: The horizontal coordinate system. `https://www.timeanddate.com/astronomy/horizontal-coordinate-system.html`. Accessed: 2019.

[44] Jacob Marsh. Solar trackers: everything you need to know. `https://news.energysage.com/solar-trackers-everything-need-know/`, 2018. Accessed: 2019.

[45] Robert Margolis Mike Woodhouse Ran Fu, David Feldman and NREL Kristen Ardani. U.s. solar photovoltaic system cost benchmark: Q1 2017. `https://www.nrel.gov/docs/fy17osti/68925.pdf`, 1982. Accessed: 2019.

[46] International Renewable Energy Agency. The power to change: Solar and wind cost reduction potential to 2025. `https://www.irena.org/publications/2016/Jun/The-Power-to-Change-Solar-and-Wind-Cost-Reduction-Potential-to-2025`, 2016. Accessed: 2019.

[47] Hamid Naseem Md Mamoon Rashid, Mohammed K. Al Mesfer and Mohd Danis. Hydrogen production technologies. `https://www.hindawi.com/journals/cpis/2013/690627/`, 2013. Accessed: 2019.

[48] F.Gallorini L.Barelli, G.Bidini and S.Servili. Hydrogen production through sorption-enhanced steam methane reforming and membrane technology: A review. `https://www.sciencedirect.com/science/article/pii/S0360544207002058`, 2008. Accessed: 2019.

[49] US DOE Office of Energy Efficiency & Renewable Energy. Hydrogen production: Natural gas reforming. `https://www.energy.gov/eere/fuelcells/hydrogen-production-natural-gas-reforming`. Accessed: 2019.

[50] Odne Stokke Burheim. *Engineering energy storage*, pages 147–190. Joe Hayton, 2017.

[51] Olga Kasian Serhiy Cherevko Maximilian Schalenbach, Aleksandar R. Zeradjanin and Karl J.J. Mayrhofer. A perspective on low-temperature water electrolysis–challenges in alkaline and acidic technology. `http://www.electrochemsci.org/papers/vol13/130201173.pdf`, 2017. Accessed: 2019.

[52] Hamid Naseem Mamoon Rashid, Mohammed K. Al Mesfer and Mohd Danis. Hydrogen production by water electrolysis. `https://citeseerx.ist.psu.edu/viewdoc/download?doi=10.1.1.673.5912&rep=rep1&type=pdf`, 2015. Accessed: 2019.

[53] Alfredo Ursúa and Pablo Sanchis. Static–dynamic modelling of the electrical behaviour of a commercial advanced alkaline water electrolyser. `https://www.sciencedirect.com/science/article/pii/S036031991202191X`, 2012. Accessed: 2019.

[54] Ioannis Papagiannakis. Studying and improving the efficiency of water electrolysis using a proton exchange membrane electrolyser. `http://www.esru.strath.ac.uk/Documents/MSc_2003/papagiannakis_i.pdf`, 2005. Accessed: 2019.

[55] Greenlysis. Hydrogen and oxygen production via electrolysis powered by renewable energies to reduce environmental footprint of a wwtp. `http://ec.europa.eu/environment/life/project/Projects/index.cfm?fuseaction=home.showFile&rep=file&fil=LIFE08_ENV_E_000118_LAYMAN.pdf`, 2012. Accessed: 2019.

[56] Roy A. Parisher and Robert A. Rhea. Pipe drafting and design (third edition) pages 259-268. `https://www.sciencedirect.com/science/article/pii/B9780123847003000128`, 2012. Accessed: 2019.

[57] The Engineering ToolBox. Specific heat of common substances. `https://www.engineeringtoolbox.com/specific-heat-capacity-d_391.html`. Accessed: 2019.

[58] Odne S.Burheim Md H.Islam and Bruno G.Pollet. Sonochemical and sonoelectrochemical production of hydrogen. `https://www.sciencedirect.com/science/article/pii/S1350417718309702#b0280`, 2018. Accessed: 2019.

[59] I.Staffell A.Hawkes J.Nelson O.Schmidt, A.Gambhir and S.Fewa. Future cost and performance of water electrolysis: An expert elicitation study. `https://www.`

sciencedirect.com/science/article/pii/S0360319917339435, 2017. Accessed: 2019.

[60] Greig Chisholm and Leroy Cronin. Hydrogen from water electrolysis. http://www.chem.gla.ac.uk/cronin/media/papers/Chisholm-Chapter_16_2016.pdf. Accessed: 2019.

[61] Bjørn Halvorsen. Nel hydrogen. Mail correspondence and interviews.

[62] Ju Irgen Mergela Marcelo Carmoa, David L. Fritza and Detlef Stolten. A comprehensive review on pem water electrolysis. https://www.sciencedirect.com/science/article/pii/S0360319913002607, 2012. Accessed: 2019.

[63] Samir Boulfrada Lei Bi and Enrico Traversa. Steam electrolysis by solid oxide electrolysis cells (soecs) with proton-conducting oxides. https://pubs.rsc.org/en/content/articlelanding/2014/cs/c4cs00194j#!divAbstract, 2014. Accessed: 2019.

[64] Lan Hu. Molten carbonate fuel cells for electrolysis. https://www.diva-portal.org/smash/get/diva2:920605/FULLTEXT01.pdf, 2016. Accessed: 2019.

[65] The Pacific Northwest National Laboratory. Comparative properties of hydrogen and other fuels. https://h2tools.org/hyarc/hydrogen-data/comparative-properties-hydrogen-and-other-fuels. Accessed: 2019.

[66] Department of Energy (US). Hydrogen storage. https://www.energy.gov/eere/fuelcells/fuel-cell-technologies-office. Accessed: 2019.

[67] Farida Lamari-Darkrim Billur Sakintuna and Michael Hirscher. Metal hydride materials for solid hydrogen storage: A review. https://www.sciencedirect.com/science/article/pii/S0360319906005866, 2007. Accessed: 2019.

[68] E.MacA. Gray S.S. Mohammadshahi and C.J. Webb. A review of mathematical modelling of metal-hydride systems for hydrogen storage applications. https://www.researchgate.net/publication/290788587_A_review_of_mathematical_modelling_of_metal-hydride_systems_for_hydrogen_storage_applications, 2015. Accessed: 2019.

[69] Fraunhofer IFAM Dresden. Schematic hydride formation. `https://forschung-energiespeicher.info/en/projektschau/gesamtliste/projekt-einzelansicht/95/Metallhydride_speichern_schneller_mit_Graphit/`, 2016. Accessed: 2019.

[70] Michael Felderhoff Ulrich Eberle and Ferdi Schüth. Chemical and physical solutions for hydrogen storage. `https://www.researchgate.net/publication/26666827_Chemical_and_Physical_Solutions_for_Hydrogen_Storage`, 2009. Accessed: 2019.

[71] Office of Energy Efficiency & Renewable Energy US DOE. Chemical hydrogen storage materials. `https://www.energy.gov/eere/fuelcells/chemical-hydrogen-storage-materials`. Accessed: 2019.

[72] Chris Cone. Battery energy storage systems (bess) - worthwhile investment? `https://www.renewableenergyworld.com/ugc/articles/2018/08/23/battery-energy-storage-systems-bess--worthwhile-investment.html`, 2018. Accessed: 2019.

[73] Research Interface. Operation optimization of standalone microgrids considering lifetime characteristics of battery energy storage system. `https://ieeexplore.ieee.org/abstract/document/6510510`, 2013. Accessed: 2019.

[74] Spirit. Battery storage knowledge bank. `https://www.spiritenergy.co.uk/kb-batteries-understanding-batteries`. Accessed: 2019.

[75] Energysage. How to choose the best battery for a solar energy system. `https://www.energysage.com/solar/solar-energy-storage/what-are-the-best-batteries-for-solar-panels/`, 2019. Accessed: 2019.

[76] Alistair Davidson Geoffrey J. May and Boris Monahov. Lead batteries for utility energy storage: A review. `https://www.sciencedirect.com/science/article/pii/S2352152X17304437`, 2018. Accessed: 2019.

[77] Aristides E. Kiprakis Siraj Sabihuddin and Markus Mueller. A numerical and graphical review of energy storage technologies. `https://www.mdpi.com/1996-1073/8/1/172/htm`, 2014. Accessed: 2019.

[78] Siraj Sabihuddin. A numerical and graphical review of energy storage and energy production technologies v3. `https://figshare.com/articles/A_Numerical_and_Graphical_%20Review_of_%20Energy_Storage_and_Energy_Production_Technologies/1096289`, 2014. Accessed: 2019.

[79] Lan Ma Jihong Wang Mark Dooner Shihong Miao Jian Li Jidai Wang, Kunpeng Lu and Dan Wang. Overview of compressed air energy storage and technology development. `http://wrap.warwick.ac.uk/91858/7/WRAP-overview-compressed-air-energy-storage-technology-development-Wang-2017.pdf`, 2017. Accessed: 2019.

[80] Hydro Tasmania. Pumped hydro. `https://www.hydro.com.au/clean-energy/battery-of-the-nation/pumped-hydro`, 2019. Accessed: 2019.

[81] O. Achkari and A. El Fadar. Renewable energy storage technologies - a review. `https://www.researchgate.net/publication/326352395_Renewable_Energy_Storage_Technologies-A_Review`, 2018. Accessed: 2019.

[82] Ziyad Salameh. Renewable energy system design. `https://www.sciencedirect.com/science/article/pii/B9780123749918000040`, 2014. Accessed: 2019.

[83] Beacon Power. Carbon fiber flywheels. `https://beaconpower.com/carbon-fiber-flywheels/`, 2018. Accessed: 2019.

[84] Hans Bernhoff Björn Bolund and Mats Leijon. A numerical and graphical review of energy storage technologies. `https://www.sciencedirect.com/science/article/pii/S1364032105000146`, 207. Accessed: 2019.

[85] Hans Bernhoff Björn Bolund and Mats Leijon. Flywheel energy and power storage systems. `https://www.sciencedirect.com/science/article/pii/S1364032105000146`, 2007. Accessed: 2019.

[86] Comindware Inc. What is capex and opex. `https://www.comindware.com/blog-what-is-capex-and-opex/`, 2018. Accessed: 2019.

[87] Jordan Hanania Bethel Afework, Lyndon G. and Jason Donev. Levelized cost of energy. `https://energyeducation.ca/encyclopedia/Levelized_cost_of_energy`, 2018. Accessed: 2019.

[88] California Energy Commission. Assessment of time and cost needed to attain 100 hydrogen refueling stations in california. `https://www.energy.ca.gov/2015publications/CEC-600-2015-016/CEC-600-2015-016.pdf`, 2015. Accessed: 2019.

[89] Office of Energy Efficiency & Renewable Energy US DOE. Doe technical targets for hydrogen production from electrolysis. `https://www.energy.gov/eere/fuelcells/doe-technical-targets-hydrogen-production-electrolysis/`, 2011. Accessed: 2019.

[90] NEL. The world's most efficient and reliable electrolyser. `https://nelhydrogen.com/assets/uploads/2017/01/Nel_Electrolyser_brochure.pdf`. Accessed: 2019.

[91] Kailyn Stenhouse Brodie Yyelland Bethel Afework, Jordan Hanania and Jason Donev. Us solar market boom cuts o&m costs years ahead of forecast. `http://newenergyupdate.com/pv-insider/us-solar-market-boom-cuts-om-costs-years-ahead-forecast`, 2019. Accessed: 2019.

[92] Eystein Helland. Norconsult. Mail correspondence.

[93] Globalpetrolprices.com. Usa gasoline prices, us gallon. `https://www.globalpetrolprices.com/USA/gasoline_prices/`, 2019. Accessed: 03.05.2019.

[94] Globalpetrolprices.com. Zambia gasoline prices, us gallon. `https://www.globalpetrolprices.com/Zambia/gasoline_prices/` , 2019. Accessed: 03.05.2019.

[95] NEL. Nels m-series hydrogen generation systems. `https://www.protononsite.com/sites/default/files/2019-03/M%20Series%20Spec%20Sheet.pdf`, 2019. Accessed: 2019.

[96] NEL. Nels atmospheric alkaline electrolyzer. `https://nelhydrogen.com/product/atmospheric-alkaline-electrolyser-a-series/`, 2019. Accessed: 2019.

[97] Sapp members. `http://www.sapp.co.zw/about-sapp#structure`, 2019. Accessed: 2019.

[98] Canadian Solar. Kudymond cs3u-335—340—345p-fg. `https://www.canadiansolar.com/upload/c2332dfde10c8c9a/1d8727f427cf0855.pdf`. Accessed: 2019.

A Appendix: NEL M-series datasheet

nel·

PROTON® PEM

M Series

Hydrogen Generation Systems

MODEL	M100	M200	M400
	Fully-automated MW-class on-site hydrogen generator utilizing a modular skid-based design Tri-mode operation (selectable): • Command-following mode allows operation based on available input power • Load following mode automatically adjusts output 0-100% to match demand • Tank filling mode operates with power-conservation mode during standby		
ELECTROLYTE			
	Proton Exchange Membrane (PEM) – Caustic-Free		
HYDROGEN PRODUCTION			
Nominal Production Rate Nm³/hr @ 0°C, 1 bar SCF/hr @ 70°F, 1 atm SLPM @ 70°F, 1 atm kg per 24 hours	100 Nm³/hr 3,804 SCF/hr 1,795 SLPM 216 kg/24 hr	200 Nm³/hr 7,608 SCF/hr 3,590 SLPM 431 kg/24 hr	400 Nm³/hr 15,217 SCF/hr 7,180 SLPM 864 kg/24 hr
Delivery Pressure – Nominal	30 barg (435 psig); full differential pressure H_2 over O_2		
Power Consumed at Stack by System	0.51 MW 0.55 MW	1.0 MW 1.1 MW	2.1 MW 2.2 MW
Power Consumption at Stack per Volume of H_2 Gas Produced[1]	4.95 kWh/Nm³		
Power Consumed at Stack per Mass of H_2 Gas[1]	55 kWh/kg		
Purity (Concentration of Impurities)	99.9% H_2O < 500 ppm, N_2 < 2 ppm, O_2 < 1 ppm, all others undetectable		
Purity (Concentration of Impurities with Optional High Purity Dryer)	ISO 14687-1:1999 Type 1 Grade C / ISO 14687-2:2012 Type 1 Grade D 99.9995% H_2O < 2 ppm, N_2 < 2 ppm, O_2 < 1 ppm, all others undetectable		
Start-Up Time (from Off State)	<5 min		
Ramp-Up Time (Minimum to Full Load)	<10 Sec		
Ramp Rate (% of Full-Scale)	≥ 15% per sec (Power Input Mode)		
Turndown Range	10-100% (Input Power Mode); 0-100% (H_2 Demand Mode)		
Upgradeability	Field upgradeable in 250 kW (52 Nm³/hr) increments		
DI WATER REQUIREMENT			
Consumption Rate at Maximum Production	93 L/hr (25 gal/hr)	187 L/hr (49 gal/hr)	373 L/hr (99 gal/hr)
Temperature	5°C to 40°C (41°F to 104°F)		
Input Water Quality	Required: ASTM Type II Deionized Water, < 1 µS/cm (> 1 MΩ-cm) Preferred: ASTM Type I Deionized Water, < 0.1 µS/cm (> 10 MΩ-cm)		

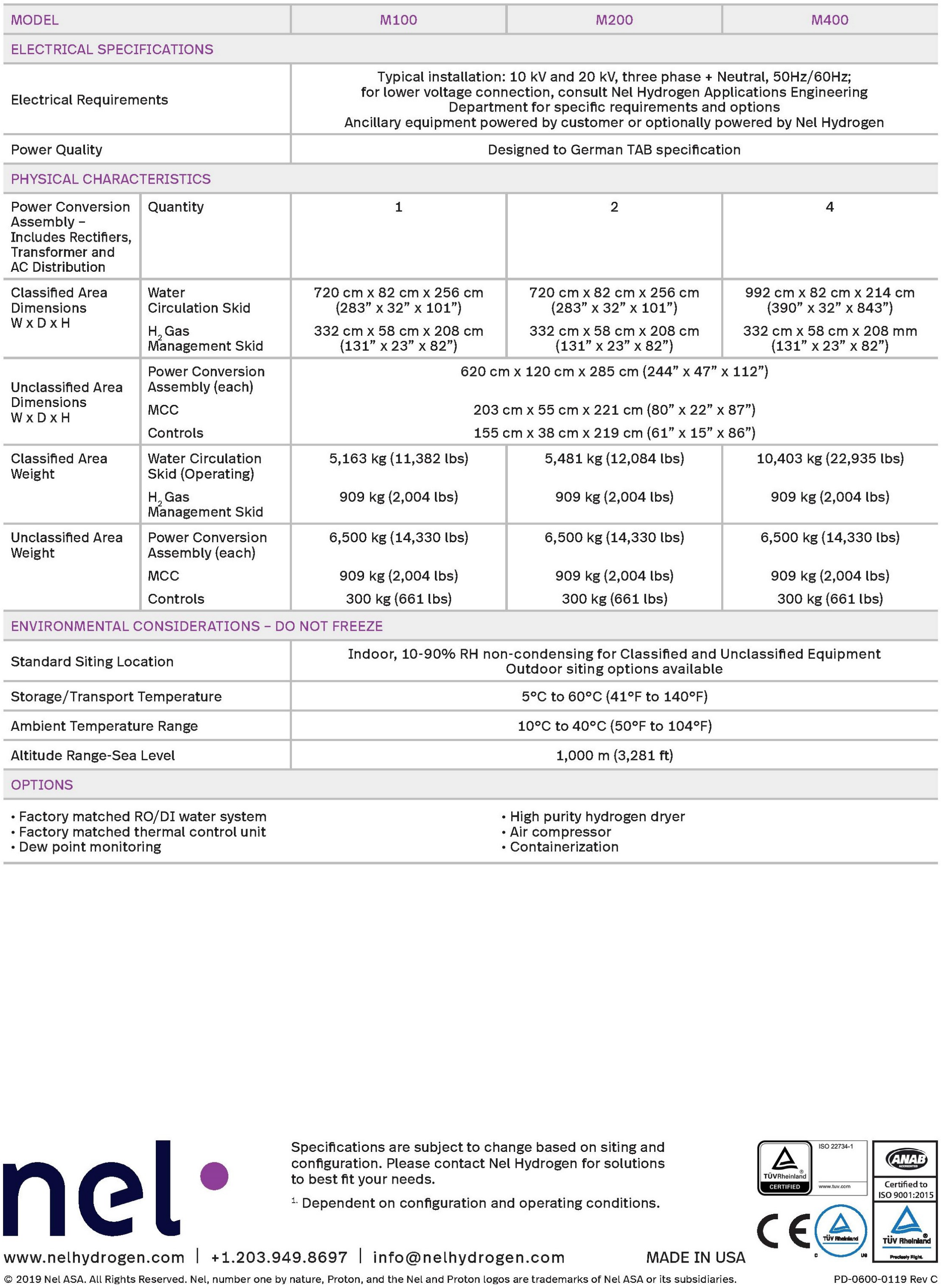

MODEL		M100	M200	M400
ELECTRICAL SPECIFICATIONS				
Electrical Requirements		Typical installation: 10 kV and 20 kV, three phase + Neutral, 50Hz/60Hz; for lower voltage connection, consult Nel Hydrogen Applications Engineering Department for specific requirements and options Ancillary equipment powered by customer or optionally powered by Nel Hydrogen		
Power Quality		Designed to German TAB specification		
PHYSICAL CHARACTERISTICS				
Power Conversion Assembly – Includes Rectifiers, Transformer and AC Distribution	Quantity	1	2	4
Classified Area Dimensions W x D x H	Water Circulation Skid	720 cm x 82 cm x 256 cm (283” x 32” x 101”)	720 cm x 82 cm x 256 cm (283” x 32” x 101”)	992 cm x 82 cm x 214 cm (390” x 32” x 843”)
	H_2 Gas Management Skid	332 cm x 58 cm x 208 cm (131” x 23” x 82”)	332 cm x 58 cm x 208 cm (131” x 23” x 82”)	332 cm x 58 cm x 208 mm (131” x 23” x 82”)
Unclassified Area Dimensions W x D x H	Power Conversion Assembly (each)	620 cm x 120 cm x 285 cm (244” x 47” x 112”)		
	MCC	203 cm x 55 cm x 221 cm (80” x 22” x 87”)		
	Controls	155 cm x 38 cm x 219 cm (61” x 15” x 86”)		
Classified Area Weight	Water Circulation Skid (Operating)	5,163 kg (11,382 lbs)	5,481 kg (12,084 lbs)	10,403 kg (22,935 lbs)
	H_2 Gas Management Skid	909 kg (2,004 lbs)	909 kg (2,004 lbs)	909 kg (2,004 lbs)
Unclassified Area Weight	Power Conversion Assembly (each)	6,500 kg (14,330 lbs)	6,500 kg (14,330 lbs)	6,500 kg (14,330 lbs)
	MCC	909 kg (2,004 lbs)	909 kg (2,004 lbs)	909 kg (2,004 lbs)
	Controls	300 kg (661 lbs)	300 kg (661 lbs)	300 kg (661 lbs)
ENVIRONMENTAL CONSIDERATIONS – DO NOT FREEZE				
Standard Siting Location		Indoor, 10-90% RH non-condensing for Classified and Unclassified Equipment Outdoor siting options available		
Storage/Transport Temperature		5°C to 60°C (41°F to 140°F)		
Ambient Temperature Range		10°C to 40°C (50°F to 104°F)		
Altitude Range-Sea Level		1,000 m (3,281 ft)		
OPTIONS				

- Factory matched RO/DI water system
- Factory matched thermal control unit
- Dew point monitoring
- High purity hydrogen dryer
- Air compressor
- Containerization

Specifications are subject to change based on siting and configuration. Please contact Nel Hydrogen for solutions to best fit your needs.

[1] Dependent on configuration and operating conditions.

ISO 22734-1

Certified to ISO 9001:2015

www.nelhydrogen.com | +1.203.949.8697 | info@nelhydrogen.com

MADE IN USA

PD-0600-0119 Rev C

Figure A.1: *Datasheet of the M-Series electrolyzers produced by NEL. [95]*

B Appendix: NEL A-series datasheet

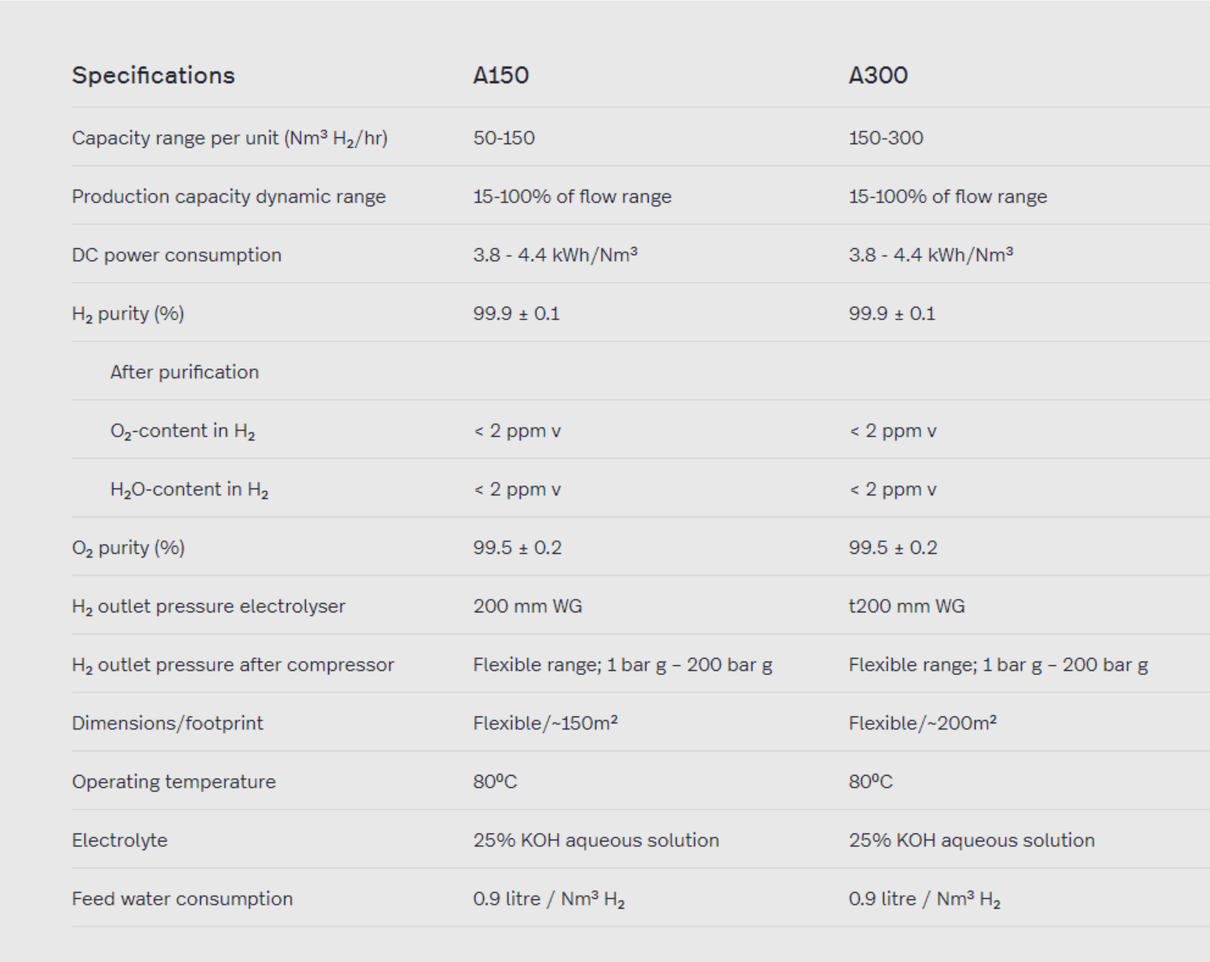

Specifications	**A150**	**A300**
Capacity range per unit (Nm^3 H_2/hr)	50-150	150-300
Production capacity dynamic range	15-100% of flow range	15-100% of flow range
DC power consumption	3.8 - 4.4 kWh/Nm^3	3.8 - 4.4 kWh/Nm^3
H_2 purity (%)	99.9 ± 0.1	99.9 ± 0.1
After purification		
O_2-content in H_2	< 2 ppm v	< 2 ppm v
H_2O-content in H_2	< 2 ppm v	< 2 ppm v
O_2 purity (%)	99.5 ± 0.2	99.5 ± 0.2
H_2 outlet pressure electrolyser	200 mm WG	t200 mm WG
H_2 outlet pressure after compressor	Flexible range; 1 bar g – 200 bar g	Flexible range; 1 bar g – 200 bar g
Dimensions/footprint	Flexible/~150m^2	Flexible/~200m^2
Operating temperature	80ºC	80ºC
Electrolyte	25% KOH aqueous solution	25% KOH aqueous solution
Feed water consumption	0.9 litre / Nm^3 H_2	0.9 litre / Nm^3 H_2

Figure B.1: *Datasheet of the A150 and A300 A-series electrolyzer produced by NEL. [96]*

C Appendix: SAPP Members

Figure C.1: *The companies involved in the Southern African Power Pool. [97]*

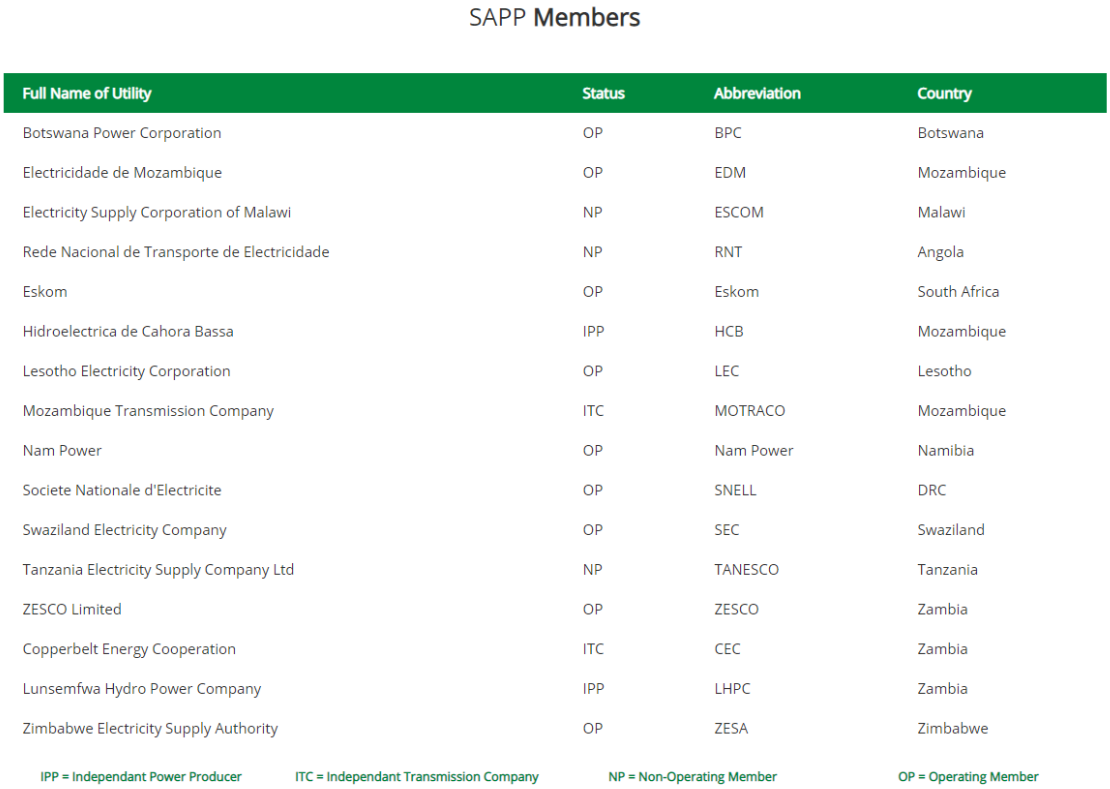

SAPP **Members**

Full Name of Utility	Status	Abbreviation	Country
Botswana Power Corporation	OP	BPC	Botswana
Electricidade de Mozambique	OP	EDM	Mozambique
Electricity Supply Corporation of Malawi	NP	ESCOM	Malawi
Rede Nacional de Transporte de Electricidade	NP	RNT	Angola
Eskom	OP	Eskom	South Africa
Hidroelectrica de Cahora Bassa	IPP	HCB	Mozambique
Lesotho Electricity Corporation	OP	LEC	Lesotho
Mozambique Transmission Company	ITC	MOTRACO	Mozambique
Nam Power	OP	Nam Power	Namibia
Societe Nationale d'Electricite	OP	SNELL	DRC
Swaziland Electricity Company	OP	SEC	Swaziland
Tanzania Electricity Supply Company Ltd	NP	TANESCO	Tanzania
ZESCO Limited	OP	ZESCO	Zambia
Copperbelt Energy Cooperation	ITC	CEC	Zambia
Lunsemfwa Hydro Power Company	IPP	LHPC	Zambia
Zimbabwe Electricity Supply Authority	OP	ZESA	Zimbabwe

IPP = Independant Power Producer

ITC = Independant Transmission Company

NP = Non-Operating Member

OP = Operating Member

D Appendix: Canadian Solar datasheet

NEW

CanadianSolar

KuDymond

CS3U-335|340|345P-FG

***Transparent doubleglass module can be provided upon request.**

MORE POWER

Low power loss in cell connection

Low NMOT: 42 ± 3 °C
Low temperature coefficient (Pmax): -0.38 % / °C

Better shading tolerance

MORE RELIABLE

Lower hot spot temperature

Minimizes micro-cracks

Heavy snow load up to 5400 Pa,
wind load up to 2400 Pa

Fire Class A and Type 3 / Type 13 certified according to IEC 61730-2 / MST 23 and UL 1703

30 years **linear power output warranty**

10 years **product warranty on materials and workmanship**

MANAGEMENT SYSTEM CERTIFICATES

ISO 9001:2015 / Quality management system
ISO 14001:2015 / Standards for environmental management system
OHSAS 18001:2007 / International standards for occupational health & safety

PRODUCT CERTIFICATES*

IEC 61215 / IEC 61730: VDE / CE / CEC AU
UL 1703: CSA / IEC61701 ED2: VDE / IEC62716: VDE
Take-e-way

*We can provide this product with special BOM specifically certified with salt mist, ammonia and sand blowing tests. Please talk to our local technical sales representatives to get your customized solutions.

CANADIAN SOLAR INC. is committed to providing high quality solar products, solar system solutions and services to customers around the world. No. 1 module supplier for quality and performance/price ratio in IHS Module Customer Insight Survey. As a leading PV project developer and manufacturer of solar modules with over 30 GW deployed around the world since 2001.

CANADIAN SOLAR INC.
545 Speedvale Avenue West, Guelph, Ontario N1K 1E6, Canada, www.canadiansolar.com, support@canadiansolar.com

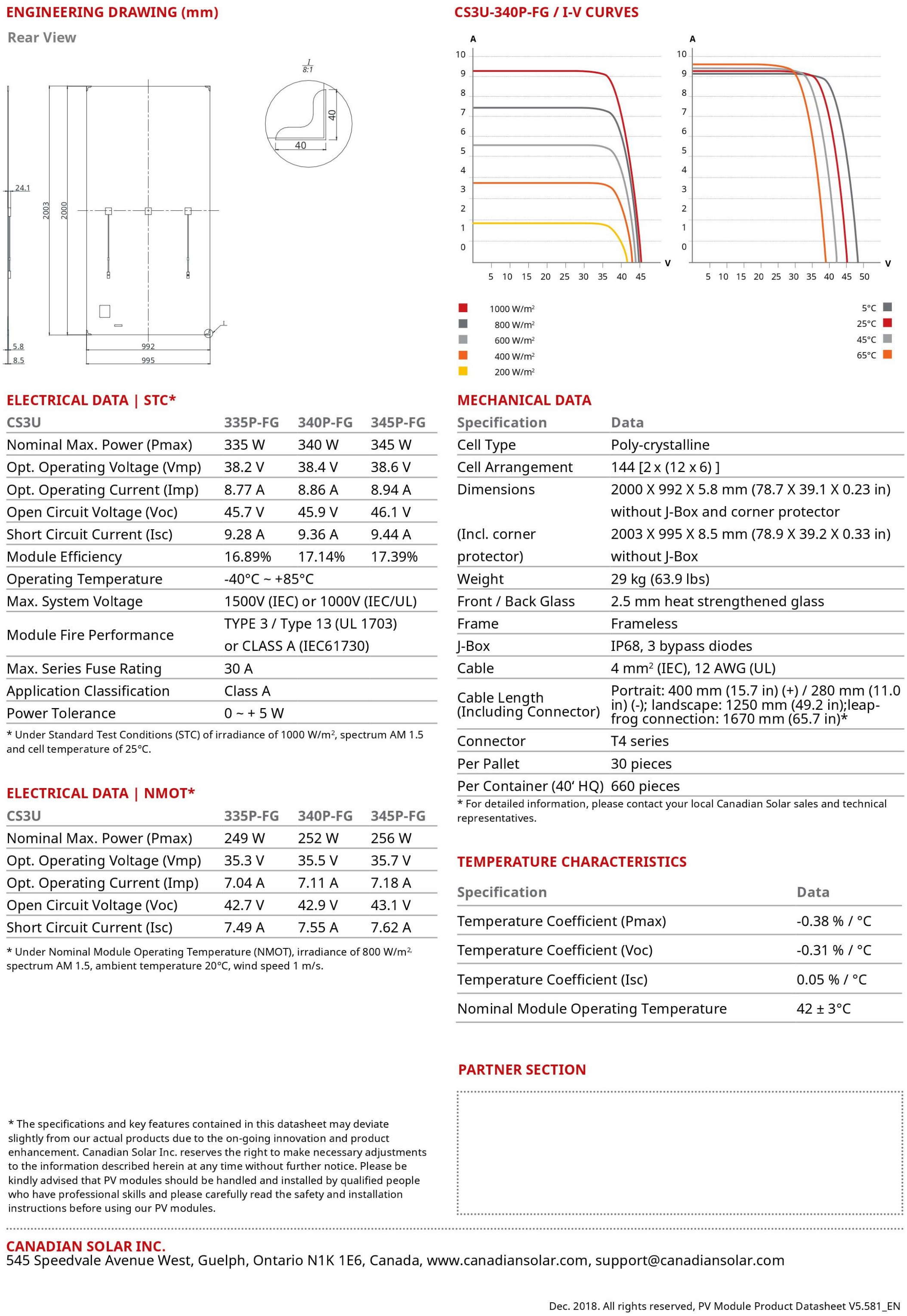

ENGINEERING DRAWING (mm)

CS3U-340P-FG / I-V CURVES

ELECTRICAL DATA | STC*

CS3U	335P-FG	340P-FG	345P-FG
Nominal Max. Power (Pmax)	335 W	340 W	345 W
Opt. Operating Voltage (Vmp)	38.2 V	38.4 V	38.6 V
Opt. Operating Current (Imp)	8.77 A	8.86 A	8.94 A
Open Circuit Voltage (Voc)	45.7 V	45.9 V	46.1 V
Short Circuit Current (Isc)	9.28 A	9.36 A	9.44 A
Module Efficiency	16.89%	17.14%	17.39%
Operating Temperature	-40°C ~ +85°C		
Max. System Voltage	1500V (IEC) or 1000V (IEC/UL)		
Module Fire Performance	TYPE 3 / Type 13 (UL 1703) or CLASS A (IEC61730)		
Max. Series Fuse Rating	30 A		
Application Classification	Class A		
Power Tolerance	0 ~ + 5 W		

* Under Standard Test Conditions (STC) of irradiance of 1000 W/m^2, spectrum AM 1.5 and cell temperature of 25°C.

ELECTRICAL DATA | NMOT*

CS3U	335P-FG	340P-FG	345P-FG
Nominal Max. Power (Pmax)	249 W	252 W	256 W
Opt. Operating Voltage (Vmp)	35.3 V	35.5 V	35.7 V
Opt. Operating Current (Imp)	7.04 A	7.11 A	7.18 A
Open Circuit Voltage (Voc)	42.7 V	42.9 V	43.1 V
Short Circuit Current (Isc)	7.49 A	7.55 A	7.62 A

* Under Nominal Module Operating Temperature (NMOT), irradiance of 800 W/m^2, spectrum AM 1.5, ambient temperature 20°C, wind speed 1 m/s.

MECHANICAL DATA

Specification	Data
Cell Type	Poly-crystalline
Cell Arrangement	144 [2 x (12 x 6)]
Dimensions	2000 X 992 X 5.8 mm (78.7 X 39.1 X 0.23 in) without J-Box and corner protector
(Incl. corner protector)	2003 X 995 X 8.5 mm (78.9 X 39.2 X 0.33 in) without J-Box
Weight	29 kg (63.9 lbs)
Front / Back Glass	2.5 mm heat strengthened glass
Frame	Frameless
J-Box	IP68, 3 bypass diodes
Cable	4 mm^2 (IEC), 12 AWG (UL)
Cable Length (Including Connector)	Portrait: 400 mm (15.7 in) (+) / 280 mm (11.0 in) (-); landscape: 1250 mm (49.2 in);leap-frog connection: 1670 mm (65.7 in)*
Connector	T4 series
Per Pallet	30 pieces
Per Container (40' HQ)	660 pieces

* For detailed information, please contact your local Canadian Solar sales and technical representatives.

TEMPERATURE CHARACTERISTICS

Specification	Data
Temperature Coefficient (Pmax)	-0.38 % / °C
Temperature Coefficient (Voc)	-0.31 % / °C
Temperature Coefficient (Isc)	0.05 % / °C
Nominal Module Operating Temperature	42 ± 3°C

PARTNER SECTION

* The specifications and key features contained in this datasheet may deviate slightly from our actual products due to the on-going innovation and product enhancement. Canadian Solar Inc. reserves the right to make necessary adjustments to the information described herein at any time without further notice. Please be kindly advised that PV modules should be handled and installed by qualified people who have professional skills and please carefully read the safety and installation instructions before using our PV modules.

CANADIAN SOLAR INC.
545 Speedvale Avenue West, Guelph, Ontario N1K 1E6, Canada, www.canadiansolar.com, support@canadiansolar.com

Dec. 2018. All rights reserved, PV Module Product Datasheet V5.581_EN

Figure D.1: *Datasheet for the PV-module used in PVsyst [98]*

E Appendix: PV land coverage

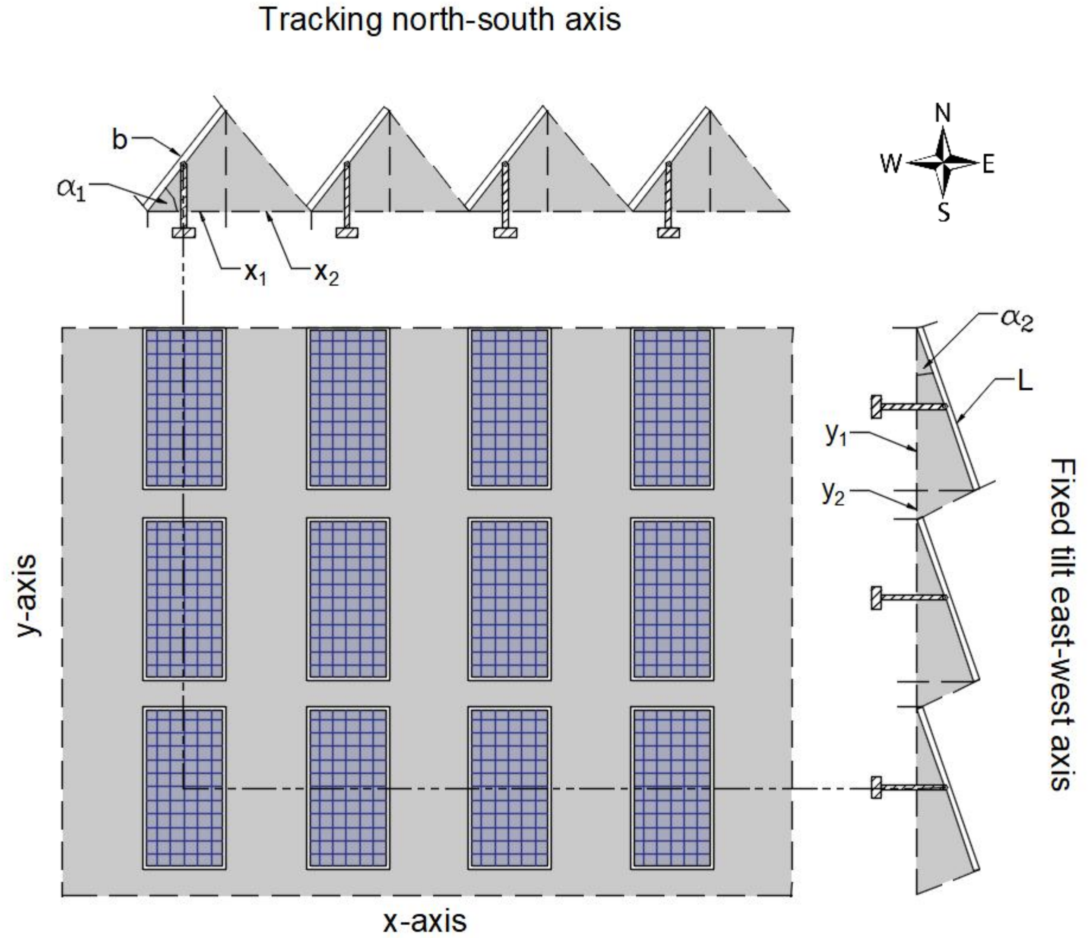

Figure E.1: *Land coverage due to shading from PV, made in Autocad.*

$$x = x_1 + x_2 = \left(cos(\alpha_1) + \frac{sin^2(\alpha_1)}{cos(\alpha_1)} \right) \cdot b \tag{E.1}$$

$$y = y_1 + y_2 = \left(cos(\alpha_2) + \frac{sin^2(\alpha_2)}{cos(\alpha_2)} \right) \cdot L \tag{E.2}$$

F Appendix: DOE hydrogen production targets

Figure F.1: *DOE Technical Targets for Hydrogen Production from Electrolysis. [89]*

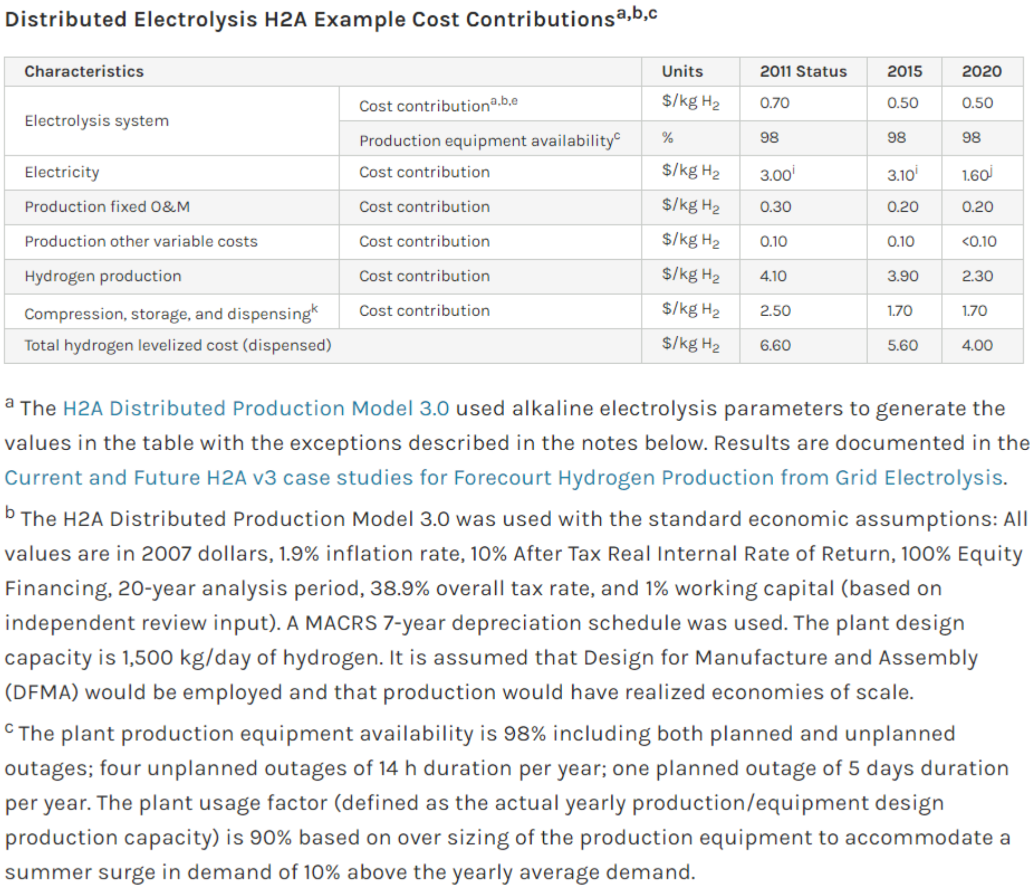

Distributed Electrolysis H2A Example Cost Contributions[a,b,c]

Characteristics		Units	2011 Status	2015	2020
Electrolysis system	Cost contribution[a,b,e]	$/kg H_2	0.70	0.50	0.50
	Production equipment availability[c]	%	98	98	98
Electricity	Cost contribution	$/kg H_2	3.00[i]	3.10[i]	1.60[j]
Production fixed O&M	Cost contribution	$/kg H_2	0.30	0.20	0.20
Production other variable costs	Cost contribution	$/kg H_2	0.10	0.10	<0.10
Hydrogen production	Cost contribution	$/kg H_2	4.10	3.90	2.30
Compression, storage, and dispensing[k]	Cost contribution	$/kg H_2	2.50	1.70	1.70
Total hydrogen levelized cost (dispensed)		$/kg H_2	6.60	5.60	4.00

[a] The H2A Distributed Production Model 3.0 used alkaline electrolysis parameters to generate the values in the table with the exceptions described in the notes below. Results are documented in the Current and Future H2A v3 case studies for Forecourt Hydrogen Production from Grid Electrolysis.

[b] The H2A Distributed Production Model 3.0 was used with the standard economic assumptions: All values are in 2007 dollars, 1.9% inflation rate, 10% After Tax Real Internal Rate of Return, 100% Equity Financing, 20-year analysis period, 38.9% overall tax rate, and 1% working capital (based on independent review input). A MACRS 7-year depreciation schedule was used. The plant design capacity is 1,500 kg/day of hydrogen. It is assumed that Design for Manufacture and Assembly (DFMA) would be employed and that production would have realized economies of scale.

[c] The plant production equipment availability is 98% including both planned and unplanned outages; four unplanned outages of 14 h duration per year; one planned outage of 5 days duration per year. The plant usage factor (defined as the actual yearly production/equipment design production capacity) is 90% based on over sizing of the production equipment to accommodate a summer surge in demand of 10% above the yearly average demand.

G Appendix: Hydrogen price equivalent

The conversion rates used:
1 US gallon = 3.785 Liters
1 US mile = 1.609 km

In equation G.1 the USD/km prices for driving a CGV in the USA, with the national average gasoline prices in January 2019 is described [93, 88]. In equation G.2 the USD/km prices for driving a CGV is described for Zambia, with the national average gasoline prices in January 2019 [94, 88].

$$\text{CGV (USA)} = \frac{2.83\text{USD/gal gas}}{27\,\text{mi/gal gas}} = \frac{0.75\text{ USD/L gas}}{11.5\text{km/L gas}} = 0.065\text{USD/km} \tag{G.1}$$

$$\text{CGV (Zambia)} = \frac{6.27\,\text{USD/gal gas}}{27\,\text{mi/gal gas}} = \frac{1.66\text{ USD/L gas}}{11.5\,\text{km/L gas}} = 0.144\,\text{USD/km} \tag{G.2}$$

As seen in equation G.1 and G.2 the price of driving a CGV is substantial higher in Zambia than the US. The fuel price when driving a FCEV in California, USA (2015) is shown in equation G.3.[88]

$$\text{FCEV (USA)} = \frac{14\,\text{USD/kg H}_2}{66\,\text{mi/kg H}_2} = \frac{14\,\text{USD/kg H}_2}{106.2\,\text{km/kg H}_2} = 0.132\,\text{USD/km} \tag{G.3}$$

In equation G.4, the USD/km of driving a CGV in Zambia is multiplied by the km/kg H_2 for a FCEV. The result is the value of hydrogen per kg, that corresponds to the gasoline price in Zambia,

$$\text{FCEV (Zambia)} = 0.144\,\text{USD/km} \;\cdot 106.2\,\text{km/kg H}_2 = 15.3\,\text{USD/kg H}_2 \tag{G.4}$$

From equation G.4 one can estimate the feasible fuel price when driving a FCEV in Zambia.